MANIPULATIONS OF SUCROSE/PROTON SYMPORTERS AND PROTON-PUMPING PYROPHOSPHATASE LEAD TO ENHANCED PHLOEM TRANSPORT BUT HAVE CONTRASTING EFFECTS ON PLANT BIOMASS

Aswad S. Khadilkar, B.S., M.S.

Dissertation Prepared for the Degree of

DOCTOR OF PHILOSOPHY

UNIVERSITY OF NORTH TEXAS

May 2015

APPROVED:

Brian Ayre, Major Professor
Kent Chapman, Committee Member
Jyoti Shah, Committee Member
Vladimir Shulaev, Committee Member
Stevens Brumbley, Committee Member
Art Goven, Chair of the Department of Biological Sciences
Costas Tsatsoulis, Interim Dean of the Toulouse Graduate School

Khadilkar, Aswad S. Manipulations of Sucrose/Proton Symporters and Proton-Pumping Pyrophosphatase Lead to Enhanced Phloem Transport but have Contrasting Effects on Plant Biomass. Doctor of Philosophy (Biochemistry), May 2015, 121 pp., 4 tables, 23 figures, 198 chapter references.

Delivery of photoassimilate, mainly sucrose (Suc) from photoautotrophic source leaves provides the substrate for the growth and maintenance of sink tissues such as roots, storage tissues, flowers and fruits, juvenile organs, and seeds. Phloem loading is the energized process of accumulating solute in the sieve element/companion cell complex of source leaf phloem to generate the hydrostatic pressure that drives long-distance transport. In many plants this is catalyzed by Suc/Proton (H^+) symporters (SUTs) which are energized by the proton motive force (PMF). Overexpression of *SUTs* was tested as means to enhance phloem transport and plant productivity. Phloem specific overexpression of *AtSUC2* in wild type (WT) tobacco resulted in enhanced Suc loading and transport, but against the hypothesis, plants were stunted and accumulated carbohydrates in the leaves, possibly due to lack of sufficient energy to support enhanced phloem transport.

The energy for SUT mediated phloem loading is provided from the PMF, which is ultimately supplied by the oxidation of a small proportion of the loaded photoassimilates. It was previously shown that inorganic pyrophosphate (PP_i) is necessary for this oxidation and overexpressing a proton-pumping pyrophosphatase (*AVP1*) enhanced both shoot and root growth, and augmented several energized processes like nutrient acquisition and stress responses. We propose that AVP1 localizes to the PM of phloem cells and uses PMF to synthesize PP_i rather than hydrolyze it, and in doing so, maintains PPi levels for efficient Suc

oxidation and ATP production. Enhanced ATP production in turn strengthens the PMF via plasma membrane (PM) ATPase, increasing phloem energization and phloem transport. Phloem-specific and constitutive *AVP1* overexpressing lines showed increased growth and more efficiently moved carbohydrates to sink organs compared to WT. This suggested changes in metabolic flux but diagnostic metabolites of central metabolism did not show changes in steady state levels. This research focuses on fundamental aspects of carbon utilization and transport, and has a strong applied component, since increased H^+-PPase activity enhances plant biomass, nutrient up-take capacities, and stress tolerance for as yet not fully characterized reasons.

Copyright 2015

by

Aswad S. Khadilkar

ACKNOWLEDGEMENTS

I would like to express my gratitude and most thanks to my advisor Dr. Brian Ayre for his expert insights, recommendations, guidance and persuasion. Especially the last one, because without that, this work would not have been possible.

I would like to thank my committee members, Dr. Kent Chapman, Dr. Jyoti Shah, Dr. Vladimir Shulaev and Dr. Stevens Brumbley for their feedbacks and support. I would like to especially thank Dr. Stevens Brumbley for letting me use his genogrinder and qPCR machine, and Dr. Vladimir Shulaev for training in UPLC-MS. I thank the University of North Texas, Department of Biological Sciences for funding and amenities.

Thanks to all past and present members of Ayre lab: Te Cao, Dr. Kasturi Dasgupta, Ipsita Lahiri, Dr. Umesh Prasad Yadav, Dr. Roisin Mcgarry, Sarah Prewitt, Tristan Britt, Bernice Yau, Angela Chia-chi Fu, Justin Laughlin, Heather Thames. Especially, Dr. Umesh Prasad Yadav for training with enzyme-based, high-throughput metabolite assays. Also, thanks to our collaborators on the AVP1 project at Arizona State University, Dr. Julio Paez-Valencia for immunohistochemistry results and Roberto Gaxiola for providing *AVP1* cDNA and consultation.

My parents, Nila and Sunil Khadilkar have been the pillar behind me during my entire education that provided the foundation for this work. Last but not the least; (In fact the most), I would like to thank my best friend and wife Ananya Sen Chowdhury for her immense support, love, patience and for being with me in thick and thin. I am truly indebted to her, and it's because of her strength and compassion that this dissertation was possible.

TABLE OF CONTENTS

Page

LIST OF TABLES

Page

LIST OF FIGURES

Page

LIST OF ABBREVIATIONS

CC	Companion cell
C	Carbon
CoYMV	Commelina Yellow Mottle Virus
dpg	Days post germination
EDTA	Ethylene diamine tetraacetic acid
EF	Elongation factor
ESI	Electrospray ionization
Fru	Fructose
FW	Fresh weight
G6P	Glucose-6-Phosphate
Glc	Glucose
H+-PPase	Proton-pumping pyrophosphatase
HPAEC-PAD	High performance anion exchange chromatography- pulsed amperometric detection
HPLC	High performance liquid chromatography
IRGA	Infra red gas analyzer
MRM	Multiple reaction monitoring
NaCl	Sodium Chloride
NaHCO3	Sodium Bicarbonate
P	Phosphorous
PCR	Polymerase chain reaction
Pi	Orthphosphate
PM	Plasma membrane
PMF	Proton motive force

PPi	Pyrophosphate
qRT-PCR	Quantitative reverse transcription polymerase chain reaction
RH	Relative humidity
SE	Standard error
SE-CCC	Sieve element-companion cell complex
Suc	Sucrose
UBQ	Ubiquitin
UPLC-ESI-MS/MS	Ultra-performance liquid chromatography- electrospray ionization-tandem mass spectroscopy
WT	Wild type

CHAPTER 1

INTRODUCTION

Plant yield is largely determined by the efficient delivery of photoassimilates from source tissue to sink organs: mainly Suc from source leaves which provides the substrate for the growth and maintenance of non-photosynthetic sink tissues such as fruits, grains and tubers (Figure 1.1). Source tissues are most prominently photosynthetic leaves, but could also be storage organs from which reserves are being utilized. Thus, source tissues are net exporters of fixed carbon (C). Alternatively, sink organs are net importers and include roots, storage tissues accumulating reserves and secondary growth tissues such as reproductive organs (flowers, fruits and seeds).

The allocation of carbon fixed during photosynthesis is complex. CO_2 that is fixed during photosynthesis is the carbon gain. Part is transiently stored in chloroplast as starch during the day and later utilized during the night when photosynthesis is not occurring. Part is respired in the leaf for leaf functions. Part is converted to Suc in the cytoplasm and transported to the sink tissues where it is utilized for growth, storage and maintenance of heterotrophic tissues. For human exploitation of plants, “yield” refers to any harvested organ, and yield is generally derived from transported assimilates. 50-80 % of the assimilated CO_2 is provided from the source leaf to the phloem stream to fulfill demands of heterotrophic sink tissues (Ainsworth and Bush, 2011).

The phloem network contains files of living cells which form the sieve-tube system. A complex is formed with the sieve element and its connected companion cell. Sieve tube members are linked end to end by sieve plates; to compose a sieve tube, which lack the

tonoplast, nucleus, and have few mitochondria or plastids. Companion cells have dense cytoplasm, all organelles, and carry out active processes and generate energy needed for phloem transport. The two cells are connected via symplasmic connections of plasmodesmata. Phloem loading is the active (i.e. energy requiring) accumulation of solute, principally sugars, in to the sieve element-companion cell complex (SE-CCC). This decreases the solute potential and causes uptake of water from the apoplasm by osmosis. Increased hydrostatic pressure promotes bulk flow of water and solutes through the sieve tube system to sink organs with lower pressure. In the sink tissues, utilization of solute for growth, storage and metabolism causes increase in solute potential, and lowers the turgor pressure by allowing removal of water by osmosis. This hydrostatic pressure gradient drives the flow of water and photoassimilates from source to sink tissues (Taiz and Zeiger, 2010). These critical operating procedures of the phloem are well established. Nevertheless, the mechanism by which plants control carbon partitioning to disparate sink tissues is not well understood. Whether competing sink strengths determine the distribution processes or plants have systemic process at the whole-plant level that coordinates allocation is an issue (Ruiz-Medrano et al., 2001).

1.1 Phloem Loading in Source Leaves

In source leaves, Suc produced in mesophyll cells must first move toward the phloem. The generally accepted model is that this is passive cell to cell movement via plasmodesmata. In some families, plasmodesmata connect the mesophyll directly to the SE-CCC. Although, referred to as passive loading, true phloem “loading” (i.e. energized accumulation of solute in the phloem) does not occur and the highest photoassimilate concentration is maintained in mesophyll cells (Turgeon and Medville, 1998; Rennie and Turgeon, 2009). Transport is thus

entirely through the symplasm, with bulk flow initiating at the point where the pressure gradient in the source to sink continuum exceeds the resistance to flow within the path. In other families, plasmodesmata also connect the mesophyll to SE-CCC, but phloem loading occurs by a polymer trap mechanism. Here, Suc enters the intermediary cells (specialized CC) passively through plasmodesmata and is converted to raffinose family oligosaccharides that are too large to diffuse back. These are thus trapped in the phloem and contribute to the hydrostatic pressure. (Turgeon and Medville, 1998; Rennie and Turgeon, 2009).

In the best studied phloem loading system, and the one that operates in the majority of crop plants as well as in the model plant Arabidopsis, mesophyll cells and the phloem cells are not connected by plasmodesmata and phloem loading occurs from the apoplasm (Slewinski and Braun, 2010; Ayre, 2011; Braun, 2012). Historically, it was thought that, in mesophyll, Suc moves cell to cell through plasmodesmata and is effluxed into the apoplasm via facilitated diffusion (Bush, 1993). Recently identified AtSWEET11 and 12 have been shown to be involved in facilitating Suc movement from mesophyll cell to the apoplasmic space in Arabidopsis and OsSWEET11 and 14 may do the same in rice (Chen et al., 2012). Suc effluxers *AtSWEET11* and *12* are expressed in the phloem parenchyma cells adjacent to the companion cells. Double mutants (atsweet11/12) show defects in the phloem transport. Suc facilitators have also been identified in pea and bean, which allow Suc movement in both directions (Zhou et al., 2007). In the minor vein of phloem, Suc from the apoplasm is loaded into the companion cell by Suc/Proton (H^+) symporters (SUTs) and is energized by PMF (Gottwald et al., 2000; Ayre, 2011). Once into the phloem Suc travels by bulk flow along the hydrostatic pressure gradient.

1.2 Apoplasmic Phloem Loading

In apoplasmic phloem loading, carbohydrates from mesophyll cells are released into the cell wall space/apoplasm. The sugars from the apoplasm are then loaded into the SE-CCC by SUTs. Since, Suc is in low concentration in the apoplasm and high concentration in the SE-CCC, this loading step is an active process which requires PMF. For each molecule of Suc loaded into the SE-CCC, one H^+ is also pumped in the same direction indicating symport. The PMF is generated by the plasma membrane (PM) H^+-ATPase which hydrolyzes ATP and pumps H^+ into the apoplasmic space (Sauer, 2007; Ayre, 2011). Figure 1.2 describes the mechanism of apoplasmic phloem loading and the role of SUTs.

In most plant species studied, families of genes encoding SUTs have been identified and these phylogenetically related SUTs show alterations in the ability to transport Suc. Their expression patterns also vary depending on type of tissue or organ and its developmental stage (Ayre, 2011). SUTs operate throughout the plant, since apoplasm to symplasm Suc movement occur at several interfaces. The photoassimilate supply to the organs adjacent to the transport phloem (e.g. in stems) generally occurs through the apoplasm (Minchin and Thorpe, 1996; Meyer et al., 2000; Ayre, 2011). In strong sink tissues, terminal Suc delivery may occur through the symplasm or the apoplasm. Suc may be recovered from apoplasm by SUTs or could be hydrolyzed by cell-wall invertase and the resultant hexose molecules may be transported by hexose transporters (Godt and Roitsch, 2006; Zhang et al., 2006) (Figure 1.1). Further discussion focuses on SUTs involved in phloem transport.

SUTs have evolutionary diverse substrate affinity and specificity. Symporter activity and kinetics of SUTs have been studied in Xenopus oocytes (Chandran et al., 2003; Sivitz et al., 2007;

Reinders et al., 2008) and yeast (Sauer and Stolz, 1994; Meyer et al., 2000; Zhou et al., 2007). The roles of SUTs have been studied by using techniques like immunolocalizations, *in situ* hybridizations and promoter:reporter gene fusions (Truernit and Sauer, 1995; Barker et al., 2000; Meyer et al., 2000; Kuhn et al., 2003). On the other hand, in *planta* functions have been deciphered based on T-DNA insertional mutagenesis studies in Arabidopsis, over expression studies with constitutive or tissue-specific promoters and RNAi-mediated suppression studies (Gottwald et al., 2000; Srivastava et al., 2008; Srivastava et al., 2009). Detailed explanation of Suc transporters will be discussed in the Chapter 2. In Chapter 2, we hypothesized that *SUT* over-expression specifically with phloem companion cell specific promoter would enhance carbon partitioning and improve growth.

A plant's ability to acquire, supply and partition nutrients depend on H^+ gradients primarily generated by P-type H^+-ATPases (Figure 1.2). The PMF required for apoplasmic phloem loading is ultimately provided by the oxidation of a small proportion of the loaded photoassimilates. Complete oxidation of one loaded Suc molecule generates as much as 72 ATP (Taiz and Zeiger, 2010). Plant cells spend large amounts of energy reserves to maintain proton (H^+) gradients.

In addition to P-type ATPases, plants possess H^+-pyrophosphatases (H^+-PPases) which utilize the energy of pyrophosphates (PP_i) to create PMF across endomembranes. PP_i is by-product of many biological reactions, including synthesis of DNA, RNA, proteins, Suc, starch and cell wall carbohydrates. Since it is a product, PP_i accumulation would cause feedback inhibition on these essential reactions. Most organisms hydrolyze PPi with a soluble enzyme, and the energy is lost as heat. The H^+-PPase of plants conveniently capture this energy of PPi hydrolysis

by creating a proton gradient. In germinating seedlings, the role of H^+-PPase in removal of PP_i is more important than its role in the acidification of vacuoles (Ferjani et al., 2011; Ferjani et al., 2012).

Plants have two distinct H^+-PPases. Type-I depend on cytosolic K^+ and are slightly inhibited by Ca^{2+}. Type-II are insensitive to K^+ but sensitive to Ca^{2+} (Reaa et al., 1992; Maeshima, 2000; Segami et al., 2010). An example of a type-I H^+-PPase is *Arabidopsis Vacuolar Pyrophosphatase (AVP1)* which encodes a tonoplast-localized, pyrophosphate-dependent H^+ pump (Li et al., 2005).

1.3 Relation of Suc and PPi

PP_i is an essential intermediate in both Suc synthesis and respiration: low levels of PP_i pull the reaction in the direction of Suc synthesis and high PP_i levels push the reaction toward Suc oxidation. During Suc synthesis, UDP-Glc pyrophosphorylase (UGPase) catalyzes conversion of Glc-1-P and UTP to UDP-Glc and PP_i. Removal of PP_i leads to increased formation of UDP-Glc. UDP-Glc is further utilized in Suc synthesis. Plants overexpressing the soluble *E.coli* PPase (*ppa1)* from the *Cauliflower mosaic virus* 35S promoter showed enhanced accumulation of UDP-Glc and Suc in the source leaves, consistent with ppa1 driving the reaction toward Suc. But, these plants were stunted and had reduced root formation (Sonnewald, 1992). *E.coli* PPase is a cytosolic enzyme and activity is not coupled to H^+ translocation. PP_i is required for Suc synthase mediated Suc oxidation, and plants with *Pro35S:ppa1* likely had impeded Suc oxidation and consequently phloem loading, explaining the diminutive root phenotype. As carbohydrate transport to other organs is not enhanced in these plants, carbohydrates

accumulated in the source tissue, resulting in a diminutive phenotype, reduced root growth and signs of necrosis in the mature leaves (Jelitto et al., 1992).

In phloem companion cells, a portion of loaded Suc is oxidized to generate the ATP needed to create the PM PMF. During this process of Suc oxidation, several steps utilize PP_i. Firstly, Suc synthase breaks Suc into Fru and UDP-Glc. UDP-Glc pyrophosphorylase then utilizes UDP-Glc and PP_i to generate Glc-1-P and UTP. In glycolysis, PP_i-dependent phosphofructokinase utilizes PP_i and Fru-6-P to produce Fru-1, 6-bisphosphate. In phloem, as PP_i is necessary for efficient Suc oxidation, plants with *ppa1* overexpression may have blocked Suc oxidation. Sonnewald and colleagues showed that *Pro35S:ppa1* plants were stunted but accumulated more sugars. This result argued that reducing PP_i levels enhance Suc synthesis, but also suggested limited transport, which also would lead to Suc accumulation (Sonnewald, 1992).

Phloem-specific expression of *ppa1* with *Agrobacterium rhizogenes Ri plasmid rolC* promoter resulted in removal of cytosolic PP_i specifically from companion cells. The resultant phenotype was similar to *Pro35S:ppa1* plants, confirming that ppa1 in companion cells inhibited phloem transport, thus the Suc synthase pathway which requires PPi predominates. Phloem-specific expression of yeast invertase (Pro*rolC:Suc2)* rescued the phenotype by bypassing the PP_i dependent Suc synthase pathway (Lerchl et al., 1995). Compared to *Pro35S:pp1* which are debilitated, *Pro35S:AVP1* plants show enhanced growth compared to WT, indicating that *AVP1* overexpression may enhance phloem transport. Overexpression of *AVP1* in Arabidopsis showed improved salt tolerance due to enhanced Na^+ uptake in the vacuoles and drought resistance due to increased vacuolar osmoregulation (Gaxiola et al., 2001; Gaxiola et al., 2002). Such increased salt and drought resistance have been reported in several species (Yang et al., 2007;

Bao et al., 2009; Li et al., 2010). In addition, enhanced biomass and yield, increased root acidification, and improved nutrient use efficiencies were described (Lv et al., 2008; Arif et al., 2012; Pei et al., 2012; Paez-Valencia et al., 2013). It is difficult to attribute all of these effects to H^+-PPase role in energizing the vacuole. Thus, understandings of alterations in primary metabolism and nutrient partitioning were needed (Discussed in Chapter 3 and 4). Our objective was to investigate whether overexpression of *AVP1* improves plant growth by altering carbon utilization, allocation, phloem loading and transport (Discussed in Chapter 3 and 4). In Chapter 3 and 4 we test the hypothesis that H^+-PPase stimulate phloem loading and long distance transport by acting as PPi synthase on the CC PM rather than PPase on endomembranes.

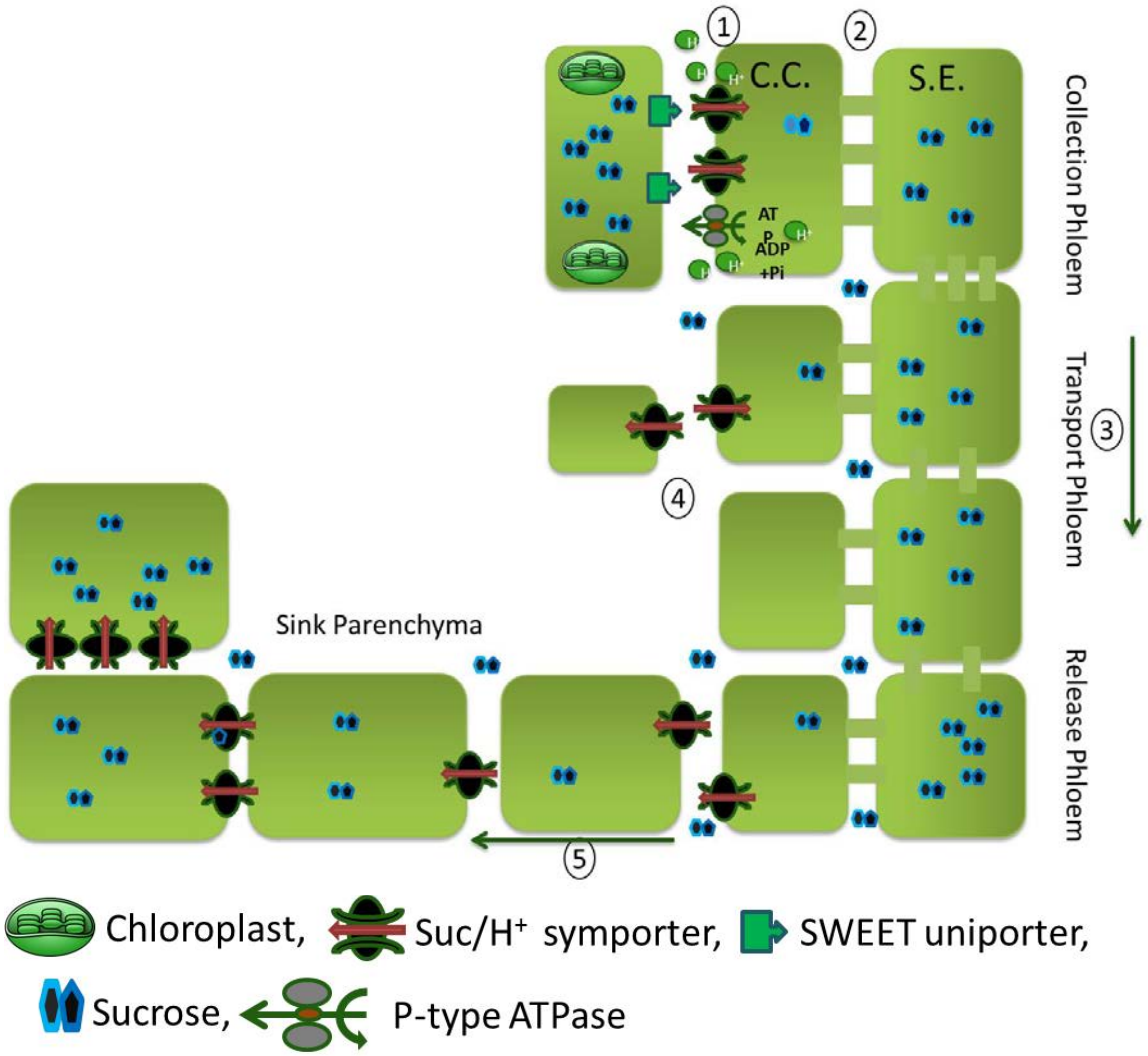

Figure1-1: Pathway of delivery of photoassimilates (mainly Suc) from source to sink tissues. Suc is loaded into the phloem by an energized process (explained in detail in Figure 1.2). Once loaded in the phloem, Suc travels through complex network of phloem cells. In the sink tissues, Suc is delivered either via passive diffusion through plasmodesmata or by active un-loading process facilitated by SUTs (Truernit and Sauer, 1995). Step 1: Suc from parenchyma cells is released in the apoplasm by SWEET effluxers, uptake in companion cell (C.C.) occurs via SUTs which utilize PMF. PMF is generated by ATP hydrolysis by P-type ATPase. Step 2: Photoassimilate enters sieve element (S.E.) via plasmodesmata. Step 3: Increased hydrostatic pressure promotes bulk flow of water and solutes through the sieve tube system to sink organs with lower pressure. Suc is retrieved into the phloem by SUTs. Step 4: Suc is released symplasmically by plasmodesmata or delivered by SUTs through apoplasm. Figure adapted and modified from (Ayre, 2011). Role of SWEET effluxers from(Braun, 2012).

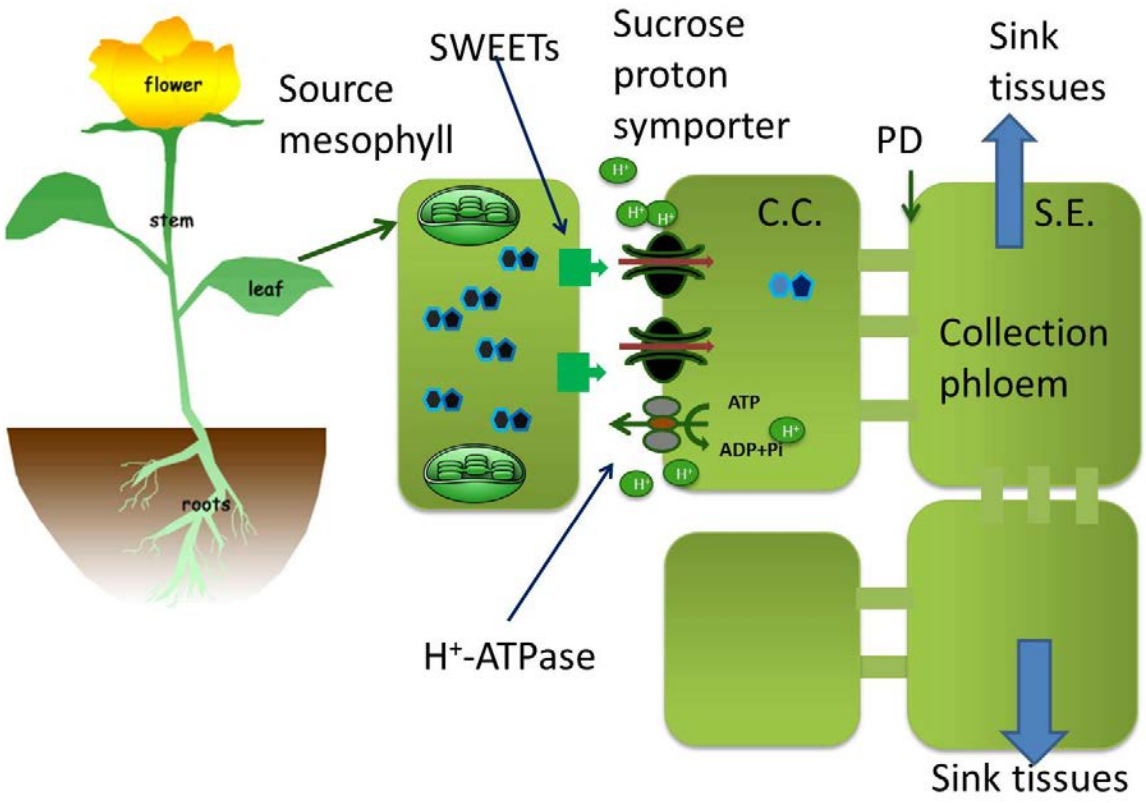

Figure 1-2: Active process of phloem loading.
Suc generated through photosynthesis in mesophyll cells is released in to the apoplasm with the aid of recently identified SWEET effluxers. From the apoplasm the Suc is pumped into the companion cell of the SE-CC complex with the aid of SUTs. SUTs utilize the energy of PMF which is generated by PM ATPase which hydrolyze ATP and generate PMF. Once in the CC the Suc enters SE through plasmodesmata and further delivered to sink tissues such as flowers, fruits or roots. Plants spend significant amount of energy to maintain that PMF which is key during this process (Haruta and Sussman, 2012). PD, plasmodesmata; C.C, companion cell; S.E, sieve element.

1.4 Chapter References

Ainsworth EA, Bush DR (2011) Carbohydrate export from the leaf: a highly regulated process and target to enhance photosynthesis and productivity. Plant Physiology 155: 64-69

Arif A, Zafar Y, Arif M, Blumwald E (2012) Improved growth, drought tolerance, and ultrastructural evidence of increased turgidity in tobacco plants overexpressing Arabidopsis vacuolar pyrophosphatase (*AVP1*). Molecular Biotechnology 54: 379-392

Ayre BG (2011) Membrane-transport systems for sucrose in relation to whole-plant carbon partitioning. Molecular Plant 4: 377-394

Bao A, Suo-Min W, Guo-Qiang W, Jie-Jun X, Jin-Lin Z, Chun-Mei W (2009) Overexpression of the *Arabidopsis* H^+-PPase enhanced resistance to salt and drought stress in transgenic alfalfa (*Medicago sativa* L.). Plant Science 176: 232-240

Barker L, Kuhn C, Weise A, Schulz A, Gebhardt C, Hirner B, Hellmann H, Schulze W, Ward JM, Frommer WB (2000) SUT2, a putative sucrose sensor in sieve elements. The Plant Cell 12: 1153-1164

Braun DM (2012) SWEET! The pathway is complete. Science 335: 173-174

Bush DR (1993) Proton-coupled sugar and amino acid transporters in plants. Annual Review of Plant Physiology and Plant Molecular Biology 44: 513-542

Chandran D, Reinders A, Ward JM (2003) Substrate specificity of the *Arabidopsis thaliana* sucrose transporter AtSUC2. The Journal of Biological Chemistry 278: 44320-44325

Chen LQ, Qu XQ, Hou BH, Sosso D, Osorio S, Fernie AR, Frommer WB (2012) Sucrose efflux mediated by SWEET proteins as a key step for phloem transport. Science 335: 207-211

Ferjani A, Segami S, Horiguchi G, Muto Y, Maeshima M, Tsukaya H (2011) Keep an eye on PPi: the vacuolar-type H^+-pyrophosphatase regulates postgerminative development in Arabidopsis. The Plant Cell 23: 2895-2908

Ferjani A, Segami S, Horiguchi G, Sakata A, Maeshima M, Tsukaya H (2012) Regulation of pyrophosphate levels by H^+-PPase is central for proper resumption of early plant development. Plant Signaling & Behavior 7: 38-42

Gaxiola RA, Fink GR, Hirschi KD (2002) Genetic manipulation of vacuolar proton pumps and transporters. Plant Physiology 129: 967-973

Gaxiola RA, Li J, Undurraga S, Dang LM, Allen GJ, Alper SL, Fink GR (2001) Drought- and salt-tolerant plants result from overexpression of the *AVP1* H^+-pump. Proceedings of the National Academy of Sciences of the United States of America 98: 11444-11449

Godt D, Roitsch T (2006) The developmental and organ specific expression of sucrose cleaving enzymes in sugar beet suggests a transition between apoplasmic and symplasmic phloem unloading in the tap roots. Plant Physiology and Biochemistry 44: 656-665

Gottwald JR, Krysan PJ, Young JC, Evert RF, Sussman MR (2000) Genetic evidence for the in planta role of phloem-specific plasma membrane sucrose transporters. Proceedings of the National Academy of Sciences of the United States of America 97: 13979-13984

Haruta M, Sussman MR (2012) The effect of a genetically reduced plasma membrane protonmotive force on vegetative growth of Arabidopsis. Plant Physiology 158: 1158-1171

Jelitto T, Sonnewald U, Willmitzer L, Hajirezeai M, Stitt M (1992) Inorganic pyrophosphate content and metabolites in potato and tobacco plants expressing *E. coli* pyrophosphatase in their cytosol. Planta 188: 238-244

Kuhn C, Hajirezaei MR, Fernie AR, Roessner-Tunali U, Czechowski T, Hirner B, Frommer WB (2003) The sucrose transporter StSUT1 localizes to sieve elements in potato tuber phloem and influences tuber physiology and development. Plant Physiology 131: 102-113

Lerchl J, Geigenberger P, Stitt M, Sonnewald U (1995) Impaired photoassimilate partitioning caused by phloem-specific removal of pyrophosphate can be complemented by a phloem-specific cytosolic yeast-derived invertase in transgenic plants. The Plant Cell 7: 259-270

Li J, Yang H, Peer WA, Richter G, Blakeslee J, Bandyopadhyay A, Titapiwantakun B, Undurraga S, Khodakovskaya M, Richards EL, Krizek B, Murphy AS, Gilroy S, Gaxiola R (2005) Arabidopsis H^+-PPase AVP1 regulates auxin-mediated organ development. Science 310: 121-125

Li Z, Baldwin CM, Hu Q, Liu H, Luo H (2010) Heterologous expression of Arabidopsis H^+-pyrophosphatase enhances salt tolerance in transgenic creeping bentgrass (*Agrostis stolonifera L.*). Plant, Cell & Environment 33: 272-289

Lv S, Zhang K, Gao Q, Lian L, Song Y, Zhang J (2008) Overexpression of an *H^+-PPase* gene from *Thellungiella halophila* in cotton enhances salt tolerance and improves growth and photosynthetic performance. Plant & Cell Physiology 49: 1150-1164

Maeshima M (2000) Vacuolar H^+-pyrophosphatase. Biochimica et Biophysica Acta 1465: 37-51

Meyer S, Melzer M, Truernit E, Hummer C, Besenbeck R, Stadler R, Sauer N (2000) *AtSUC3*, a gene encoding a new Arabidopsis sucrose transporter, is expressed in cells adjacent to the vascular tissue and in a carpel cell layer. The Plant Journal 24: 869-882

Minchin PE, Thorpe MR (1996) What determines carbon partitioning between competing sinks? Journal of Experimental Botany 47: 1293-1296

Paez-Valencia J, Sanchez-Lares J, Marsh E, Dorneles LT, Santos MP, Sanchez D, Winter A, Murphy S, Cox J, Trzaska M, Metler J, Kozic A, Facanha AR, Schachtman D, Sanchez CA, Gaxiola RA (2013) Enhanced proton translocating pyrophosphatase activity improves nitrogen use efficiency in romaine lettuce. Plant Physiology 161: 1557-1569

Pei L, Wang J, Li K, Li Y, Li B, Gao F, Yang A (2012) Overexpression of *Thellungiella halophila* H^+-pyrophosphatase gene improves low phosphate tolerance in maize. PLOS ONE 7: e43501

Reaa P, Kima Y, Sarafiana V, Pooleb R, Daviesc J, Sanders D (1992) Vacuolar H^+-translocating pyrophosphatases: a new category of ion translocase. Trends in Biochemical Sciences 17: 348-353

Reinders A, Sivitz AB, Starker CG, Gantt JS, Ward JM (2008) Functional analysis of LjSUT4, a vacuolar sucrose transporter from Lotus japonicus. Plant Molecular Biology 68: 289-299

Rennie EA, Turgeon R (2009) A comprehensive picture of phloem loading strategies. Proceedings of the National Academy of Sciences of the United States of America 106: 14162-14167

Ruiz-Medrano R, Xoconostle-Cázares B, Lucas WJ (2001) The phloem as a conduit for inter-organ communication. Current Opinion in Plant Biology 4: 202-209

Sauer N (2007) Molecular physiology of higher plant sucrose transporters. FEBS Letters 581: 2309-2317

Sauer N, Stolz J (1994) SUC1 and SUC2: two sucrose transporters from Arabidopsis thaliana; expression and characterization in baker's yeast and identification of the histidine-tagged protein. The Plant Journal 6: 67-77

Segami S, Nakanishi Y, Sato M, Maeshima M (2010) Quantification, organ-specific accumulation and intracellular localization of type II $H(^+)$-pyrophosphatase in Arabidopsis thaliana. Plant Cell Physiology 51: 1350-1360

Sivitz AB, Reinders A, Johnson ME, Krentz AD, Grof CP, Perroux JM, Ward JM (2007) Arabidopsis sucrose transporter AtSUC9. High-affinity transport activity, intragenic control of expression, and early flowering mutant phenotype. Plant Physiology 143: 188-198

Slewinski T, Braun DM (2010) Current perspectives on the regulation of whole-plant carbohydrate partitioning. Plant Science 178: 341-349

Sonnewald U (1992) Expression of *E. coli* inorganic pyrophosphatase in transgenic plants alters photoassimilate partitioning. The Plant Journal 2: 571-581

Srivastava AC, Dasgupta K, Ajieren E, Costilla G, McGarry RC, Ayre BG (2009) Arabidopsis plants harbouring a mutation in *AtSUC2*, encoding the predominant sucrose/proton symporter necessary for efficient phloem transport, are able to complete their life cycle and produce viable seed. Annals of Botony 104: 1121-1128

Srivastava AC, Ganesan S, Ismail IO, Ayre BG (2008) Functional characterization of the Arabidopsis AtSUC2 Sucrose/H^+ symporter by tissue-specific complementation reveals an essential role in phloem loading but not in long-distance transport. Plant Physiology 148: 200-211

Taiz L, Zeiger E (2010) Plant Physiology, Ed 5. Sinauer Associates, Inc., Sunderland, MA

Truernit E, Sauer N (1995) The promoter of the *Arabidopsis thaliana SUC2 sucrose-H^+ symporter* gene directs expression of beta-glucuronidase to the phloem: evidence for phloem loading and unloading by SUC2. Planta 196: 564-570

Turgeon R, Medville R (1998) The absence of phloem loading in willow leaves. Proceedings of the National Academy of Sciences of the United States of America 95: 12055-12060

Yang H, Knapp J, Koirala P, Rajagopal D, Peer WA, Silbart LK, Murphy A, Gaxiola RA (2007) Enhanced phosphorus nutrition in monocots and dicots over-expressing a phosphorus-responsive type I H^+-pyrophosphatase. Plant Biotechnology Journal 5: 735-745

Zhang XY, Wang XL, Wang XF, Xia GH, Pan QH, Fan RC, Wu FQ, Yu XC, Zhang DP (2006) A shift of phloem unloading from symplasmic to apoplasmic pathway is involved in developmental onset of ripening in grape berry. Plant Physiology 142: 220-232

Zhou Y, Qu H, Dibley KE, Offler CE, Patrick JW (2007) A suite of sucrose transporters expressed in coats of developing legume seeds includes novel pH-independent facilitators. The Plant Journal 49: 750-764

CHAPTER 2

HETEROLOGOUS EXPRESSION OF ARABIDOPSIS SUCROSE TRANSPORTER *AtSUC2* INCREASES PHLOEM LOADING AND TRANSPORT IN *Nicotiana tobaccum* (TOBACCO)

2.1 Abstract

Delivery of carbohydrates from photosynthetic source leaves provide the substrate for the growth and maintenance of non-photosynthetic sink tissues such as fruits, grains and tubers. This long distance transport is mediated by the phloem vascular system. Suc is the predominant form in which photoassimilate are transported. The phloem of source leaves has higher concentration of sugars and other nutrients than sink tissues, and this creates a hydrostatic pressure gradient which drives the bulk flow of phloem sap from source to sink tissues. Phloem loading of Suc into SE/CCC from the surrounding apoplasm is mediated by SUTs and energized by the PMF. In a previous study, we tested the potential of phloem-specific overexpression of *SUTs* to enhance phloem transport and increase plant productivity in Arabidopsis. Enhanced Suc loading and transport was achieved but growth was reduced due to disturbed C/P homeostasis. To corroborate our findings, here we present results of phloem specific overexpression of *Arabidopsis thaliana AtSUC2* in tobacco. Similar to Arabidopsis, tobacco plants were stunted, had increased phloem loading and transport, and plants were moderately rescued with additional phosphate.

2.2 Introduction

Reduced *SUT* expression leads to negative impact on plant growth and development. Alternatively, enhanced *SUT* expression might improve plant productivity by improving phloem transport and enhancing photoassimilate supply to heterotrophic tissues (Ainsworth and Bush,

2011). There are two reasons for a potential increase, 1) increased photoassimilate transport and 2) reduced feedback inhibition on photosynthesis. Studies with constitutive or organ specific overexpression of SUTs are not well represented in the literature. Seed-specific overexpression of *StSUT1* with the vicilin promoter resulted in enhanced Suc uptake and growth of developing pea cotyledons (Rosche et al., 2002). In another example, constitutive overexpression of *SoSUT1* in potato led to reduction in Suc levels in the leaves, reduced amino acid levels in leaves and enhanced Suc uptake capacity but did not have significant impact on tuber yield (Leggewie et al., 2003). In barley, *HvSUT1* overexpression with endosperm specific Hordein B1 promoter led to increased seed protein levels, and alterations in carbon-nitrogen metabolism (Weichert et al., 2010). Since, these studies showed an impact on carbon metabolism and partitioning, manipulations of SUTs for enhancing phloem transport capacity needs to be explored further.

SUTs genes have been identified and form a small gene family in all plants where they have been sought. Based on sequence similarities, SUTs are classified in five distinct groups (Braun and Slewinski, 2009). Group I contains monocot-specific, high-affinity SUTs which are primarily involved in phloem loading. Similarly, group V contains monocot specific SUTs which have not been well characterized. Group II contains dicot-specific, high affinity SUTs which play a role in both source and sink tissues (Lalonde et al., 2003; Lalonde et al., 2004; Sauer, 2007). Group III contains both monocot and dicot specific SUTs which are structurally different from other groups, have low affinity, and unclear function. Group IV contains both monocot and dicot specific SUTs which are mostly tonoplast localized and are presumably involved in transport of Suc from vacuole to cytoplasm, as dictated by the prevailing PMF.

Amongst these SUTs, those involved mainly in phloem loading have been characterized to greatest extent. ZmSUT1 belonging to monocot-specific group 1 is involved in phloem loading in source leaves and may also be involved in Suc efflux (Carpaneto et al., 2005; Slewinski and Braun, 2010). In Arabidopsis, AtSUC2 catalyzes phloem loading (Truernit and Sauer, 1995; Gottwald et al., 2000; Srivastava et al., 2008) and belongs to group II whereas LeSUT1 is the main phloem loader in source leaves of tomato (Weise et al., 2008). Mutation in *AtSUC2* and anti-sense inhibition of *LeSUT1* results in diminutive plants which accumulate high amounts of soluble sugar and starch compared to WT, as they are compromised in transport of photoassimilate (Hackel et al., 2006; Srivastava et al., 2008). These SUTs localize to companion cells of minor veins, where the first step of phloem loading occurs (Stadler et al., 2005; Schmitt et al., 2008). In addition, these *SUTs* are expressed in the transport phloem, presumably to retrieve Suc that leaks from the phloem or to retrieve Suc from transient reserves.

In addition to roles in phloem transport *SUTs* are expressed throughout the plant where energized Suc uptake is necessary. AtSUC1*,* also belonging to group II is involved in providing photoassimilate to developing pollen and elongating roots, both strong sinks. It is also thought to be involved in signaling in vegetative tissues and male gametophyte functions (Stadler et al., 1999; Sivitz et al., 2008). AtSUC9 (group II) is a high affinity SUT involved in transport of Suc in shoots and flowers. Both *AtSUC9* and *AtSUC1* have regulatory sequence in their introns which controls their expression patterns in different tissues (Sauer et al., 2004; Sivitz et al., 2007). LeSUT1 from group II is involved in phloem loading and accumulation of Suc in certain sink tissues. AtSUC3 belonging to group III is involved in transport of Suc to pollen, wounded tissue and developing seed (Meyer et al., 2000; Meyer et al., 2004). LeSUT2 belonging to group III is

involved in Suc transport to developing sink tissue like pollen (Hackel et al., 2006). NtSUT3 belonging to group III is involved in Suc transport and signaling into pollen tubes (Lemoine et al., 1999). LeSUT4 belonging to group IV is involved in Suc signaling and transport to sink tissues like developing ovaries and fruits (Weise et al., 2000). Apart from sequence, not much is known about group V SUTs.

Our objective was to uncouple the regulation on phloem loading by using a heterologous promoter that is not controlled by endogenous regulation. This strategy may be a useful tool to maintain constant elevated levels of phloem loading and consequently phloem transport (Srivastava et al., 2009). To test phloem-specific *SUT* overexpression as a mechanism to improve carbon partitioning, in a previous study, phloem-specific CoYMV (Commelina Yellow Mottle Virus) promoter was shown to be superior compared to other exotic promoters for expressing *AtSUC2* in homozygous *atsuc2* knockout condition. Compared to *ProrolC:SUC2*, a promoter element from *Agrobacterium rhizogenes*, *ProCoYMV:SUC2* was able to rescue the mutant to up to WT levels (Srivastava et al., 2009). Activity of *ProCoYMV* was compared to *AtSUC2p* and *rolCp* for its activity in different Suc concentrations. *ProCoYMV* activity was enhanced by added Suc while *ProAtSUC2* was repressed (Dasgupta et al., 2014). In addition, representative SUTs from each of the sub-family group were tested for capacity to restore phloem loading and long-distance transport in the *atsuc2-4* mutant. Out of the SUTs tested, only group 2 SUTs, *AtSUC2* and *AtSUC1,* and monocot-specific group I member *ZmSUT1* were able to rescue the deleterious *Atsuc2-4* mutant phenotype and restored phloem transport.

Since these lines could rescue the *atsuc2-4* phenotype, we rationalized that the same expression level in a WT background would have additive impacts on carbon partitioning.

Contrary to our hypothesis, plants overexpressing *AtSUC1, AtSUC2* and *ZmSUT1* were stunted and showed a phosphate starvation response (Dasgupta et al., 2014). Further experimentation showed that phloem loading and transport was enhanced, but the disruption in C/P homeostasis resulted in overall stunting. As Arabidopsis is not a typical model plant for biomass or starch accumulation, we correlated our results here in tobacco. Hence, the most promising construct ProCoYMV:AtSUC2 from our Arabidopsis study (Dasgupta et al., 2014) was transformed into WT tobacco.

2.3 Results

Similar to Arabidopsis, *AtSUC2* overexpressing tobacco showed enhanced Suc loading and transport, accumulated Suc and other carbohydrates in the source leaves, and were stunted compared to the WT (Figure 2.1 A and B). Additive expression of *AtSUC2* in tobacco was confirmed by RT-qPCR. Expression of cDNA from the companion cell specific *ProCoYMV* surpassed that of the endogenous *NtSUT1* in two representative lines Suc2-2-2 and Suc2-3-1 (Figure 2.1 C). To establish that the *ProCoYMV* promoter is functional and phloem-specific in tobacco, qualitative GUS staining assays were performed to show that the enzyme is expressed only in the phloem cells (Figure 2.1 D).

As shown before (Dasgupta et al., 2014), additive *SUT* expression led to reduction in growth of plants overexpressing *AtSUC2* compared to WT tobacco. Figure 2.1 A shows representative WT, uidA, Suc2-2-2 and Suc2-3-1 lines four weeks post germination. Also, shown here is the fresh weight of the sixth leaf from control and transgenic plants (Figure 2.1B). To evaluate if the observed phenotype is associated to carbon partitioning, major transient carbohydrates were quantified at the middle of the day from the sixth fully expanded source

leaf counting up, excluding cotyledons, and with eight total visible leaves. Major soluble carbohydrates Glc, Fru and Suc were significantly enhanced in the transgenic lines compared to WT (Figure 2.2 A). Starch levels were significantly reduced in the ProCoYMV:*AtSUC2* lines compared to WT (Figure 2.2 B). This alteration was not observed in Arabidopsis (Dasgupta et al., 2014). Also, other prominent carbon-containing compounds were also measured to evaluate the overall carbon-status of the plants. Suc2-2-2 lines showed significantly reduced levels of malate (Figure 2.2 C) and fumarate (Figure 2.2 D) compared to control WT and uidA lines. These results correlate with higher levels of carbohydrates and decreased biomass.

Earlier, we proposed that stunting despite increased partitioning was the result of C/P imbalance (Dasgupta et al., 2014). Carbohydrates need to be phosphorylated for utilization in respiration and metabolism. Also, sugars stimulate growth, which has a high demand for phosphate-containing nucleic acids and lipids. Thus, the availability of phosphate determines the plants ability to utilize available carbon. Furthermore, essential genes involved in the photosynthetic machinery and in carbon metabolism were shown to be controlled by inorganic phosphate levels (Paul and Foyer, 2001) .

Based on studies in Arabidopsis (Dasgupta et al., 2014) two models for potential relationships between C and P availability were proposed. In the first, *SUT* overexpression in companion cells of source leaves led to added Suc transport to sink tissues. In regular phosphate levels, there could be inadequate phosphate to phosphorylate carbohydrates or for generating added growth leading to biochemical phosphate deficiency. In the second model, sink organs may recognize a disruption in C/P homeostasis and activate a signaling pathway in preparation for a P starvation. In either case less utilization of available carbon resources in sink

tissues may lead to feedback regulation on the source. Hence, to test if the phosphate levels are altered in the plants overexpressing *ProCoYMV:AtSUC2*, inorganic phosphate levels were measured (Figure 2.2 F). No significant changes in the levels of inorganic phosphate were observed. This indicates that ProCoYMV:AtSUC2 plants may not have a biochemical inorganic phosphate deficiency, and supports the alternative perceived deficiency due to signaling generated by carbon to phosphorous imbalance.

Since, *SUT* overexpression appears to create a C/P imbalance within the plant, we tested if an external C/P imbalance has a similar effect. To test the impact of carbon availability with and without phosphate supplementation on plant growth, and to show that the effects of *SUT* overexpression is tightly linked to the P availability, Arabidopsis *AtSUC1* overexpressing line At-1-4-4, *AtSUC2* line At-2-1-6 and ZmSUT1 line Zm-1-6-8 (Dasgupta et al., 2014) were grown on 0 % Suc/ 0.6mM PO_4 (insufficient phosphate condition), 1 % Suc/0.6mM PO_4 (insufficient phosphate condition), 0 % Suc/ 1.8 mM PO_4 (sufficient phosphate condition) or 1 % Suc/ 1.8 mM PO_4 (sufficient phosphate condition) media. Plants were grown for 2 weeks in the respective media, harvested and fresh weights measured (Figure 2.3). In the absence of Suc or phosphate supplementation, the three overexpression lines are significantly stunted compared to WT. But, with phosphate supplementation (1.8 mM PO_4) or in presence of 1 % Suc and phosphate supplementation (1.8 mM PO_4), the *SUT* overexpressing lines do not show differences compared to WT. Thus, supplement of phosphate is sufficient for the rescue of *SUT* overexpressing lines. Additional carbohydrates are not sufficient to rescue plants in phosphate insufficient conditions.

As high levels of photoassimilates negatively affect photosynthesis rates, photosynthesis was measured using a Li-6400 XT infrared gas analyzer. Rates of CO_2 uptake and H_2O loss determine the stomatal conductance. Therefore, stomatal conductance influences the photosynthetic rates and in turn photosynthetic capacity controls conductance at guard cells, via signaling from mesophyll (von Caemmerer et al., 2004) Dynamic changes in stomatal aperture triggers changes in intercellular CO_2 concentration which impacts CO_2 assimilation capacity of plants (Farquhar and Sharkey, 1982). *ProCoYMV: AtSUC2* showed reduced stomatal conductance measured as moles of H_2O $m^{-2}s^{-1}$ (Figure 2.4A), CO_2 assimilation rate measured as µmol m^{-2} s^{-1} (Figure 2.4B) and intercellular CO_2 concentration measured in µbar (Figure 2.4C) compared to WT plants (Figure 2.4). This signifies that photosynthetic rate is reduced in ProCoYMV:AtSUC2 compared to WT.

To compare phloem loading among *AtSUC2* overexpression lines and wild type, uptake of [^{14}C]-Suc into leaf veins was measured. For this, 5 mm diameter leaf discs were infiltrated with [^{14}C]-Suc solution for 20 min, thoroughly washed, snap frozen in powdered dry ice, and freeze dried to avoid leakage and spread of labeled Suc. Incorporated label was quantified by autoradiography and scintillation counting. The results, represented as cpm (counts per minute) per mm^2, indicate that *AtSUC2* overexpression lines have significantly higher phloem loading compared to wild type (Figure 2.5 A).

To further investigate if *ProCoYMV:AtSuc2* in tobacco leads to increased phloem transport from source to sink tissues and if phloem transport is affected by the additional phosphate, WT, Suc2-2-2 and Suc2-3-1 were germinated on 1 % Suc, transferred to either phosphate deficient media, (0.6 mM) or to phosphate sufficient media, (3.0 mM) and grown for

21 days. Source leaves were photosynthetically labeled with [^{14}C]-CO_2 for 20 min in the middle of the 12 hour light period, excess [^{14}C]-CO_2 was removed and plants were allowed to photosynthesize for another 40 min in ambient air. Then shoots and roots were separated. Roots were further dissected into a 1 cm section from the tip of the root and the remainder of the root to establish where [^{14}C] label accumulates. The Suc2-2-2 and Suc2-3-1 lines retained a lower ratio of label in the shoots compared to WT, indicating higher partitioning of incorporated photoassimilates to roots of *ProCoYMV:AtSUC2* overexpressing plants (Figure 2.5 B). The lowest 1 cm of root, representing the growing tip of the primary root, is where the most growth occurs. An increased ratio of ^{14}C was incorporated in this section of Suc2-2-2 and Suc2-3-1 lines in P insufficient and supplemented P conditions compared to WT (Figure 2.5 C). Also, Suc2-2-2 and Suc2-3-1 lines transported a higher ratio of label to the remaining root section in both phosphate deficient and sufficient conditions, indicating that enhanced phloem transport occurs in the ProCoYMV:AtSUC2 plants compared to WT (Figure 2.4 C). Together, phloem loading and phloem transport experiments indicate that more photoassimilate was getting loaded in the phloem during the labeling period (Figure 2.5). Altogether, experiments done in this study show that *ProCoYMV:AtSUC2* plants have enhanced phloem loading and transport. But, also have higher accumulation of soluble sugars in the source tissues leading to negative feedback on photoassimilate generation. These results are consistent with those in Arabidopsis (Dasgupta et al., 2014)

2.4 Discussion

Understanding how photoassimilate transport is controlled to provide sufficient nutrients to growing tissues or for storage is critical. Enhancing phloem transport could be an

important mean to enhance plant productivity by increasing carbon supply to sink tissues and reducing negative feedback on photoassimilate generation (Ainsworth and Bush, 2011). We hypothesized that overexpressing *SUTs* specifically in the phloem would enhance partitioning and improve growth. In spite of increased phloem loading and transport, unpredicted stunting and soluble carbohydrate accumulation in Arabidopsis (Dasgupta et al., 2014)) and in tobacco was observed (Figure 2.1).Transgenic plants showed ~2 fold expression of *AtSUC2* over *NtSUT1* expression. Stunted plants showed increased accumulation of soluble carbohydrates which probably contributed to decreased photosynthesis (Figure 2.2 and 2.4). Starch levels were significantly reduced compared to controls, possibly due to an unbalanced increase in soluble sugars. To establish that overexpression of companion cell-specific *AtSUC2* led to enhanced phloem loading and transport compared to WT, [^{14}C]-Suc uptake into the veins of leaf disks, which is direct measure of phloem loading, showed that *AtSUC2* overexpression lines had enhanced phloem loading capacity (Figure 2.3). Phloem transport experiments were carried out in phosphate limited and phosphate sufficient conditions. In both conditions transgenic plants accumulated proportionately less [^{14}C] in shoots and more in roots compared to WT, indicating higher partitioning to the roots. In growing tip of root, bottom 1 cm section and remaining root section, ProCoYMV:*AtSUC2* lines showed enhanced phloem un-loading represented by higher ^{14}C accumulation, in phosphate limiting and sufficient conditions. Improved transport to sink organs likely creates a drain on source leaf carbohydrates to limit the accumulation of transient starch in mature leaves. Higher levels of soluble sugars may result from this repression of starch synthesis. If starch synthesis is reduced, but midday photosynthesis exceeds transport ratios, higher soluble sugars would be expected.

In spite of increased phloem loading and transport, plants were debilitated. The role of C/P homeostasis in maintaining health of plants is well known in the literature (Baltscheffsky et al., 1966; Chiou et al., 2006; Karthikeyan et al., 2007; Hammond and White, 2008, 2011). A link between SUTs and phosphate homeostasis was shown in an activation tagging experiments with CaMV 35S enhancers: *AtSUC2* was identified to play a role in causing phosphate limitation and the phenotype could be rescued by providing additional phosphate supplements (Lei et al., 2011). In addition, a phosphate starvation response gene, purple acid phosphatase, was reduced in *pho3* mutants of Arabidopsis. *PHO3* was identified as an allele of *AtSUC2* (Lloyd and Zakhleniuk, 2004). AtSUC2 is involved in phloem loading and carbon partitioning (Srivastava et al., 2008; Srivastava et al., 2009). Previous studies show the importance of carbohydrate partitioning in initiating a P deficiency response (Hammond and White, 2011). In stem girdling experiments, which block phloem transport, expression of phosphate starvation induced (*PSI*) genes was inhibited in white lupin (Zhou et al., 2008). Expression of *PSI* genes was strongly reduced when bean plants were grown in the dark without Suc supply. Sustained expression was achieved when plants were supplied with external Suc (Liu et al., 2010). Enhanced biosynthesis of Suc has been observed in Arabidopsis, spinach and soybean grown in P starved condition (Hammond and White, 2008). The importance of Suc partitioning in these studies is logical because P-starvation leads to lateral root growth, alterations in gene expression and altered metabolic flux, all of which have higher photoassimilate demand. One prior study indicated a role of increased Suc transport in inducing a P-deficiency response. *Hypersensitive to phosphate starvation1 (hps1)* was shown to be hypersensitive to phosphate deficiency in

activation-tagging screens. This mutant was shown to be overexpression allele of *AtSUC2* (Lei et al., 2011).

For efficient metabolism, enhanced production of carbohydrates, as well as better conversion into usable form of energy is required. When cellular respiration is constrained due to a lack of phosphate, primary sugars tend to accumulate within the source tissues. The stunted growth could be due to lack of sufficient energy (Lei et al., 2011). Surprisingly, the levels of free phosphate were not significantly affected in ProCoYMV:AtSUC2 plants compared to WT, indicating that there was not a biochemical deficiency. Rather, a signaling pathway between C/P may be inadequate to co-ordinate higher transport rates and metabolic requirements of P. Thus, a PSI response is activated in response to a perceived disruption in C/P balance. A model for possible disruption of C-P homeostasis in plants was proposed earlier (Dasgupta et al., 2014).

In the work presented here, the endogenous expression of *SUTs* in tobacco was not altered but phloem-specific expression of *AtSUC2* still led to phosphate limited phenotype. Here, we show that *AtSUC2* overexpressing tobacco plants show a significantly stunted phenotype compared to WT in phosphate limiting conditions. Stunting is rescued to 70-95 % of WT in phosphate sufficient conditions, indicating that phosphate is necessary for phenotype rescue of *ProCoYMV:AtSUC2* expressing Arabidopsis lines (Figure 2.3). Hence, the phenomenon observed in Arabidopsis is not limited to a single plant, but may be widely observed. Our findings with *SUT* overexpression are distinct from earlier work. Earlier work showed that more carbohydrates are needed to mount a response to phosphate deficiency, but our work shows that excess C may “trick” the plant into thinking it has a deficiency.

2.5 Material and Methods

2.5.1 Plasmid Constructions and Plant Transformation

For tobacco transformation, explants were cut from internodal stem and leaf sections of *Nicotiana tabacum L.*cv. Petit Havana from young greenhouse grown plants. Tissues were surface sterilized in 5 % domestic bleach with 0.01 % Silwett and washed four times with sterile H_2O. Stem disks of 2-3 mm thickness were cut and leaf explants were damaged with a sterile scalpel blade. These tissues were placed on callus induction medium (CIM) containing 1X MS (Murashige and Skoog) plus Gambourg vitamins, 2.4 g/L gelrite, Suc 20 g/L, pH 5.7, 6-Benzylaminopurine (BAP) 1mg/L (Phytotechnology Laboratories, Shawnee Mission, KS) and α-Naphthaleneacetic acid (NAA) 0.1 mg/L (Phytotechnology Laboratories). pGPTV:ProCoYMV:AtSUC2 (Dasgupta et al., 2014), and pGPTV:ProCoYMV:uidA were electroporated into *Agrobacterium tumefaciens* strain GV3101 *mp90* as described before (Dasgupta et al., 2014). Freshly grown overnight culture of Agrobacterium was diluted 1:10 with sterile MS pH 5.4. Explants were incubated with Agrobacterium in MS liquid medium at room temperature for 15 min with occasional stirring. Explants were washed with sterile MS and blot dried. Explants were placed on CIM co-cultivation medium in the dark for three days. Explants were washed in MS containing 400 mg/L Timentin (Phytotechnology Laboratories) to wash out excess Agrobacterium. Tissues were transferred to CIM containing Phosphinothricin and Timentin (Phytotechnology Laboratories) and grown for four weeks. Once callus growth was evident, tissues were transferred to shoot induction medium (SIM) which contains 1X MS, 2.4 g/L gelrite, Suc 20 g/L, pH 5.7,Gibberelic acid (GA) 20 mg/L (Phytotechnology Laboratories) and BAP 20 mg/L and 40 mg/L DL-Phosphinothricin (Phytotechnology Laboratories). After 4 weeks,

when shoots were visible, they were transferred to root induction medium (RIM). RIM contained 1X MS, 2.4 g/L gelrite, Suc 20 g/L, pH 5.7, zeatin riboside (Phytotechnology Laboratories) 1 mg/L and NAA 0.1 mg/L and 40 mg/L DL-Phosphinothricin (Protocol adapted and modified from (Beaujean et al., 1998; Park et al., 2005). After 4 weeks, plantlets were transferred to soil and grown to seed. T1 generation was selected on 40 mg/L DL-Phosphinothricin, healthy green seedlings were transferred to 6 inch pots, one week later plants were sprayed with 20mg/L glufosinate ammonia (Finale, Farnam Companies, Phoenix, AZ) , allowed to self-pollinate and T2 seeds were collected. Homozygous lines were identified based on 100 % resistance to glufosinate ammonia in the T3 generation. T3 seeds of two transgenic lines were used for all further experiments, which were Suc2-3-1-and Suc2-2-2.

2.5.2 Plant Material

For soil grown plants, 4-6 seeds were sown on 6 inch pot and post-germination, a single plant was retained per pot. Plants were transferred to a growth chamber (Percival AR95L, Percival Scientific, Perry IA) in 12 hours light at 22°C and 12 hours dark at 18°C, 180 µmol photons m^{-2} s^{-1}. Plants were photographed at emergence of sixth leaf stage. Sixth-eighth leaves of control and transgenic plants were harvested in the middle of the day, fresh weight was determined, and leaves were placed in aluminum foil envelopes and frozen in liquid N_2. Tissues were stored at -80 °C until further processing. For cryogenic grinding, tissues were transferred to pre-cooled 15 ml polycarbonate vials (OPS Diagnostics, Lebanon NJ) precooled in liquid N_2, each containing three 5 mm stainless steel grinding balls. Lined screw caps of vials were also pre-chilled during this process. Tissues were ground in a 2010 Geno Grinder (SPEX SamplePrep, Metuchen, NJ) at 1200 strokes / minute for 20 seconds. 18-20 mg aliquots were made for

carbohydrate determination and 100 mg for RNA extraction and gene expression analysis. For plants grown on solid media, plants were grown on 0.5 MS for phosphate deficiency (contains 0.6 mM PO_4) and 0.5 MS supplemented with an addition of 1.2 mM phosphate (1.8 mM PO_4 final) for sufficient conditions. Plants were harvested after growing for 15 days.

2.5.3 Transcript Analysis

Total RNA was isolated from the 100 mg of sixth leaf tissue of T3 plants and controls using Trizol (Life Technologies) according to manufacturer's instructions and further treated with RNAase free DNase-I (Life Technologies). The quantity of RNA was estimated by spectrophotometry. 600 ng of RNA in 10 µl H_2O was reverse transcribed with Superscript III reverse transcriptase and 50 µM oligo (dT) (Life Technologies) according to the manufacturer's instructions. Gene specific primers used for the real-time quantitative PCR (RT-qPCR) are listed in Table: 2.I. RT-qPCR was carried out with SybrGreen PCR Master Mix (Sigma-Aldrich, St. Louis, MO) on an Applied Biosystems ViiA 7 (Life Technologies) using the following protocol: 10 min denaturation at 95 °C followed by 40 cycles of 95 °C for 10 s, 58 °C for 30 s, and 72 °C for 30 s. A melting curve was obtained at the end of the program to confirm a single PCR product. The levels of genomic *NtSUT1* and *AtSUC2* cDNA expression were normalized to that of *NtEF1α* (AF120093.1). Three biological and three technical replicates were used for these measurements. GUS staining was performed with eighth leaf of WT and ProCoYMV:uidA line using 3 mM potassium ferrocyanide and ferricyanide to restrict diffusion of GUS reaction products (Ayre and Turgeon, 2004)

2.5.4 Photosynthesis Measurement

Photosynthesis per unit surface area was measured on greenhouse grown plants with a Li-6400XT infra-red gas analyzer (IRGA) with LED Light source 6400-02B (red / blue). The seventh-eighth leaves of each plant were clamped and allowed to acclimate for 120 s in the chamber before taking measurements. Gas exchange measurements were determined with 400 µmol mol^{-1} of CO_2, RH 60 %, 23°C temperature, a gas flow rate of 400 µmol s^{-1} and photosynthetically active radiation (PAR) of 240 µmol $m^{-1}s^{-1}$. The acclimatization time was determined empirically. Two measurements were taken per plant in 30 s intervals, and combined for data analysis.

2.5.5 Metabolite Analysis

The major transient soluble carbohydrates were extracted with 80 % ethanol or tri-chloroacetic acid (Gibon et al., 2002) and quantified enzymatically (Stitt et al., 1989) using a Synergy H Reader (Bio Tek, USA). Starch was measured enzymatically from the insoluble material after ethanolic extraction of soluble carbohydrates (Hendriks et al., 2003). Total protein was measured using the Bradford Assay (Bradford, 1976). Malate and fumarate were also determined by standard protocol (Cross et al., 2006). Inorganic phosphate was measured using an ammonium molybdate assay (Chiou et al., 2006).

2.5.6 Phloem Loading in Leaf Discs with [^{14}C]-Suc Labeling

To test for phloem loading capacity of transgenic and control plants [^{14}C]-Suc uptake studies were conducted. The eighth leaf of WT, Suc2-2-2 and Suc2-3-1 were harvested, leaves were submerged in MES [2(*N*-morpholino) ethane-sulfonic acid] buffer (20 mM MES, 2 mM $CaCl_2$, pH 5.5 with KOH) and leaf discs were derived with a cork borer of 5 mm diameter. Once

all leaf discs were collected, previous solutions were replaced with [^{14}C]-Suc (1 mM Suc, 0.81 µCi ml^{-1}) (MP Biomedicals, Solon, OH) in MES buffer. Discs were held down with 4 mm glass beads in a 24-well microtiter plate. Each replicate contained 6 leaf discs from one biological replicate and 6 biological replicates were used for one genotype. The leaf discs were vacuum infiltrated to allow for absorption of labeled solution and incubated at room temperature for 20 min. Excess solution was removed, followed by three washes in MES buffer. The leaf discs were gently blotted dry, placed in aluminum foil envelopes and placed in powdered dry ice. Frozen discs were lyophilized in -30 °C for 48 hour, pressed between steel plates in vice clamps and exposed to X-ray film (Kodak Biomax MR Film, Rochester NY) for 24 hour. The leaf discs were cleared with 1 ml 95 % ethanol for 30 min, and then bleached with commercial bleach for 15 min. Counts were measured after adding scintillation fluid and [^{14}C]-Suc uptake calculated as cpm per surface area.

2.5.7 Radiolabeling with [^{14}C]-CO_2 to Measure Rates of Phloem Transport

Transgenic and control plants were germinated on 0.5 MS with 1 % Suc and transferred to 0 % Suc plates to grow vertically for 16 days. Plants were labeled with [^{14}C]-CO_2 which was generated by acidification of 5 µl (5 µCi, 0.185 MBq) of [^{14}C]-HCO_3 (MP Biomedicals) by using 15 µl of lactic acid. Plants were allowed to photosynthesize for 20 min. Excess of [^{14}C]-CO_2 was removed by an air pump connected to soda lime. Plants were allowed to photosynthesize for another 40 min in normal air. Shoots and roots were separated and put in scintillation vials containing 500 µl household bleach. After pigments were removed, 5 ml ScintiSafe Plus 50 % (Phenylxylylethane) scintillation solution (Thermo Fisher Scientific) was added and cpm determined in a scintillation counter. For experiments with roots, roots were divided as 1 cm

from the tip of the root and remainder of the root. Roots from two plants were pooled for analysis. Counts were normalized as ratio of label in shoots, 1 cm terminal root and remainder of the root, compared to total incorporation (Figure 2.5 E).

Table 2-1: Primers used for cloning and qPCR.

Tobacco	Forward	Reverse
Actin	CCTGAGGTCCTTTTCCAACCA	GGATTCCGGCAGCTTCCATT
Elongation factor 1a	TGAGATGCACCACGAAGCTC	CCAACATTGTCACCAGGAAGTG
Ubiquitin-conjugating enzyme E2 (Ntubc2)	CTGGACAGCAGACTGACATC	CAGGATAATTTGCTGTAACAGATTA
Protein phosphatase 2A (PP2A)	GTGAAGCTGTAGGGCCTGAGC	CATAGGCAGGCACCAAATCC
Transgene Specific primers (ProCoYMV:AtSUC2)		
NtSUT1-L (Sameeullah et al., 2013)	CGTCTTCCTTCTACTCAGCTTAACAATCT	CCAAAAACTCCACACTTAGCGACATA

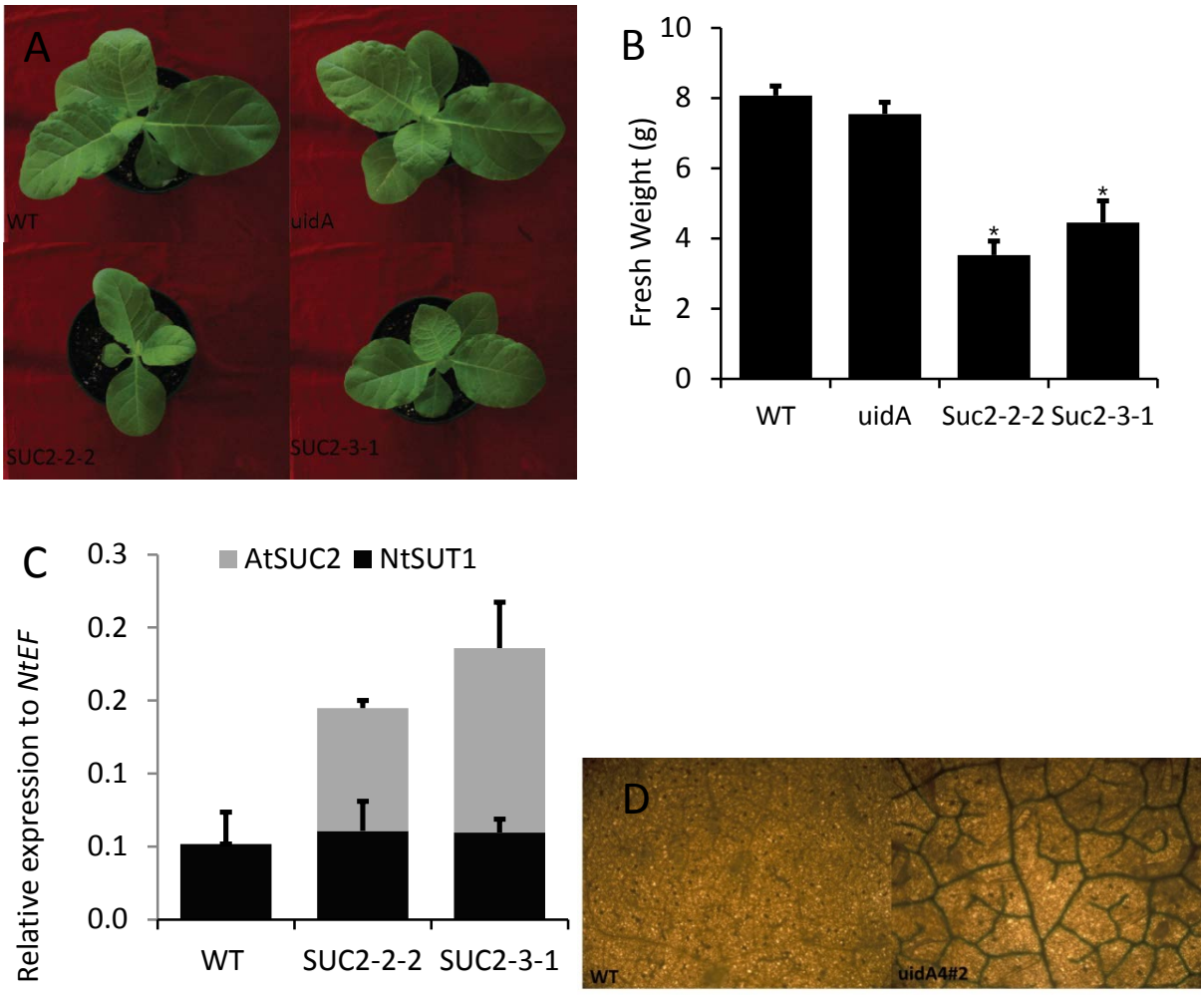

Figure 2-1: Growth characteristics of wild type (WT), *uidA* and ProCoYMV:AtSUC2 lines Suc2-2-2 and Suc2-3-1. **A**, Representative 28-d-old WT, ProCoYMV:SUC2-2-2 and ProCoYMV:SUC2-3-1 lines. For scale, the round pots are 6 inch. **B**, Fresh weights of 6th leaf of tobacco plants.Variation is expressed as SE; n = 6. **C**, RT-qPCR results of WT, Suc2-2-2 and Suc2-3-1 compared to *Nicotiana tabacum Elongation factor-1α* (*NtEF1α*), black bars: phloem localized endogenous Suc transporter *NtSUT1*, grey bars: *AtSUC2*. **D**, XGlcA staining in the source leaves of, left: WT and Right: ProCoYMV:uidA-4#2. Significant differences from WT are based on Student's T-Test: *, P ≤ 0.05; **, P ≤ 0.01; ***, P ≤ 0.001.

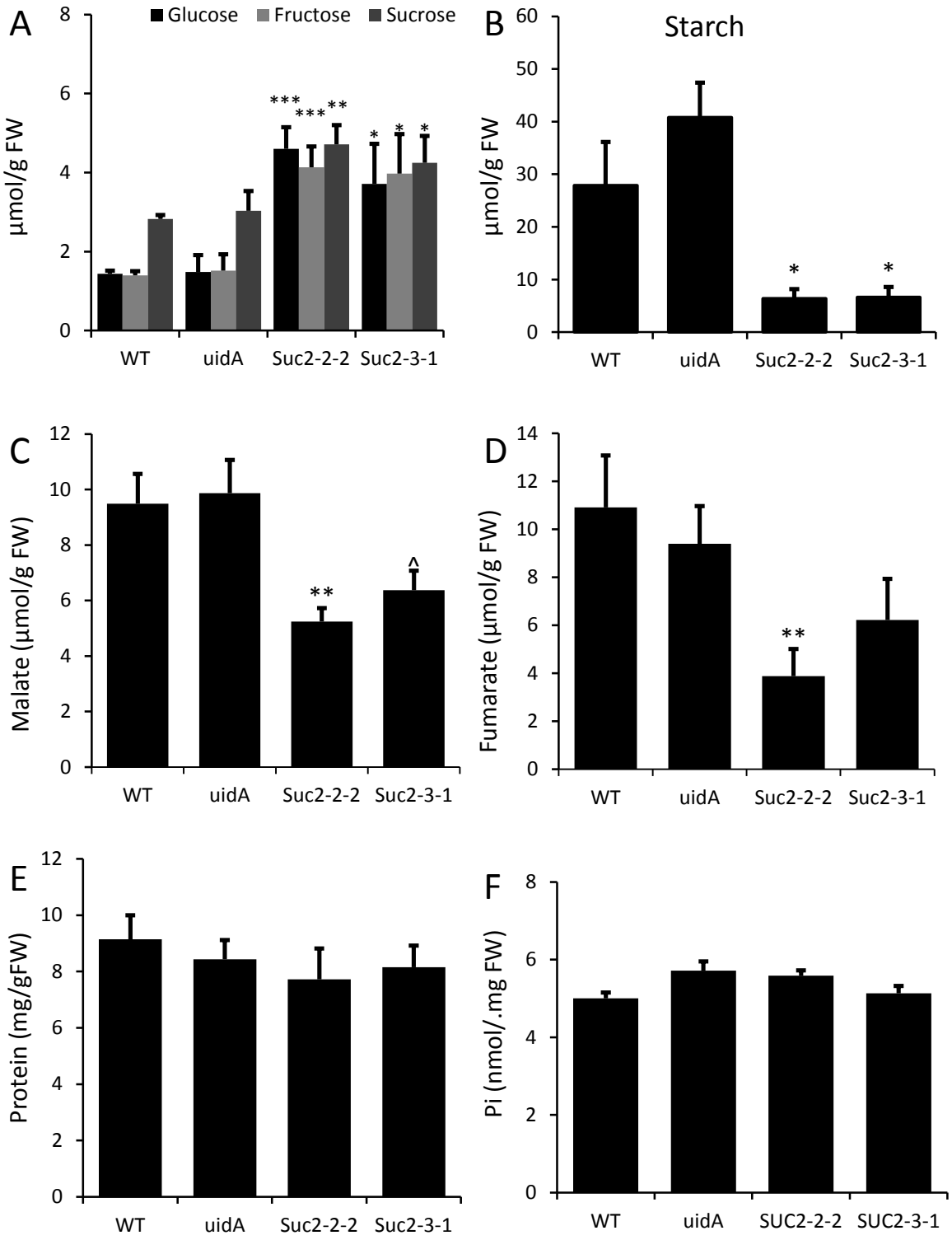

Figure 2-2: Metabolic analysis of WT, *uidA* and ProCoYMV:AtSUC2 lines Suc2-2-2 and Suc2-3-1. Metabolites extracted from sixth matured leaf. **A**, Principal soluble sugars:Glc, Fru and Suc. **B**, starch; **C**,malate; **D**, fumarate; expressed as µmol/g fw; **E**, total protein; **F**, inorganic phosphate; expressed as mg/g fw. Variation is SE; n=6. Significant differences from WT are based on Student's T-Test: ^, P ≤0.1 ;*, P ≤ 0.05; **, P ≤ 0.01; ***, P ≤ 0.001.

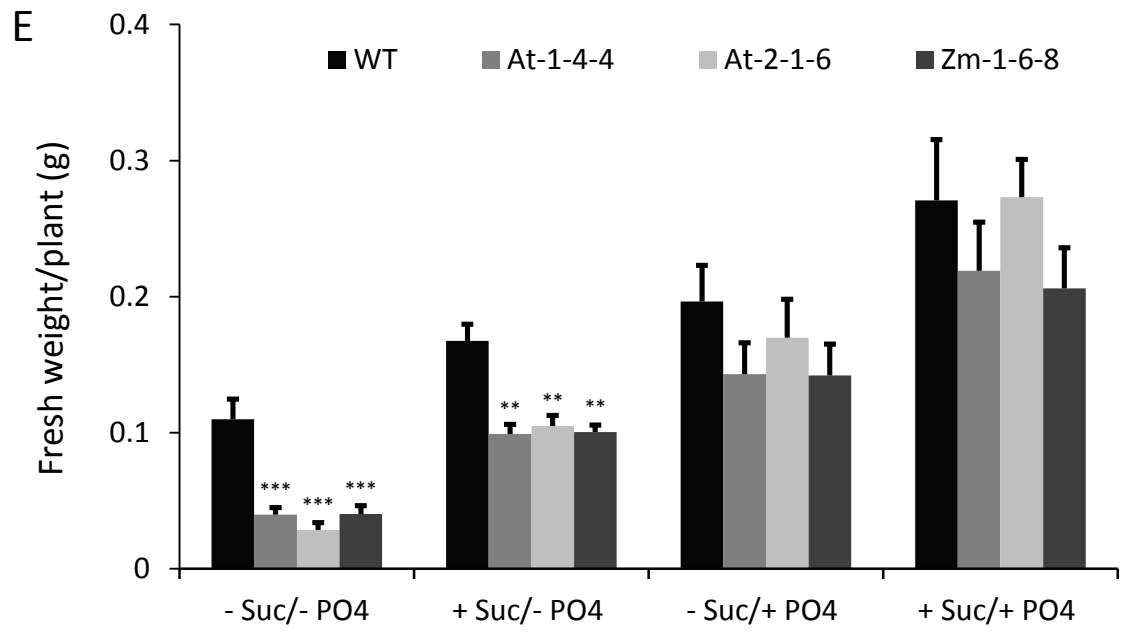

Figure 2-3: Effect of external C/P imbalance on the Arabidopsis *SUT* over-expressing lines. Arabidopsis WT, At-1-4-4, At-2-1-6 and Zm-1-6-8 lines grown in –Suc/-PO_4 (0 % Suc/0.6 mM PO_4), +Suc/- PO_4 (1 % Suc/0.6 mM PO_4),-Suc/+PO_4 (0 % Suc/1.8 mM mM PO_4), +Suc/+PO_4 (0 1 % Suc/1.8 mM mM PO_4) conditions. Variation is expressed as SE; n = 6, plants were at 15 dpg at the time of harvest. Significant differences from WT are based on Student's T-Test: *, P ≤ 0.05; **, P ≤ 0.01; ***, P ≤ 0.001.

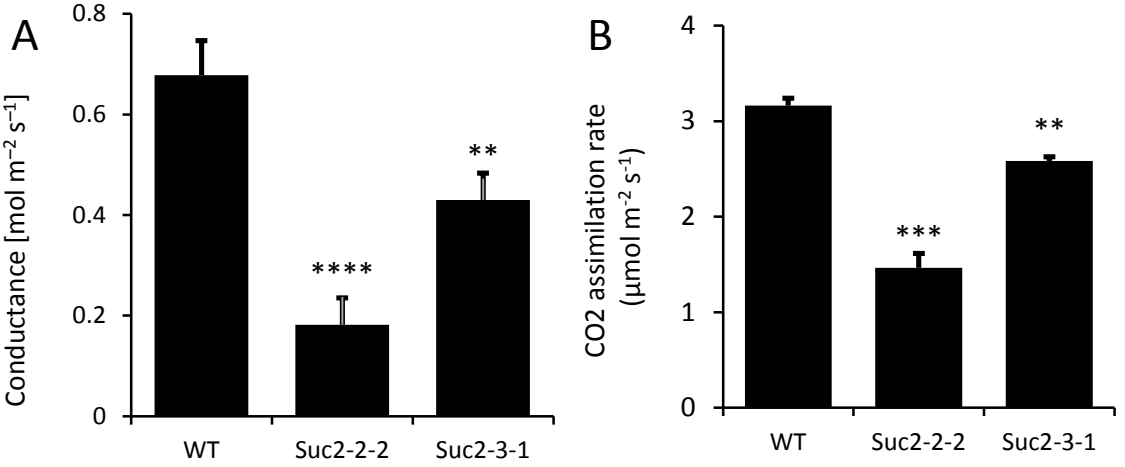

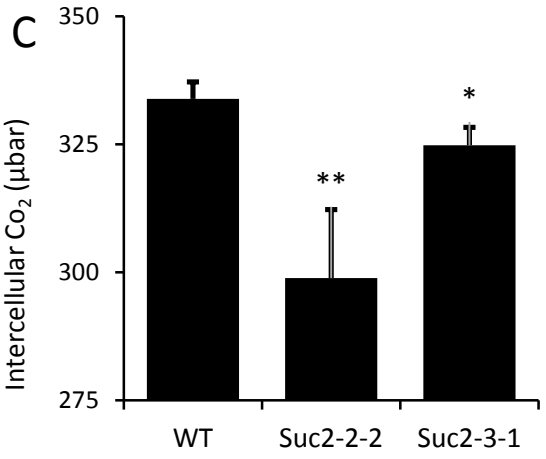

Figure 2-4: Photosynthesis is significantly reduced in *SUT* over-expression lines compared to WT. **A,** Conductance measured as mol m^{-2} s^{-1}, **B,** CO_2 assimilation rate measured as µmole m^{-2} S^{-1} and **C**, Intercellular CO_2 measured as µbar measured by LiCor Li6400-XT IRGA. All measurements show significant differences compared to WT, n=12 plants for each line. Significant differences from WT are based on Student's T-Test: *, P ≤ 0.05; **, P ≤ 0.01; ***, P ≤ 0.001.

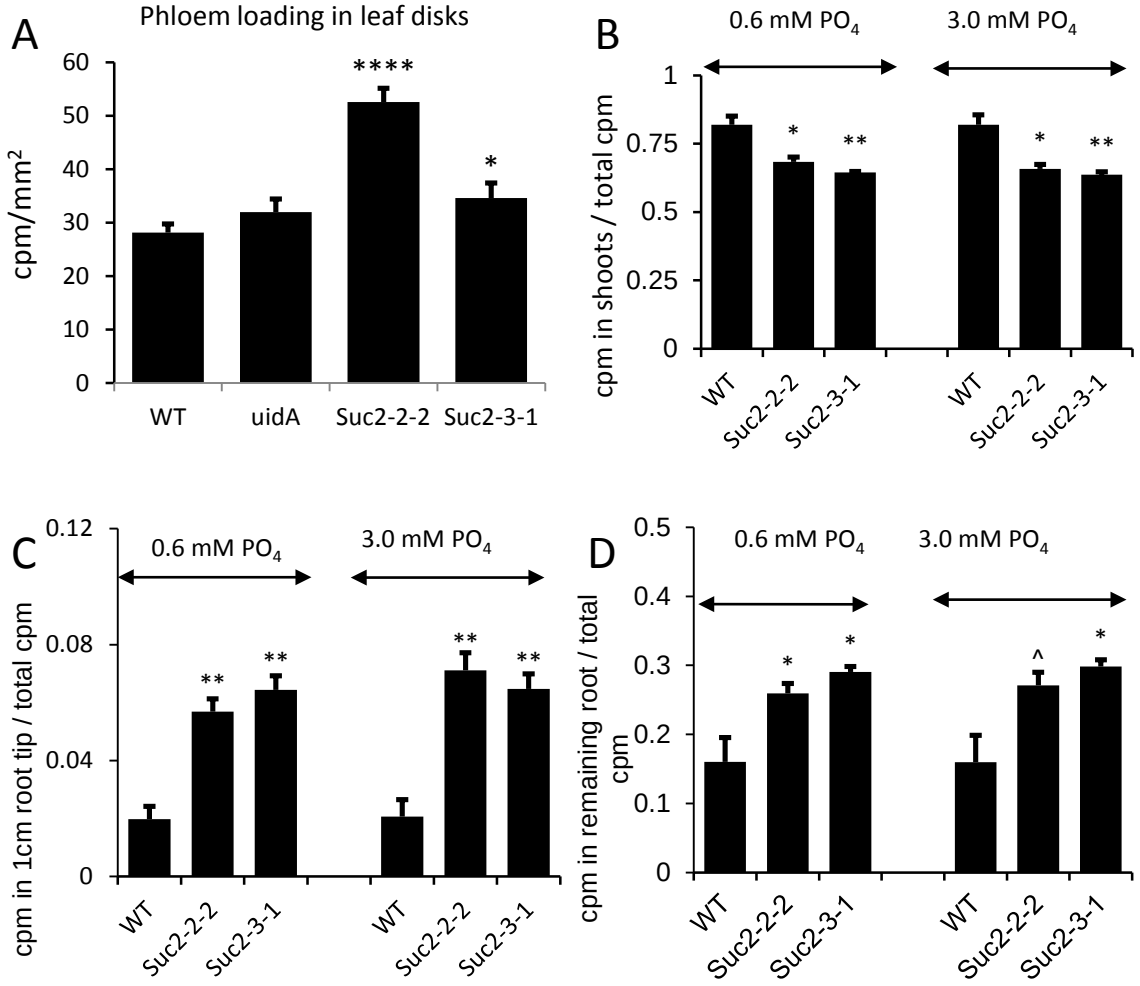

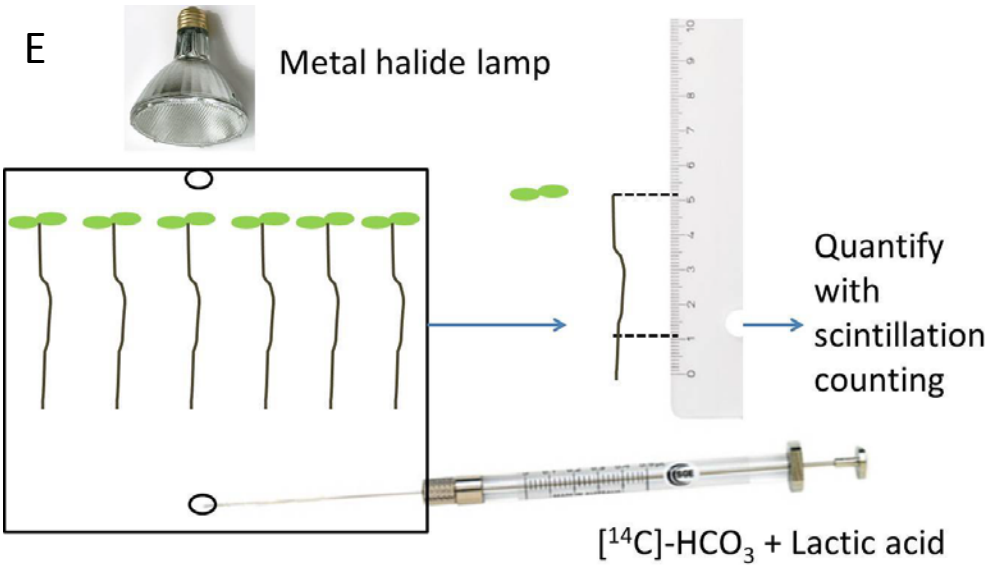

Figure 2-5: Phloem loading, phloem transport measurements of WT and ProCoYMV:AtSUC2 lines. **A**, Uptake of [^{14}C]-Suc into the leaf disks of WT and transgenic lines; expressed as cpm per mm^2 of leaf disc area. Variation is SE; n = 8, each containing three randomly pooled leaf discs (Suc2-3-1 is significant compared to WT only). Phloem-specific overexpression of *AtSUC2* enhances phloem transport determined by photosynthetic labeling with [^{14}C]-CO_2 for 20 min followed by 40 min chase in normal air. **B**, Represented as ratio of total cpm in shoots of ProCoYMV:SUC2 lines, compared to WT, in phosphate deficient (0.6 mM PO_4) and phosphate supplemented media (3.0 mM PO_4); **C**, Ratio of total cpm in 1 cm root section consisting of the lowest 1 cm; **D**, Ratio of total label in the remainder of the root. **E**, Method of radiolabeling with [^{14}C]-CO_2. Once germinated, plants are transferred to square plates and grown vertically for 15 days. Plants were labeled with [^{14}C]-CO_2, which is generated spontaneously by reacting [^{14}C]-HCO_3 and lactic acid. Plants were allowed to photosynthesize for 20 min, excess gas was removed and allowed to photosynthesize for another 40 min in normal air. Shoots, 1 cm terminal root sections, and remainder of the roots were separated and incorporated label quantified by scintillation counting. Averages and standard error, n=12. Significant differences are based on Student's T-Test: *, $P \leq 0.05$; **, $P \leq 0.01$; ***, $P \leq 0.001$.

2.6 Chapter References

Ainsworth EA, Bush DR (2011) Carbohydrate export from the leaf: a highly regulated process and target to enhance photosynthesis and productivity. Plant Physiology 155: 64-69

Ayre BG, Turgeon R (2004) Graft transmission of a floral stimulant derived from CONSTANS. Plant Physiology 135: 2271-2278

Baltscheffsky H, Von Stedingk LV, Heldt HW, Klingenberg M (1966) Inorganic pyrophosphate: formation in bacterial photophosphorylation. Science 153: 1120-1122

Beaujean A, Sangwan RS, Lecardonnel A, Sangwan-Norreel BS (1998) Agrobacterium-mediated transformation of three economically important potato cultivars using sliced internodal explants: an efficient protocol of transformation. Journal of Experimental Botany 49: 1589-1595

Bradford MM (1976) A rapid and sensitive method for the quantitation of microgram quantities of protein utilizing the principle of protein-dye binding. Analytical Biochemistry 72: 248-254

Braun DM, Slewinski TL (2009) Genetic control of carbon partitioning in grasses: roles of sucrose transporters and tie-dyed loci in phloem loading. Plant Physiology 149: 71-81

Carpaneto A, Geiger D, Bamberg E, Sauer N, Fromm J, Hedrich R (2005) Phloem-localized, proton-coupled sucrose carrier ZmSUT1 mediates sucrose efflux under the control of the sucrose gradient and the proton motive force. The Journal of Biological Chemistry 280: 21437-21443

Chiou TJ, Aung K, Lin SI, Wu CC, Chiang SF, Su CL (2006) Regulation of phosphate homeostasis by MicroRNA in Arabidopsis. The Plant Cell 18: 412-421

Cross JM, von Korff M, Altmann T, Bartzetko L, Sulpice R, Gibon Y, Palacios N, Stitt M (2006) Variation of enzyme activities and metabolite levels in 24 Arabidopsis accessions growing in carbon-limited conditions. Plant Physiology 142: 1574-1588

Dasgupta K, Khadilkar A, Sulpice R, Pant B, Scheible WR, Fisahn J, Stitt M, Ayre BG (2014) Expression of sucrose transporter cDNAs specifically in companion cells enhances phloem loading and long-distance transport of sucrose, but leads to an inhibition of growth and the perception of a phosphate limitation. Plant Physiology 165: 715–731

Farquhar GD, Sharkey TD (1982) Stomatal conductance and photosynthesis. Annual Review of Plant Physiology 33: 317-345

Gibon Y, Vigeolas H, Tiessen A, Geigenberger P, Stitt M (2002) Sensitive and high throughput metabolite assays for inorganic pyrophosphate, ADPGlc, nucleotide phosphates, and glycolytic intermediates based on a novel enzymic cycling system. The Plant Journal 30: 221-235

Gottwald JR, Krysan PJ, Young JC, Evert RF, Sussman MR (2000) Genetic evidence for the in planta role of phloem-specific plasma membrane sucrose transporters. Proceedings of the National Academy of Sciences of the United States of America 97: 13979-13984

Hackel A, Schauer N, Carrari F, Fernie AR, Grimm B, Kuhn C (2006) Sucrose transporter LeSUT1 and LeSUT2 inhibition affects tomato fruit development in different ways. The Plant Journal 45: 180-192

Hammond JP, White PJ (2008) Sucrose transport in the phloem: integrating root responses to phosphorus starvation. Journal of Experimental Botony 59: 93-109

Hammond JP, White PJ (2011) Sugar signaling in root responses to low phosphorus availability. Plant Physiology 156: 1033-1040

Hendriks JH, Kolbe A, Gibon Y, Stitt M, Geigenberger P (2003) ADP-glucose pyrophosphorylase is activated by posttranslational redox-modification in response to light and to sugars in leaves of Arabidopsis and other plant species. Plant Physiology 133: 838-849

Karthikeyan AS, Varadarajan DK, Jain A, Held MA, Carpita NC, Raghothama KG (2007) Phosphate starvation responses are mediated by sugar signaling in Arabidopsis. Planta 225: 907-918

Lalonde S, Tegeder M, Throne-Holst M, Frommer WB, Patrick JW (2003) Phloem loading and unloading of sugars and amino acids. Plant, Cell & Environment 26: 37-56

Lalonde S, Wipf D, Frommer WB (2004) Transport mechanisms for organic forms of carbon and nitrogen between source and sink. Annual Review of Plant Biology 55: 341-372

Leggewie G, Kolbe A, Lemoine R, Roessner U, Lytovchenko A, Zuther E, Kehr J, Frommer WB, Riesmeier JW, Willmitzer L, Fernie AR (2003) Overexpression of the sucrose transporter *SoSUT1* in potato results in alterations in leaf carbon partitioning and in tuber metabolism but has little impact on tuber morphology. Planta 217: 158-167

Lei M, Liu Y, Zhang B, Zhao Y, Wang X, Zhou Y, Raghothama KG, Liu D (2011) Genetic and genomic evidence that sucrose is a global regulator of plant responses to phosphate starvation in Arabidopsis. Plant Physiology 156: 1116-1130

Lemoine R, Burkle L, Barker L, Sakr S, Kuhn C, Regnacq M, Gaillard C, Delrot S, Frommer WB (1999) Identification of a pollen-specific sucrose transporter-like protein NtSUT3 from tobacco. FEBS Letters 454: 325-330

Liu JQ, Allan DL, Vance CP (2010) Systemic signaling and local sensing of phosphate in common bean: cross-talk between photosynthate and microRNA399. Molecular Plant 3: 428-437

Lloyd JC, Zakhleniuk OV (2004) Responses of primary and secondary metabolism to sugar accumulation revealed by microarray expression analysis of the Arabidopsis mutant, *pho3*. Journal of Eperimental Botany 55: 1221-1230

Meyer S, Lauterbach C, Niedermeier M, Barth I, Sjolund RD, Sauer N (2004) Wounding enhances expression of *AtSUC3*, a sucrose transporter from Arabidopsis sieve elements and sink tissues. Plant Physiology 134: 684-693

Meyer S, Melzer M, Truernit E, Hummer C, Besenbeck R, Stadler R, Sauer N (2000) *AtSUC3*, a gene encoding a new Arabidopsis sucrose transporter, is expressed in cells adjacent to the vascular tissue and in a carpel cell layer. The Plant Journal 24: 869-882

Park S, Kang T-S, Kim C-K, Han J-S, Kim S, Smith RH, Pike LM, Hirschi KD (2005) Genetic manipulation for enhancing calcium content in potato tuber. Journal of Agricultural and Food Chemistry 53: 5598-5603

Paul MJ, Foyer CH (2001) Sink regulation of photosynthesis. Journal of Experimental Botany 52: 1383-1400

Rosche E, Blackmore D, Tegeder M, Richardson T, Schroeder H, Higgins TJ, Frommer WB, Offler CE, Patrick JW (2002) Seed-specific overexpression of a potato sucrose transporter increases sucrose uptake and growth rates of developing pea cotyledons. The Plant Journal 30: 165-175

Sameeullah M, Sasaki T, Yamamoto Y (2013) Sucrose transporter NtSUT1 confers aluminum tolerance on cultured cells of tobacco (*Nicotiana tabacum* L.). Soil Science and Plant Nutrition 59: 756-770

Sauer N (2007) Molecular physiology of higher plant sucrose transporters. FEBS Letters 581: 2309-2317

Sauer N, Ludwig A, Knoblauch A, Rothe P, Gahrtz M, Klebl F (2004) *AtSUC8* and *AtSUC9* encode functional sucrose transporters, but the closely related *AtSUC6* and *AtSUC7* genes encode aberrant proteins in different Arabidopsis ecotypes. The Plant Journal 40: 120-130

Schmitt B, Stadler R, Sauer N (2008) Immunolocalization of solanaceous SUT1 proteins in companion cells and xylem parenchyma: new perspectives for phloem loading and transport. Plant Physiology 148: 187-199

Sivitz AB, Reinders A, Johnson ME, Krentz AD, Grof CP, Perroux JM, Ward JM (2007) Arabidopsis sucrose transporter AtSUC9. High-affinity transport activity, intragenic control of expression, and early flowering mutant phenotype. Plant Physiology 143: 188-198

Sivitz AB, Reinders A, Ward JM (2008) Arabidopsis sucrose transporter AtSUC1 is important for pollen germination and sucrose-induced anthocyanin accumulation. Plant Physiology 147: 92-100

Slewinski T, Braun DM (2010) Current perspectives on the regulation of whole-plant carbohydrate partitioning. Plant Science 178: 341-349

Srivastava AC, Dasgupta K, Ajieren E, Costilla G, McGarry RC, Ayre BG (2009) Arabidopsis plants harbouring a mutation in *AtSUC2*, encoding the predominant sucrose/proton symporter necessary for efficient phloem transport, are able to complete their life cycle and produce viable seed. Annals of Botony 104: 1121-1128

Srivastava AC, Ganesan S, Ismail IO, Ayre BG (2008) Functional characterization of the Arabidopsis AtSUC2 Sucrose/H^+ symporter by tissue-specific complementation reveals an essential role in phloem loading but not in long-distance transport. Plant Physiology 148: 200-211

Srivastava AC, Ganesan S, Ismail IO, Ayre BG (2009) Effective carbon partitioning driven by exotic phloem-specific regulatory elements fused to the *Arabidopsis thaliana AtSUC2* sucrose-proton symporter gene. BMC Plant Biology 9: 7

Stadler R, Truernit E, Gahrtz M, Sauer N (1999) The AtSUC1 sucrose carrier may represent the osmotic driving force for anther dehiscence and pollen tube growth in Arabidopsis. The Plant Journal 19: 269-278

Stadler R, Wright KM, Lauterbach C, Amon G, Gahrtz M, Feuerstein A, Oparka KJ, Sauer N (2005) Expression of GFP-fusions in Arabidopsis companion cells reveals non-specific protein trafficking into sieve elements and identifies a novel post-phloem domain in roots. The Plant Journal 41: 319-331

Stitt M, Lilley RM, Gerhardt R, Heldt HW (1989) Metabolite levels in specific cells and subcellular compartments of plant-leaves. Methods in Enzymology 174: 518-552

Truernit E, Sauer N (1995) The promoter of the *Arabidopsis thaliana SUC2 sucrose-H^+ symporter* gene directs expression of beta-glucuronidase to the phloem: evidence for phloem loading and unloading by SUC2. Planta 196: 564-570

von Caemmerer S, Lawson T, Oxborough K, Baker NR, Andrews TJ, Raines CA (2004) Stomatal conductance does not correlate with photosynthetic capacity in transgenic tobacco with reduced amounts of Rubisco. Journal of Experimental Botany 55: 1157-1166

Weichert N, Saalbach I, Weichert H, Kohl S, Erban A, Kopka J, Hause B, Varshney A, Sreenivasulu N, Strickert M, Kumlehn J, Weschke W, Weber H (2010) Increasing sucrose uptake capacity of wheat grains stimulates storage protein synthesis. Plant Physiology 152: 698-710

Weise A, Barker L, Kuhn C, Lalonde S, Buschmann H, Frommer WB, Ward JM (2000) A new subfamily of sucrose transporters, SUT4, with low affinity/high capacity localized in enucleate sieve elements of plants. The Plant Cell 12: 1345-1355

Weise A, Lalonde S, Kuhn C, Frommer WB, Ward JM (2008) Introns control expression of sucrose transporter *LeSUT1* in trichomes, companion cells and in guard cells. Plant Molecular Biology 68: 251-262

Zhou K, Yamagishi M, Osaki M, Masuda K (2008) Sugar signalling mediates cluster root formation and phosphorus starvation-induced gene expression in white lupin. Journal of Experimental Botany 59: 2749-2756

CHAPTER 3

OVEREXPRESSION OF *AVP1* IN THE PHLOEM ENHANCES PLANT GROWTH

3.1 Abstract

In Arabidopsis, *AVP1* encodes for a type-I proton pumping (H^+)-pyrophosphatase (PPase). The "textbook" function of H^+-PPase is to localize to the tonoplast and contribute to vacuolar PMF by capturing the energy liberated by hydrolysis of PP_i. Previous studies showed that plants overexpressing *AVP1* accumulate higher biomass, have better nutrient acquisition capacity and are better able to cope under several abiotic stress conditions. The hypothesis being tested here is that type-I H^+-PPase localizes to the companion cell PM and functions as a PPi synthase driven by apoplasmic PMF, rather than a hydrolase contributing to tonoplast PMF. By synthesizing PPi, metabolism is pushed in the direction of Suc oxidation and ATP synthesis, which in turn, via the PM ATPase, strengthens phloem PMF to energize phloem loading and transport. In this study, plants overexpressing *AVP1* with a constitutive promoter and with a phloem companion-cell specific promoter were generated and analyzed. Detailed growth characterization of transgenic and control plants showed that transgenic lines accumulate more biomass compared to WT. Certain changes were observed in accumulation of soluble sugars, namely Glc and Fru. Detailed analysis of steady-state levels of primary metabolites and photosynthetic efficiency are further discussed.

3.2 Introduction

Historically, AVP1 was described as localized on the tonoplast (Li et al., 2005). But, PM localization of AVP1 in SE-CCC complexes of *Arabidopsis* was shown by double epifluorescence microscopy and immunogold labeling. AVP1 co-localized with PM Intrinsic Protein, PIP1 (Paez-

Valencia et al., 2011). Immunolocalization studies have shown colocalization of PM H^+-ATPase and H^+-PPase in companion cells of *Ricinus commnunis* (Langhans et al., 2001) and proteomics on PM fractions of *Arabidopsis* show the presence of AVP1 (Alexandersson et al., 2004). Initially, it was proposed that AVP1 on the PM could operate with PM ATPase to contribute to PMF required for phloem loading and transport.

But, thermodynamically, H^+-PPase on the PM of phloem cells is not be able to hydrolytically pump H^+ into the apoplasm (Davies, 1997). Alternatively, it was proposed that the reverse reaction of creating PP_i by using the PMF is thermodynamically feasible (Davies, 1997). In proteobacterium *Rhodospirillum rubrum,* two distinct roles of H^+-PPase have been indicated and which vary depending on localization and cellular condition. H^+-PPase acts as a PPi hydrolase and intracellular H^+ pump in the acidocalcisomes or as PP_i synthase in membranes in fluorescing chromatophores (Baltscheffsky et al., 1966). The role of H^+-PPase in maintaining cytosolic PP_i levels was suggested in studies with tonoplast fractions of coleoptiles and seeds from maize (Rocha Facanha and de Meis, 1998). Based on this, we suggest that, the plant H^+-PPases have the ability to work as H^+ pumps or as PP_i synthase depending upon cellular demands. In the phloem companion cell, a PM localized H^+-PPases may use PMF for maintaining cytosolic PP_i levels that are needed for Suc oxidization.

3.2.1 Impact of *AVP1* Overexpression on Plant Health

In Arabidopsis, *AVP1* overexpressing lines of AVP1-1 and AVP1-2 were shown to have enhanced biomass accumulation in normal, drought, and salt-stressed conditions (Gaxiola et al., 2001; Li et al., 2005). Biomass enhancements are not limited to *AVP1* in Arabidopsis*:* heterologous overexpression of *AVP1* in alfalfa (*Medicago sativa L.)* and creeping bentgrass

(*Agrostis stolonifera L.)* with the CaMV 35S promoter resulted in increased biomass accumulation of 40-70 % and 30-40 % respectively (Li et al., 2008; Bao et al., 2009). Similarly, overexpression of orthologous *TsVP* in maize with a maize *ubiquitin* promoter and in cotton with the CaMV 35S promoter enhanced total soluble sugars by 20 % and biomass by 31-76 % and 33 % respectively (Li et al., 2008; Lv et al., 2009). Furthermore, *avp-1-1* null mutants showed severely disrupted shoot and root development and decreased auxin transport (Li et al., 2005), although it is unclear whether this phenotype is related to pyrophosphate (Ferjani et al., 2011). In tomato, RNAi-mediated suppression of type-I PPase gene resulted in fruit growth retardation of about 45-50 % in an early stage of fruit development indicating an important role in growth (Mohammed et al., 2012).

Plants overexpressing *AVP1* from constitutively active CaMV 35S promoter showed enhanced salt and drought tolerance. The proposed mechanism for salt and drought stress was that transgenic plants have increased ability of Na^+ sequestration in vacuoles, which results in enhanced water retention and turgor of the cell (Gaxiola et al., 2001; Gaxiola et al., 2002; Arif et al., 2012). Transgenic tobacco lines ectopically expressing wheat *H^+-PPase* showed enhanced tolerance to cadmium toxicity compared to WT plants (Khoudi et al., 2012). Similarly, overexpression of *AVP1* and other type I *H^+-PPase* genes has been shown to increase salt and drought tolerance in Cotton (Lv et al., 2008), alfalfa (Bao et al., 2009) and creeping bentgrass (Li et al., 2010). The importance of H^+-PPase in sodium sequestration was shown in vacuolar ATPase mutants *vha*: mutants had reduced ability to acquire nutrients but their ability to acquire ions like sodium, chloride, potassium, and nitrate was not affected, indicating the importance of AVP1 in salt tolerance (Krebs et al., 2010).

3.2.2 Enhanced Nutrient Use Efficiency in Plants Overexpressing H^+-PPase

Several mechanisms for enhanced biomass accumulation in plants overexpressing *AVP1* have been proposed, although these mechanisms may not be mutually exclusive (Gaxiola et al., 2012). One of them is the enhanced nutrient uptake capacity of the transgenic plants. *AVP1* overexpression improves the nutrient uptake capacity by influencing the activity of the PM H^+-ATPase, which leads to changes in apoplasmic pH and rhizosphere acidification (Li et al., 2005; Yang et al., 2007). *AVP1* overexpressing Arabidopsis, tomato and rice plants outperform control plants under phosphorous limiting conditions and acquire more potassium (Yang et al., 2007). In maize, overexpression of *Thellungiella halophila* H^+-PPase gene (*TsVP)* resulted in enhanced tolerance to phosphate insufficiency stress. Transgenic plants showed enhanced root growth compared to WT plants and thus were able to efficiently uptake phosphorous (Pei et al., 2012). Also, Arabidopsis and romaine lettuce plants overexpressing *AVP1* had higher biomass accumulation, rhizosphere acidification capacity and PM ATPase H^+ transport values compared to controls in the nitrate limiting conditions (Paez-Valencia et al., 2013).

In addition to enhanced stress tolerance, plants with an enhanced expression of *AVP1* have increases in shoot and root biomass due to an increase in the cell number (Li et al., 2005; Gonzalez et al., 2010). One mechanism of biomass enhancement is that AVP1 may control auxin transport (Li et al., 2005), thus regulating responses of certain auxin responsive genes (Gonzalez et al., 2010). Plants overexpressing *AVP1* had increased auxin levels (Gonzalez et al., 2010). An auxin efflux carrier Pinformed 1 (PIN1), which is the major regulator of polar auxin transport, is thought to be controlled by AVP1. *AVP1* overexpression plants had increased abundance of PIN1 on the PM (Li et al., 2005).

Another proposed mechanism for enhanced biomass accumulation in plants overexpressing *H^+-PPase* is changes in the carbohydrate distribution. In peach, a quantitative trait locus (QTL) which encodes for a type-I H^+-PPase has been implicated to enhance accumulation of organic acids and carbohydrates (Etienne et al., 2002). Also, metabolite profiling *AVP1*-overexpressing Arabidopsis plants showed alterations in composition of soluble carbohydrates, phosphorylated sugars, phosphoglycerate, succinate and some amino acids (Gonzalez et al., 2010). These measurements do not distinguish between source and sink tissues. Also, analysis was done on the plants grown *in vitro* and harvested at stage 1.03; where plants had three rosette leaves and were 13-15 d old (Boyes et al., 2001). Thus, these plants may not represent a good model for biomass measurements.

In summary, based on current literature, we propose a model (Figure 3.1) in which H^+-PPase has two seemingly contradictory roles depending on its cellular location and the cellular demands. We hypothesize that AVP1 has different functions in different cells: We propose 1) that AVP1 in mesophyll cells energizes the tonoplast while hydrolyzing PP_i produced as a byproduct of Suc synthesis and other bio-synthetic reactions in mesophyll cells (Figure 3.1). 2) That AVP1 at the phloem PM uses the PMF to synthesize PPi and provide substrate for ATP synthesis via Suc oxidation (Figure. 3.1). We further propose that this latter function helps energize the phloem and accounts for the enhanced vitality of *AVP1* overexpressing plants (Gaxiola et al., 2012) (See Chapter 4). Hence, if this hypothesis is true, plants may have enhanced phloem loading and resultant transport. Enhanced nutrient supply to sink tissues might be one of the reasons behind the witnessed benefits of *AVP1* overexpression.

For this we generated two distinct constructs for *AVP1* overexpression, one for constitutive overexpression from the *Cauliflower mosaic virus* 35S promoter. With these transgenic lines we were able to look at the effect of constitutive *AVP1* overexpression throughout the plant. But, importantly we also generated lines that would have enhanced expression specifically in companion cells with Commelina Yellow Mottle Virus *(ProCoYMV)* in order to study the role of AVP1 in phloem (Figure 3.2 A).

3.3 Results

3.3.1 Characterization of Constitutive and Phloem Specific *AVP1* Overexpression Lines

The CaMV 35S promoter is a well-established and characterized "constitutive" promoter. A promoter from Commelina Yellow Mottle Virus *(ProCoYMV)* has been shown to have strong companion cell-specific expression (Medberry et al., 1992; Matsuda et al., 2002). *ProCoYMV* is a stronger and more consistent promoter compared to other phloem specific promoters such as *rolC* and *AtSUC2* (Srivastava et al., 2009). Unlike the *AtSUC2p*, *ProCoYMV* is not feedback inhibited by Suc and thus fits well for studies where changes in Suc levels are predicted (Dasgupta et al., 2014). To dissect the role of AVP1, in enhancing biomass accumulation and carbohydrate distribution, transgenic lines were generated with constitutive and companion-cell specific promoters. Binary vectors containing the *Pro35S:AVP1:nospA* and *ProCoYMV:AVP1:nospA* cassettes (Figure 3.2 A) were transformed into WT Col-0 plants. The transgenic progeny (T1) were identified by selecting for resistance to hygromycin for *Pro35S:AVP1* plants and glufosinate ammonia for *ProCoYMV:AVP1* plants. For each construct, 25-30 independent lines, containing a transgene insertion at a single locus were identified

based on the 3:1 segregation ratio for antibiotic selection. Of those with a 3:1 ratio, T3 seeds were collected and 100 % resistance in the T3 generation identified homozygous T2 lines.

Three representative lines harboring homozygous *Pro35S:AVP1* and *ProCoYMV:AVP1* cassettes in the T3 or T4 generations were analyzed for vegetative growth. Fresh weights of plants harvested at 30-days post-germination (dpg) showed that Pro35S:AVP1 and ProCoYMV:AVP1 plants were larger and had 30-65 % higher biomass compared to WT (Figure 3.2 B and 3.2 C). 35S-1 is a previously characterized *AVP1* overexpression line (Li et al., 2005), which was generously provided by Dr. Roberto Gaxiola, Arizona State University. This line was used as a positive control in all experiments. The average rosette area of the two independent transformants of *Pro35S:AVP1* and *ProCoYMV:AVP1* were 40-55 % higher than WT (Figure 3.2 D). Furthermore, growth was measured at 16, 20, 24 and 30 dpg and growth curve established (Figure 3.2 E). These show increased rates of growth among the overexpression lines relative to WT.

AVP1 transcript levels among the three independent lines of Pro35S:AVP1 and ProCoYMV:AVP1 were analyzed relative to *GAPDH3* by RT-qPCR. Results are represented as expression of *AVP1* from the genomic copy and cDNA expression (Figure 3.3A). Based on expression level there is a positive correlation between higher transcript levels and enhancement in growth. Transgenic lines having high *AVP1* expression were selected for further experiments. For phloem-specific overexpression lines, immuno-localization of AVP1 with AVP1 antibodies was conducted on ProCoYMV:AVP1-54 and ProCoYMV:AVP1-68 by our collaborator, Dr. Julio Paez-Valencia, Arizona State University. Compared to empty-vector control plants, in both mid-rib and minor veins, two independent transgenic lines, ProCoYMV:

AVP1-54 and 68, showed higher AVP1 protein levels that were specific to phloem of the vasculature.

3.3.2 Overexpression of *AVP1* in the Phloem Influences Carbon Partitioning

In Arabidopsis, Suc is the predominant sugar transported from the source to sink tissues (Ayre, 2011). Thus, Suc accumulation in source leaves is an indicator of inefficient export leading to negative feed-back on photosynthesis and reduced productivity and growth. But, in plants with enhanced biomass, higher levels of Suc could imply enrichment in Suc synthesis due to efficient removal of PP_i (See Figure 3.1, mesophyll cell). Also, based on previous studies (Lerchl et al., 1995), our first hypothesis is that consumption of PP_i in the cytoplasm of mesophyll cells may promote Suc synthesis. Thus, to assess the effect of *AVP1* overexpression on Suc synthesis and carbohydrate distribution, the major soluble sugars, Glc, Fru and Suc and the storage carbohydrate starch were analyzed among transgenic and WT lines at 28-30 days post germination. All measurements were done at four hours into a 12 hour light period. A 38 % increase in hexose in the leaves of *AVP1* overexpressing plants relative to WT was observed in one *Pro35S:AVP1* overexpression line, 35S-30, and 61 % to 85 % increase was observed in two phloem-specific lines CoYMV-41 and CoYMV-50, respectively (Figure 3.4 A). But, alterations in Suc levels were not observed. For *Pro35S:AVP1* plants these results were not expected and do not support our model.

In order to measure transient carbohydrate reserves, starch accumulation in source leaves was measured. Line 35S-1 showed significantly higher accumulation of starch compared to WT (Figure 3.4 B), and three independent lines CoYMV-41, CoYMV-50 and CoYMV-68 showed higher levels of starch accumulation compared to WT. According to our hypothesis,

increased accumulation of soluble and stored sugar was expected in the Pro35S:AVP1 lines, but not in ProCoYMV:AVP1 lines (Gaxiola et al., 2012). Enhanced expression of *AVP1* in mesophyll cells would lead to increased removal of PP_i from the cytosol, leading to enhanced Suc synthesis. Enhanced Suc synthesis may lead to increased conversion of soluble sugars into starch. Alternatively, phloem-specific overexpression of *AVP1* should not show increased Suc synthesis and subsequent starch accumulation as these plants should not have altered *AVP1* expression in the mesophyll cells (Srivastava et al., 2009). Enhanced Suc accumulation was not observed in ProCoYMV:AVP1 plants, but enhanced accumulation of Glc was observed in shoots of CoYMV-41 and CoYMV-50, compared to WT. Enhanced Fru accumulation was observed in shoots of CoYMV-50 and CoYMV-68, compared to WT. Enhanced starch accumulation was observed in CoYMV-41, CoYMV-50 and CoYMV-68 lines, compared to WT.

As plant growth depends on its efficiency of producing, utilizing or storing nutrients, we investigated changes in metabolites of *AVP1* overexpression lines. We measured representative organic acids, phosphorylated intermediates, protein and amino acids in rosettes. Organic acids malate and fumarate are vacuolar carbon storage molecules, regulate pH of the vacuole, and are intermediates of tricarboxylic acid cycle (Fernie and Martinoia, 2009; Zell et al., 2010). We did not observe significant changes between transgenic and WT plants (Figure 3.4 C). Phosphorylated intermediates represent key steps in glycolysis and gluconeogenesis. We measured levels of glucose-6-phosphate (G6P), and lines 35S-9 and CoYMV-50 had significantly higher accumulation of G6P compared to the other lines (Figure 3.4 D). H^+-PPase hydrolyses PPi to generate inorganic phosphate, thus we measured inorganic (Figure 3.4 E) and total phosphate (Figure 3.4 F) of control and transgenic lines. We did not observe significant changes,

except 35S-1 had higher inorganic phosphate compared to WT, and 35S-9 and CoYMV-41 had less. In order to check the overall health of a plant we measured chlorophyll and did not see any significant changes in chlorophyll-a or chlorophyll-b levels (Figure 3.3 G). Total protein was measured, and 35S-9 and CoYMV-41 had less total protein than the other lines (Figure 3.4 H). Total amino acids were measured by a fluorescamine method (Bantan-Polak et al., 2001) and 35S-9 and 35S-30 had significantly less total amino acids compared to other lines. Although, there was some plant-to-plant variation among the metabolites tested, a consistent pattern was not evident.

As we did not observe prominent alterations in the measured primary metabolites from the rosettes of the transgenic lines, we measured these metabolites from shoots and roots of hydroponically grown tissues to understand the influence of AVP1 on the source-sink relationship. WT and transgenic lines were germinated in ½ strength Hoagland's solution. One week post germination, seeds were transferred to hydroponic growth tanks containing ¼ strength Hoagland's and grown for 24 days. Shoots and roots were harvested and fresh weights determined. Consistent with the increased rosette growth observed in Pro35S:AVP1 and ProCoYMV:AVP1 plants grown on potting mix (Figure 3.2 C), fresh weights of both shoot (Figure 3.5 A) and root (Figure 3.5 B) significantly exceeded that of WT when grown hydroponically. Comparing Figures 3.3 C, 3.5 A shoot and 3.5 B root shows that growth media did not differentially impact plant growth (i.e. growth ratios are the same, regardless of the medium). Expression levels of genomic *AVP1* and *AVP1* cDNA are represented in Figure 3.5, and higher expression of *AVP1* in shoots (Figure 3.5 C) and roots (Figure 3.5 D) of 35S and shoots (Figure 3.5 E) and roots (Figure 3.5 F) of CoYMV lines were observed as expected and were consistent

with the plants grown on potting mix. Significant increases in Glc were observed in the shoots of three Pro35S:AVP1 lines and one of ProCoYMV:AVP1 line namely CoYMV-68 (Figure 3.5 G). Shoots and roots (Figure 3.5 G&H) of 35S-1 had higher Glc and Fru compared to WT. In hydroponic conditions, shoots of 35S-30 and 35s-31 had less starch compared to WT (Figure 3.5 I). Arabidopsis roots do not accumulate substantial amounts of starch, and starch levels in roots of all lines were below the level of detection (data not shown)(Streb and Zeeman, 2012). No significant changes in malate and fumarate were observed in the shoots (Figure 3.5 J) and roots (Figure 3.5 K) of transgenic lines, except 35S-1 had higher malate content. No significant difference was observed in the G6P levels in the shoots (Figure 3.5 L) and roots (Figure 3.5 M). With the exception of shoots of 35S-1, no significant changes were observed in the protein content of shoots (Figure 3.5 N) and roots (Figure 3.5 O) of the other lines. Total amino acids were determined and shoots of 35S-9 had significantly less total amino acids compared to other lines (Figure 3.5 P). Whereas, roots of 35S-9 had significantly enhanced amino acids and CoYMV-50 had significantly less compared to other lines (Figure 3.5 Q).

As noted above, *Pro35S:AVP1* and *ProCoYMV:AVP1* plants are larger and some lines contain more Glc and Fru (Figure 3.4 A). Line 35S-1 and all CoYMV (Figure 4B) plants contain more starch in potting mix grown shoots, compared to the source tissues of WT (Figure 3.4 B). This implies that more photosynthesis may be occurring in the transgenic lines. Hence, instantaneous photosynthetic rates of 21 d old plants were quantified with a Li-Cor Li-6400XT photosynthesis monitoring system. Results show that 35S-1 has significant higher photosynthetic rates compared to WT. The other Pro35S:AVP1 and ProCoYMV:AVP1 lines did not show significant differences in the net photosynthesis and CO_2 assimilation rates between

transgenic and control plants indicating that other transgenic plants do not have more instantaneous photosynthesis capacity (Figure 3.6). All measurements were done between four to six hours into the light period and these are measurements of the instantaneous photosynthesis rates. Hence, small differences in photosynthesis among the lines that contribute to the growth over a long period may not be evident among the plant-to-plant variation. Another way of measuring photosynthesis is by photosynthetic labeling of source tissues with [^{14}C]-CO_2. When transgenic and control plants were allowed to photosynthesize in presence of [^{14}C]-CO_2 for 20 min and the amount of incorporated label measured, *35S* and *CoYMV* overexpression lines had higher cpm per milligram fresh weight, indicating that they have enhanced capacity to incorporate CO_2 compared to WT (Figure 3.7).

3.3.3 *AVP1* Overexpression Alters Levels of Other Primary Metabolite Like Amino Acids

Based on these experiments, some constitutive and phloem-specific *AVP1* overexpression lines showed enriched photoassimilate synthesis, augmented phloem transport capacity and increased supply of photoassimilates to the sink organs (Discussed in Chapter 4). This indicates that many compounds in addition to carbohydrates may be affected. Amino acids play a key role in nitrogen utilization and plant growth. Many metabolic pathways of plant nitrogen metabolism are regulated by concentrations of free amino acids in plants (Atilio and Causing, 1996). For example, amino acids serve as nitrogen donors during synthesis of nucleotides, hormones and secondary metabolites (Tegeder, 2012). Micro-array analyses of *AVP1* overexpressing plants indicated that several amino acid transporter genes are up-regulated (Gonzalez et al., 2010). Hence, understanding the effect of *AVP1* overexpression on individual amino acid levels was necessary. For this purpose, amino acid profiling was done with

AccQ·Tag ultra-performance liquid chromatography- electrospray ionization-tandem mass spectroscopy (AccQ Tag-UPLC-EIS-MS/MS) (Armenta et al., 2010; Salazar et al., 2012). Results show increased accumulation of several amino acids in the 35S-1 line compared to the WT, with the exception of histidine (Figure 3.8). These results indicate that the 35S-1 line has alterations in overall carbon backbone which is needed in the central metabolism.

3.4 Discussion

Adequate concentrations of PPi are necessary for plant growth, metabolism and phloem transport (Sonnewald, 1992). The Suc produced during photosynthesis is delivered to sink tissues for utilization and storage and enhanced supply may result in larger plants with energized root system and rhizosphere acidification. This may also lead to enhanced nutrient uptake and improved growth as plants have increased availability of reduced carbon. Historically, type I H^+-PPases were thought to be tonoplast localized pumps (Maeshima, 1991), but there now exists strong evidence for PM localization (Paez-Valencia et al., 2011). Nevertheless, based on free energy estimations of PPi hydrolysis for *in-vivo* conditions, type I H^+-PPases cannot pump H^+ into the apoplasm, but may instead utilize PM PMF to generate PP_i (Davies, 1997) . To test if PM localized H^+ -PPase in phloem functions as a PP_i synthase and uses the PMF to generate PP_i, we manipulated *AVP1* expression constitutively and specifically in the phloem companion cells. Pro35S:AVP1 and ProCoYMV:AVP1 lines that showed significant enhancement in shoot and root biomass compared to WT (Figure 3.2), which corresponded to higher total *cDNA* expression (Figure 3.3). Our initial hypothesis was that enhanced expression of *AVP1* in mesophyll cells would lead to increased removal of PPi from the cytosol, leading to enhanced Suc synthesis. Enhanced Suc synthesis may also lead to increased conversion of

soluble sugars into starch. Alternatively, plants overexpressing *AVP1* with a phloem-specific promoter may not show increased Suc synthesis as these plants do not have altered *AVP1* expression in the mesophyll cells. Analysis of primary metabolites from plants grown on potting mix and hydroponically grown samples revealed significant changes in Glc, Fru and starch in some lines, but a consistent pattern did not emerge. Contrasting to our hypothesis, enhanced accumulation of Suc was not observed in the Pro35S:AVP1 and ProCoYMV:AVP1 lines. In plants with enhanced phloem transport and increased delivery of reduced carbon to sink tissues (discussed in Chapter 4), osmotic status may lead to rapid breakdown of Suc into Glc and Fru (León and Sheen, 2003; Hammond and White, 2008). The proposed pathway for enhanced hexose accumulation is through enhanced generation of G6P in the calvin cycle. This further, could lead to enhanced starch synthesis in chlroplast which may be further hydrolyzed to enhanced Glc and Fru levels (Flügge et al., 2003; Hammond and White, 2008). Suc is the predominant transport sugar and not a storage sugar in Arabidopsis, thus increased Suc accumulation may not be beneficial for plants (Sturm, 1999). The Suc in the cytoplasm may be used in enhanced cytosolic glycolysis leading to organic acids which may be excreted at a higher rate in the rhizosphere for enhancing mineral nutrient acquisition. Recently, enhanced rhizosphere acidification and enhanced expression of sugar induced ion transporter genes in Pro35S:AVP1 plants was shown (Pizzio et al., 2015). Thus, even if enhanced Suc synthesis would occur in Pro35S:AVP1 plants, accumulation at the steady state level may not be observed. With respect to the rest of the metabolites analyzed, significant change in the steady state levels were not observed. The reactions of primary metabolism that involve PPi have low ΔG values and flux through the pathways is determined largely by equilibrium constants and levels of

substrate and product. Therefore, changes in steady state levels may be hard to detect and instead metabolic flux through the pathways would be more informative.

As an example, individual amino acids measured show significant changes between WT and 35S-1 line (Figure 3.8). Whereas, total amino acids measured in 35S-1 line grown on potting mix as well as hydroponically grown samples do not indicate significant changes among different lines (Figure 3.5 P-Q and Figure 3.4 I). This indicates that combined amounts of amino acids are not altered at the steady state levels. Enhancing phloem transport may eventually enhance flux or cycling of these metabolites. Amino acid permease AAP2 and AAP6 are also localized on the phloem companion cell membrane and utilizes PMF (Hirner et al., 1998; Brady et al., 2007; Hunt et al., 2010). Increased PMF may also lead to enhanced amino acid transporter activity to increase movement of several different amino acids throughout the plant. This is a highly active process and plants may constantly change their nutritional status. If this hypothesis is true the absence of congruence with respect to other metabolite levels between all Pro35S:AVP1 and ProCoYMV:AVP1 lines is not surprising. Thus, it is not immediately evident why some lines and not others have apparent significant differences in measured metabolites at the steady state levels.

The influence of constitutive and phloem specific overexpression on the photosynthetic capacity was tested with two different experiments. Instantaneous measurements of CO_2 assimilation rates with IRGA showed that 35S-1 had higher photosynthetic capacity compare to WT. The other Pro35S:AVP1 and ProCoYMV:AVP1 lines did not show significant increases. Conversely, photosynthetic labeling experiments with ^{14}C-CO_2 for 20 min, showed higher accumulation of ^{14}C in shoots of Pro35S:AVP1 and ProCoYMV:AVP1 lines. This observation is

consistent with the hypothesis that enhanced phloem transport (discussed in the Chapter 4) leads to reduced feedback inhibition on photosynthesis.

The experiments conducted in this study help us understand the importance of PPi hydrolysis and synthesis for phloem loading and long-distance transport, and its influence on plant growth. AVP1 was shown to have high levels of expression in vasculature (Figure 3.3 B)(Pizzio et al., 2015), yet in the phloem, PP_i hydrolysis hinders phloem transport by inhibiting Suc oxidation (Lerchl et al., 1995). The experimental observations in support of our hypothesis that AVP1 acts as a synthase in the phloem may significantly impact our view of how carbon-flux through central metabolism is regulated. The phloem-specific overexpression lines described above help evaluate how H^+-PPase affects carbon utilization and transport in *planta*. These results indicate that phloem-specific *AVP1* overexpression is sufficient to enhance biomass in Arabidopsis.

Based on our results and those of others, a model was proposed for the role of PM H^+-PPase in the phloem energization. In the companion cell, PM localized H^+-PPase appears to utilize the available PMF to maintain the cytosolic PPi levels needed for the Suc respiration via glycolysis. Enhanced Suc respiration may lead to generation of more ATP and PMF which are needed for the phloem loading process (discussed in the Chapter 4). In photosynthetic cells, AVP1 localizes predominantly to the tonoplast, and removes PP_i that are produced as a by-product of cellular metabolism. This study provides some insight on implication of the hydrolysis and synthesis of PP_i for phloem loading and long-distance transport, and its influence on plant growth.

3.5 Material and Methods

3.5.1 Plasmid Constructions and Plant Transformation

AVP1 cDNA was amplified from pRT103-AVP1, obtained from Dr. Roberto Gaxiola, Arizona State University. cDNA was amplified by PCR using forward oligonucleotide AVP1 F (5'-CACCATGGTGGCGCCTGCTTTGTTAC-3'). This primer contained CACC overhang at the 5' end for Directional TOPO cloning into pENTR (Life Technologies) and reverse oligonucleotide AVP1 R (5'- GAAGTACTTGAAAAGGATACCACC-3'). Phusion Hot start polymerase (NEB, Beverly, MA, USA) was used according to the manufacturer's instructions. The PCR product was cloned into pENTR/D-TOPO by using Directional TOPO Cloning Kit (Life Technologies), resulting in pENTR-AVP1. pENTR-AVP1 was recombined with pMDC32 (Curtis and Grossniklaus, 2003) in a Gateway LR recombination reaction using LR Clonase II enzyme mix, to generate pMDC32:AVP1. pMDC32 contains a 35S promoter with dual enhancer (Curtis and Grossniklaus, 2003). pENTR:AVP1 was recombined with pGPTV:ProCoYMV:cmr:ccdB to get pGPTV:ProCoYMV:AVP1. These vectors were electroporated into *Agrobacterium tumefaciens* strain GV3101mp90 as described (Ayre and Turgeon, 2004). WT Col-0 (ABRC Catalog #CS-70000) was transformed with the above constructs by the floral dip method (Clough and Bent, 1998).

3.5.2 Plant Material and Growth Conditions

WT *Arabidopsis thaliana* Col-0 was obtained from Arabidopsis Biological Research Center (ABRC) catalog # CS70000. Unless noted otherwise, seeds were stratified for 72 hour at 4°C after sowing on Fafard 3B potting mix (Agawam, MA) or on sterile MS media with 1 % Suc, as required. Plants were transferred to a growth chamber (Percival AR95L, Percival Scientific, Perry IA) with 12 hours light at 22°C and 12 hours dark at 18°C, 180 µmol photons m^{-2} s^{-1}. T1

generation seeds of plants transformed with pMDC32:AVP1 were selected on sterile medium containing 40mg/L hygromycin. After stratifying, and six hours exposure to light to induce germination, seeds were kept in darkness for five days to allow hypocotyl elongation to occur (Harrison et al., 2006). Seedlings resistant to hygromycin had twice the elongation of sensitive lines, and were transferred to potting mix. Segregation of hygromycin resistance in the T3 generation was used to identify lines homozygous for cDNA.

For selecting plants transformed with pGPTV:ProCoYMV:AVP1, T1 seeds were sown on soil and sprayed with 20mg/L glufosinate ammonia (Finale, Farnam Companies, Phoenix, AZ) post germination. Segregation of antibiotic/herbicide resistance in the T3 generation was used to identify lines homozygous for cDNA. All experiments were conducted with homozygous T_3 or T_4 generation seeds. Out of 25 or more independent lines identified for ProCoYMV:AVP1 and Pro35S:AVP1, three representative lines were selected for further experiments based on *cDNA* expression and growth morphology compared to WT. For growth analysis, seeds from all lines were sown in 1.5 inch individual pots and were photographed at 16, 18, 20, 22 and 24th days after germination. Rosette surface area was measured with ImageJ version 1.42f (Schneider et al., 2012).

Transgenic and control lines were grown on potting mix for 26-28 days under the growth conditions mentioned above. For hydroponically grown plants, seeds were germinated in 200 µl PCR tubes with 0.8 % agar and ½ strength Hoagland's solution (Phytotechnology Laboratories). One week post germination, PCR tubes with seedling were transferred to hydroponic growth tanks containing ¼ strength Hoagland's and grown for 24 days (Conn et al., 2013). Tissues were harvested between five and six hours into the light period. Rosettes (from

soil and hydroponically grown plants) and roots (from hydroponically grown plants) were excised at the hypocotyls, fresh weight was determined and samples were placed in aluminum foil envelopes and transferred to liquid N_2. Tissues were stored at -80 °C until further processing. For cryogenic grinding, tissues were transferred to pre-cooled 15 ml polycarbonate vials (OPS Diagnostics) each containing three 5 mm stainless steel grinding balls. Lined screw caps of vials were also pre-chilled during this process. Tissues were ground in 2010 Geno Grinder (SPEX SamplePrep) at 1200 strokes / minute for 20 seconds. 18-20 mg aliquots were made for carbohydrate determination, 50 mg for expression analysis and 50-100 mg for tri-chloroacetic acid extraction.

3.5.3 Transcript Analysis

Total RNA was isolated from 50 mg aliquots of ground tissues of T3 plants and controls using Trizol (Life Technologies) according to manufacturer's instructions and further treated with RNAase free DNase-I (Life Technologies). The quantity of RNA was estimated by spectrophotometry. 600 ng of total RNA in 10 µl H_2O was reverse transcribed with Superscript III reverse transcriptase and 50 µM oligo (dT) (Life Technologies) according to the manufacturer's instructions. Gene specific primers used for the real-time quantitative PCR (RT-qPCR) are listed in Table: 3.1. RT-qPCR was carried out with SybrGreen PCR Master Mix (Sigma-Aldrich) on an Applied Biosystems ViiA 7 (Life Technologies) using the following protocol: 10 min denaturation at 95 °C followed by 40 cycles of 95 °C for 10 s, 58 °C for 30 s, and 72 °C for 30 s. A final melting curve was obtained to confirm a single PCR product. The levels of genomic and cDNA expression was normalized to that of *GAPDH3* for *Pro35S:AVP1* and *ProCoYMV:AVP1*

lines. Three biological and three technical replicates were used for these measurements. Each biological replicate contained three pooled plants.

3.5.4 Extraction and Measurement of Primary Metabolites

The major transient soluble carbohydrates were extracted from 18-20 mg aliquots with 80 % ethanol or tri-chloroacetic acid (Gibon et al., 2002) and quantified enzymatically (Stitt et al., 1989) using a Synergy H microtiter plate Reader (Bio Tek, USA) or by High performance anion exchange chromatography with pulsed amperometric detection (HPAEC-PAD) (Dasgupta et al., 2014). For methanol: chloroform: water (60:25:15) (MCW) extractions, entire rosettes from soil grown plants were extracted with 5 ml of ice-cold MCW solution with 10 µM lactose, representing a minimum of 10 parts MCW to 1 part plant material. The extraction was performed at 50°C for 20 m. Samples were passed through columns containing 500 µl AG 50W-X4 cation exchange resin (hydrogen form) (Bio-Rad, Hercules, CA), 300 µl polyvinyl polypyrrolidone (Sigma-Aldrich), and 500 µl AG 1-X8 anion-exchange resin (formate form) (Bio-Rad) bed volumes, respectively (top to bottom). This collected the neutral fraction and left the cations and anions on the column. Samples were resolved and quantified against standards by HPAEC-PAD using a CarboPac PA20 column at 30°C, 50mM NaOH eluent and quadruple waveform, as recommended by manufacturer (Dionex, Sunnyvale, CA). Glc and Gal coelute under these conditions. Values were normalized against the internal lactose standard. Starch was measured enzymatically from the insoluble material after ethanolic extraction of soluble carbohydrates (Hendriks et al., 2003) or by a commercially available starch assay kit (Megazyme, Ireland). Total protein was measured using the Bradford Assay (Bradford, 1976). G6P was determined according to (Gibon et al., 2004). Malate and Fumarate were determined

according to (Cross et al., 2006). Inorganic phosphate and total phosphate were measured using an ammonium molybdate assay (Chiou et al., 2006). Total amino acids were measured using a fluorescamine method (Gibon et al., 2009). Individual amino acid levels from the source leaves of transgenic and control plants were also measured. Amino acids were derivatized with AQC and treated at 55°C by using the AccQ Tag derivatization kit (Waters Corporation, Milford, MA). UPLC-ESI-MS/MS was carried out using a Waters Acquity UPLC system aligned to a Waters Xevo TQ mass spectrometer (Salazar et al., 2012). Mass spectra were obtained using positive ESI and MRM mode. Argon gas was used as the collision gas. Calibration was done using 20 serial dilutions of amino acid mix (Sigma-Aldrich). Data acquisition and UPLC-ESI-MS/MS system control was done using Waters MassLynx software. Data analysis was done with TargetLynx software (Waters Corporation, MO).

3.5.5 Photosynthesis Measurement

Photosynthesis per unit surface area was measured with Li-6400XT Infra-red gas analyzer (IRGA) along with Li-6400-17 Whole Plant Arabidopsis (WPA) Chamber and Li-6400-18 RGB (red, green, blue) as the light source. Plants were grown for 21 days in 1.5 inch diameter round pots that fit in the WPA chamber. The surface of potting mix was sealed with pottery clay to avoid gas exchange with the potting medium. Gas exchange measurements were determined with 400 µmol mol^{-1} of CO_2, RH 60 %, 23°C temperature, a gas flow rate of 500 µmol s^{-1} and photosynthetically active radiation (PAR) 225 µmol photons $m^{-1}s^{-1}$. Plants were allowed to acclimate for 120 s in the IRGA chamber before taking measurements. The acclimatization time was determined empirically. Two IRGA measurements were taken per plant with 30 s intervals

and averaged. For each line, 8-12 plants were measured. Surface area was determined with ImageJ analysis of digital photographs of rosettes.

Table 3-1: Oligonucleotides used in this study

Oligonucleotides used for RT-qPCR			**Sequence**	
AGI code	**Location**	**Gene**	**Forward Primer (5' → 3')**	**Reverse Primer (5' → 3')**
AT1g15690	Exon	*AVP1*	GTCCTCGCCGGATCTCTTGTAT	GCTCTTTGCGTGCTCTGATAC
AT1g15690	3UTR	*AVP1*	GTCTTTGCTCCCTTCTTCGCCA	CATCATCGTCATCTTCTTCCCT
AT1g15690	Exon	*AVP1*	CACTCACGGTGGTATCCTTT	GTTTGAACGATCGGGGAAATTC
AT1g22710	Exon/Intron	*AtSUC2*	TAGCCATTGTCGTCCCTCAGATG	ATGAAATCCCATAGTAGCTTTGAAGG
AT1g13440 (3')	3UTR	*GAPDH*	TTGGTGACAACAGGTCAAGCA	AAACTTGTCGCTCAATGCAATC
AT1g13440 (5')	3UTR	*GAPDH*	TCTCGATCTCAATTTCGCAAAA	CGAAACCGTTGATTCCGATTC
Oligonucleotides used to create the *AVP1* cDNA by PCR for TOPO Directional cloning and sequencing				
AT1g15690	Exon-For cloning	*AVP1*	CACC**ATG**GTGGCGCCTGCTTTGTTAC (**ATG**-start codon)	GAAGTACTTGAAAAGGATACCACC-No stop codon
AT1g15690	Exon-For cloning	*AVP1*	GTCCTCGCCGGATCTCTTGTAT	GCTCTTTGCGTGCTCTGATAC
AT1g15690	Exon-sequencing	*AVP1*	GCCCTAGTCTCCTTGGCTCT	AGAGCTGCACTTCCCACACT
AT1g15690	Exon-sequencing	*AVP1*	GTATTGCTGAAATGGCTGGAATGAG	GAAGTACTTGAAAAGGATACCACC
AT1g15690	Exon-sequencing	*AVP1*	TGGCTTACCGACCTCCTTTACC	TCCAGCCCAAAGACCAACACAAAC

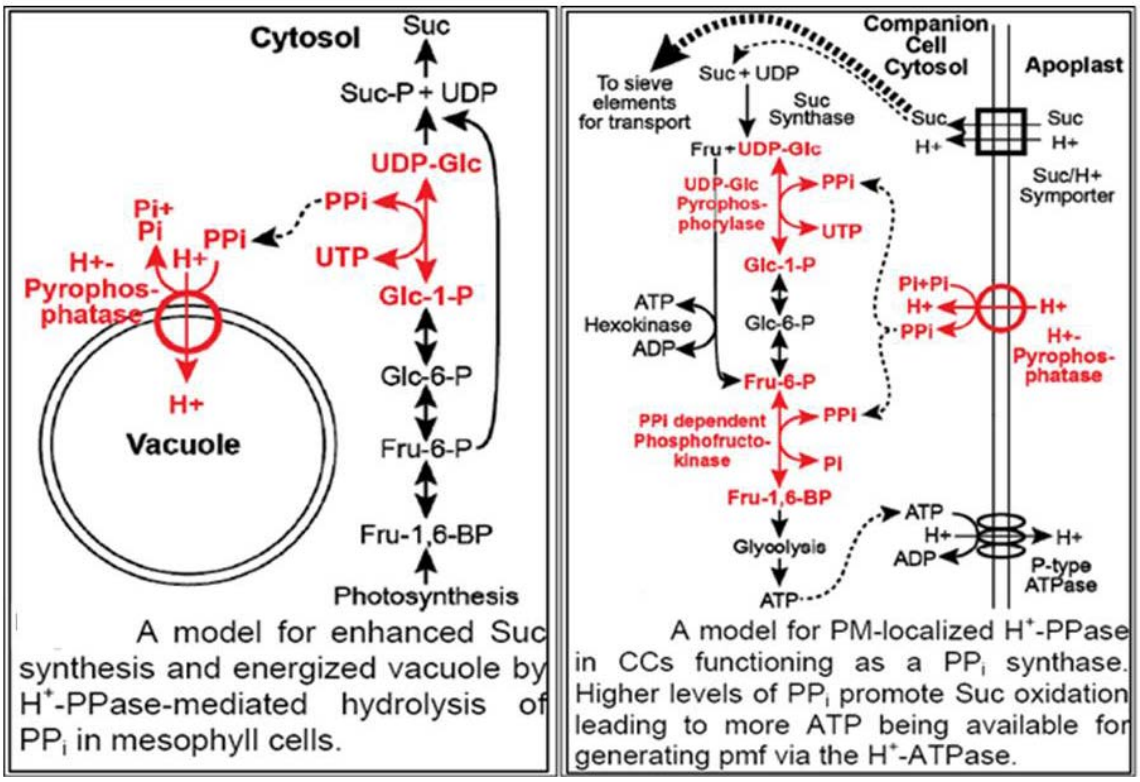

Figure 3-1: Hypothesis- AVP1 has seemingly contrasting roles based on its localization. (Left) In mesophyll cell, where Suc synthesis occurs, PPi is a product and hydrolysis by H^+-PPase leads to enhanced Suc synthesis and PMF across the tonoplast. (Right) In phloem H^+-PPase localizes to the PM of CC and uses PMF to synthesize PPi rather than hydrolyzing PPi to contribute to PMF across PM. Synthesis of more PPi promotes oxidation of Suc loaded into the phloem to create more ATP. PM ATPase would in turn use that ATP and generate more PMF. Enhanced PMF would be utilized by SUTs to pump more Suc in CC. Therefore, our hypothesis is that companion cell specific *AVP1* overexpression indirectly enhances Suc loading and transport by energizing the transport system (Image contributed by Dr. Brian Ayre, University of North Texas).

A

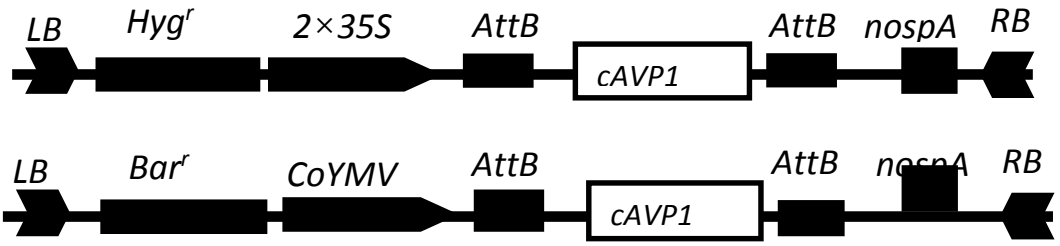
LB
Hygr
2×35S
AttB
cAVP1
AttB
nospA
RB
LB
Barr
CoYMV
AttB
cAVP1
AttB
nospA
RB

B

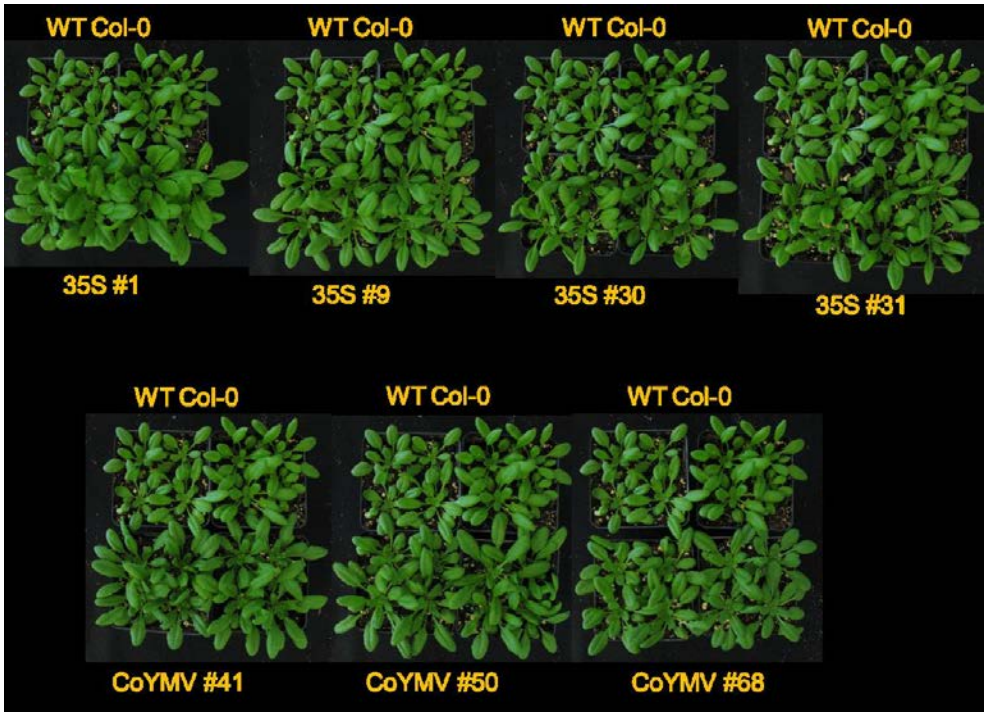
WT Col-0
WT Col-0
WT Col-0
WT Col-0
35S #1
35S #9
35S #30
35S #31
WT Col-0
WT Col-0
WT Col-0
CoYMV #41
CoYMV #50
CoYMV #68

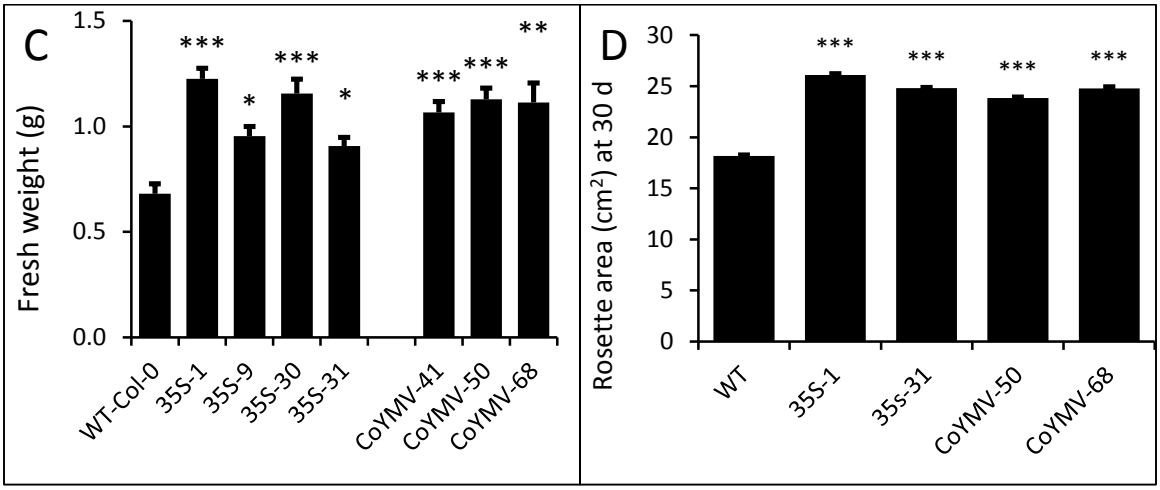
C
Fresh weight (g)
1.5
1.0
0.5
0.0
***
***
*
***
*
***
***
**
WT-Col-0
35S-1
35S-9
35S-30
35S-31
CoYMV-41
CoYMV-50
CoYMV-68
D
Rosette area (cm²) at 30 d
30
25
20
15
10
5
0
***
***
***
***
WT
35S-1
35s-31
CoYMV-50
CoYMV-68

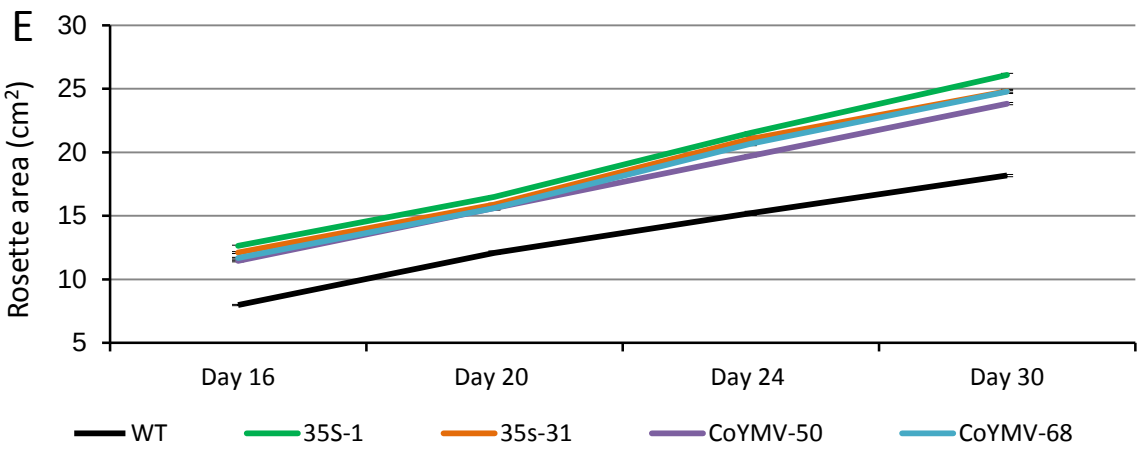

Figure 3-2: T-DNA cassettes used and growth characteristics of WT, Pro35S:AVP1 and ProCoYMV:AVP1 lines. **A,** Structure of *pMDC32:Pro35S:AVP1*, *pGPTV:ProCoYMV:AVP1*. *AVP1* cDNA was sub-cloned into pMDC32 to generate pMDC32:AVP1 and downstream of pGPTV-*ProCoYMV* by Gateway recombination. LB: T-DNA left border; RB: T-DNA right border; *Bar*^{r}: glufosinate ammonium resistance; *Hyg*^{r}*:* Hygromycin resistance; *nospA*: Nopaline synthase terminator; *2×35S*: CaMV 35S promoter with dual enhancers; *ProCoYMV:* Phloem-specific promoter from *Commelina yellow mottle virus; attB*: Gateway recombination sites. **B,** Representative 28-d-old WT, Pro35S:AVP1 and ProCoYMV:AVP1 lines. For scale, the square pots are 3.5 inch. **C,** Fresh weights of rosettes harvested from 28-d-old plants, pools of three per replicate. **D,** rosette area of WT, Pro35S:AVP1 and ProCoYMV:AVP1 lines at day 30. **E,** Rosette area of 16, 20, 24, 30 d old WT, Pro35S:AVP1 and ProCoYMV:AVP1 lines. Variation is expressed as SE; n = 12. Constitutive and phloem-specific *AVP1* overexpression results in larger plants relative to WT. Significant differences from WT are based on Student's T-Test: *, $P \leq 0.05$; **, $P \leq 0.01$; ***, $P \leq 0.001$.

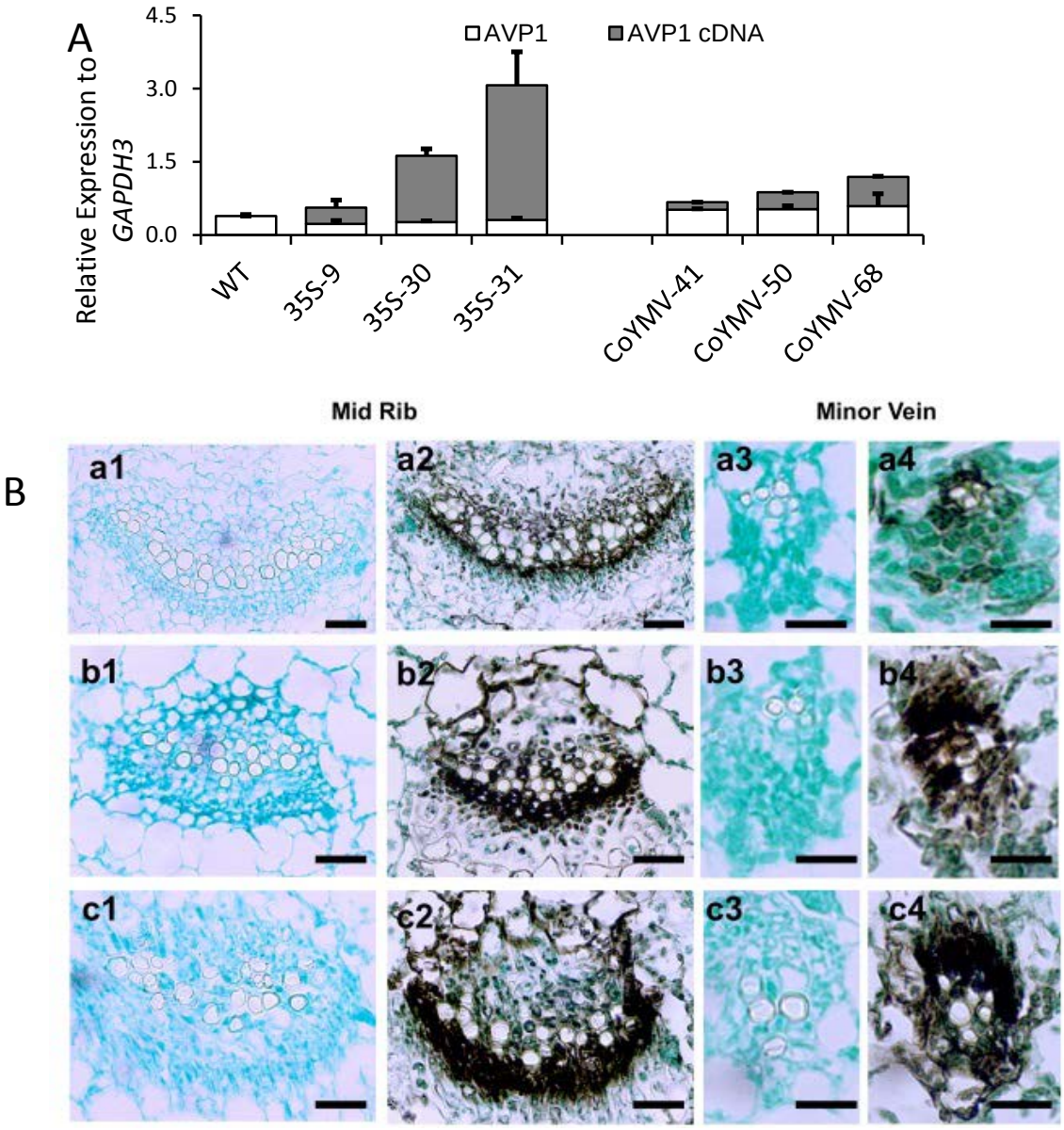

Figure 3-3: Transcript abundance of *AVP1* and immunolocalizations of AVP1 in ProCoYMV:AVP1 lines. **A**, RT-qPCR results of *AVP1* expression from genomic loci and cDNA driven by *Pro35S* and *ProCoYMV* promoters compared to *GAPDH3* from shoots of soil grown samples, white bars represent the genomic *AVP1* expression and grey bars represent the *AVP1* cDNA expression. **B,** Immunolocalization of AVP1, in leaf sections of an empty vector control and ProCoYMV:AVP1 lines. **a**, Empty vector control; **b**, ProCoYMV: AVP1-54 (not described here); **c**, ProCoYMV:AVP1-68. Preimmune sera negative controls: a, b, c odd numbers; 1 and 2, major vein; 3 and 4, minor vein. H^+-PPase sera positive a, b, c even numbers. Bars in a, b and c 1 and 2= 50 µm; Bars in a, b and c 3 and 4=10 µm. Compared to the empty vector control, phloem-specific overexpression lines; CoYMV-54 and CoYMV-68 have higher AVP1 expression in the leaf mid rib and minor vein (Image, B contributed by Dr. Julio Paez Valencia and Dr. Roberto Gaxiola, Arizona State University).

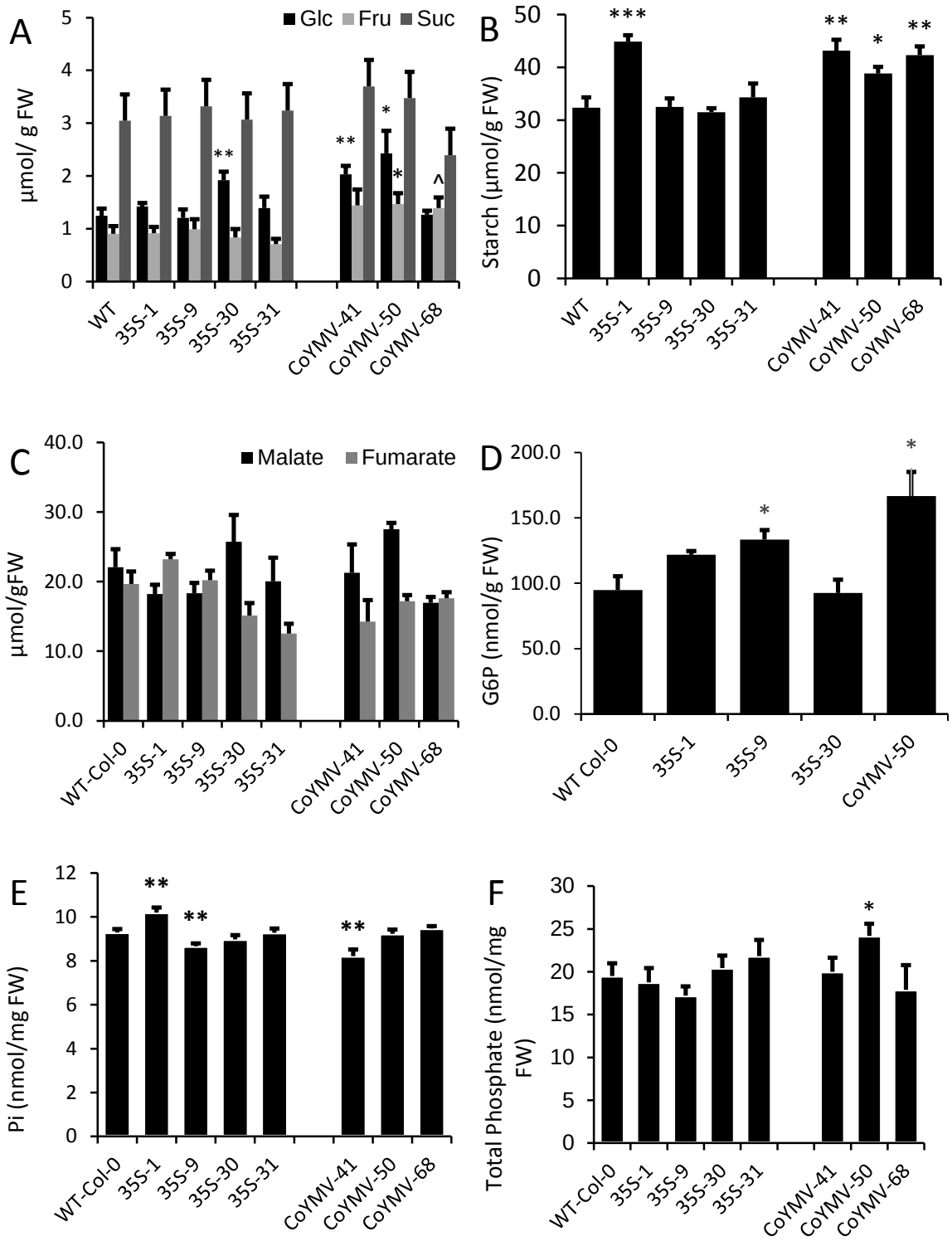
A
Glc
Fru
Suc
µmol/ g FW
WT
35S-1
35S-9
35S-30
35S-31
CoYMV-41
CoYMV-50
CoYMV-68
B
Starch (µmol/g FW)
C
Malate
Fumarate
µmol/gFW
WT-Col-0
D
G6P (nmol/g FW)
E
Pi (nmol/mg FW)
F
Total Phosphate (nmol/mg FW)

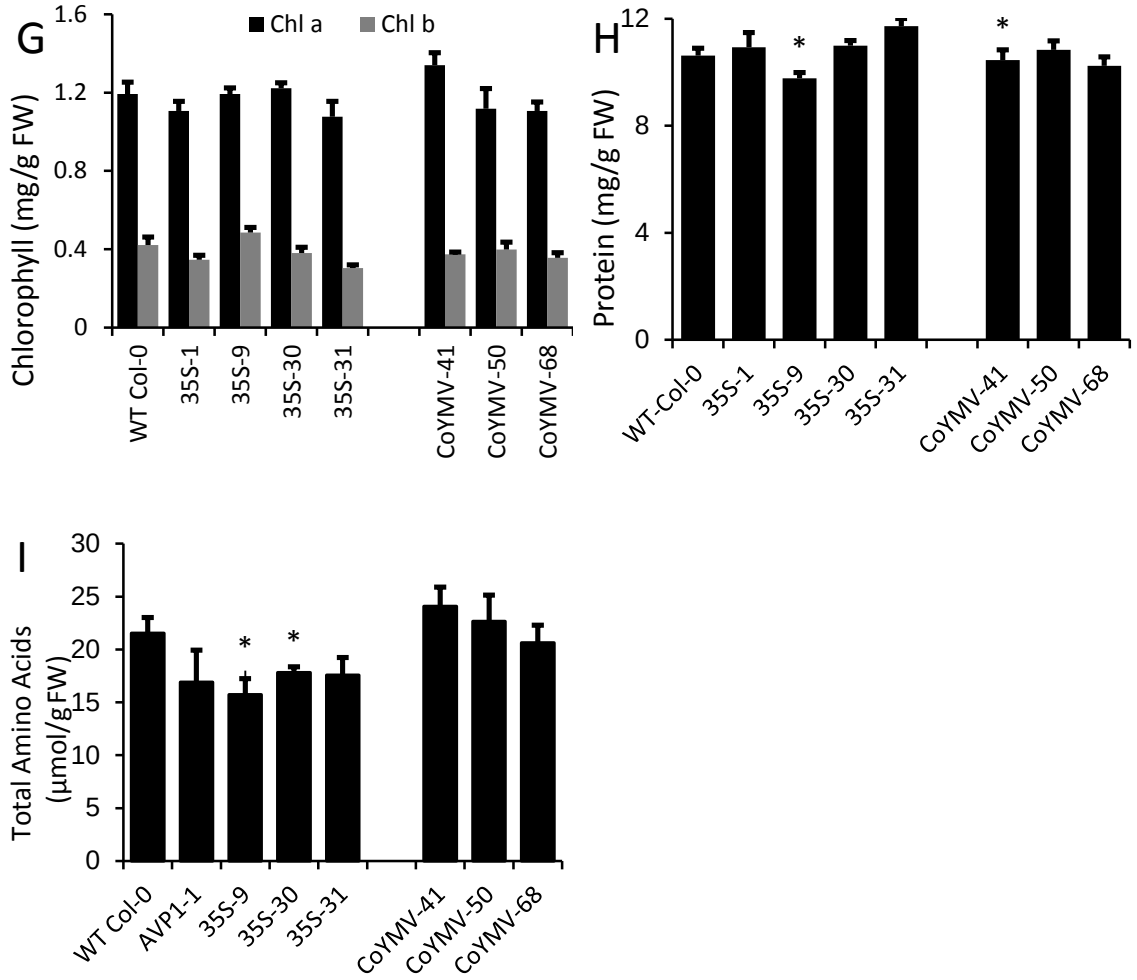

Figure 3-4: Accumulation of transient carbohydrates and other primary metabolites from whole rosettes. **A**, Principal soluble sugars, Glc, Fru and Suc as indicated in the color key, for the indicated WT, Pro35S and ProCoYMV lines; **B**, starch levels (Glc equivalents) in the indicated lines; **C**, malate and fumarate; **D**, glucose-6-phosphate, in the indicated lines; **E**, Inorganic phosphate (P_i); **F**, total phosphate; **G**, chlorophyll-a and b as labeled; **H**, total protein as labeled; **I**, total amino acids expressed as µmol per gram fresh weight. Variation is SE; n=6 pools, each consisting of four rosettes; significant differences from WT are based on Student's T-Test: ^,P ≤0.07; *, P ≤ 0.05; **, P ≤ 0.01; ***, P ≤ 0.001.

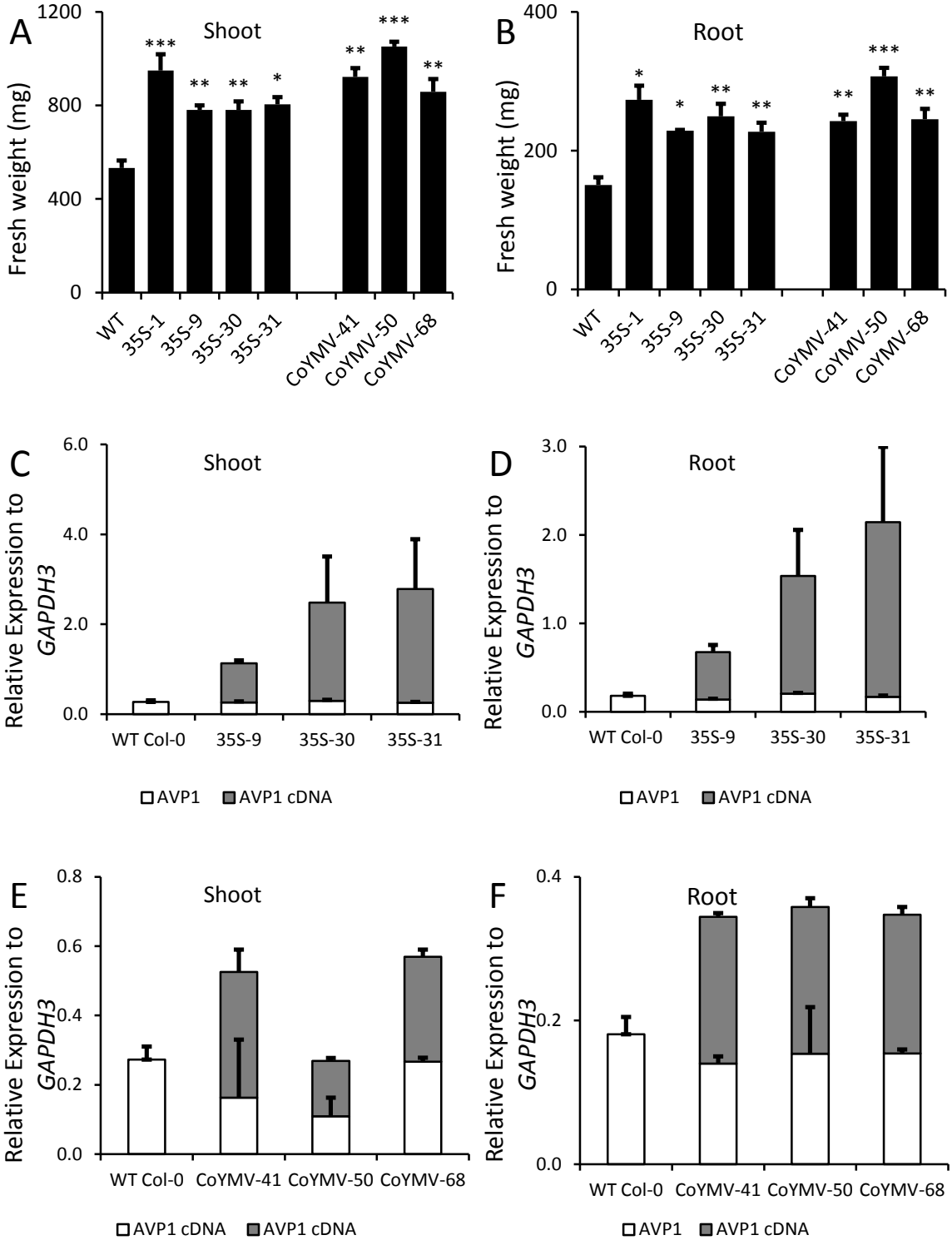
A
Shoot
Fresh weight (mg)
1200
800
400
0
***
**
**
*
**
***
**
WT
35S-1
35S-9
35S-30
35S-31
CoYMV-41
CoYMV-50
CoYMV-68
B
Root
Fresh weight (mg)
400
200
0
*
*
**
**
**
***
**
WT
35S-1
35S-9
35S-30
35S-31
CoYMV-41
CoYMV-50
CoYMV-68
C
Shoot
Relative Expression to GAPDH3
6.0
4.0
2.0
0.0
WT Col-0
35S-9
35S-30
35S-31
AVP1
AVP1 cDNA
D
Root
Relative Expression to GAPDH3
3.0
2.0
1.0
0.0
WT Col-0
35S-9
35S-30
35S-31
AVP1
AVP1 cDNA
E
Shoot
Relative Expression to GAPDH3
0.8
0.6
0.4
0.2
0.0
WT Col-0
CoYMV-41
CoYMV-50
CoYMV-68
AVP1 cDNA
AVP1 cDNA
F
Root
Relative Expression to GAPDH3
0.4
0.2
0.0
WT Col-0
CoYMV-41
CoYMV-50
CoYMV-68
AVP1
AVP1 cDNA

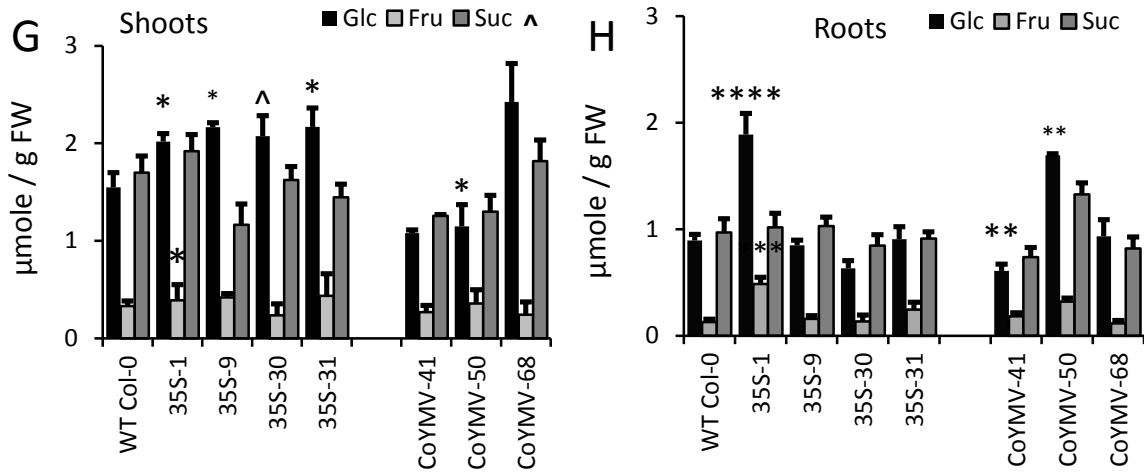
G
Shoots
Glc Fru Suc ^
µmole / g FW
3
2
1
0
WT Col-0
35S-1
35S-9
35S-30
35S-31
CoYMV-41
CoYMV-50
CoYMV-68
H
Roots
Glc Fru Suc
µmole / g FW

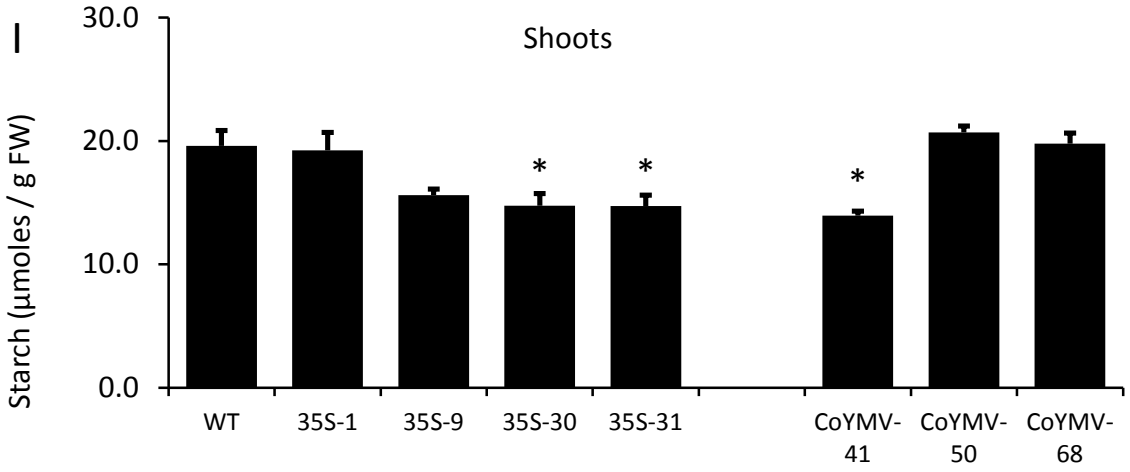
I
Shoots
Starch (µmoles / g FW)
30.0
20.0
10.0
0.0
WT
35S-1
35S-9
35S-30
35S-31
CoYMV-41
CoYMV-50
CoYMV-68

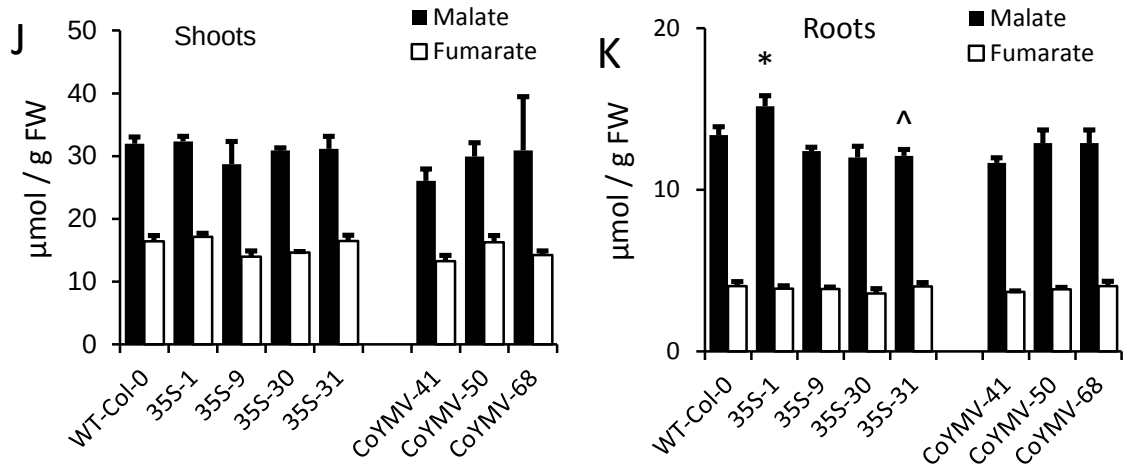
J
Shoots
Malate
Fumarate
µmol / g FW
50
40
30
20
10
0
WT-Col-0
35S-1
35S-9
35S-30
35S-31
CoYMV-41
CoYMV-50
CoYMV-68
K
Roots
Malate
Fumarate
µmol / g FW

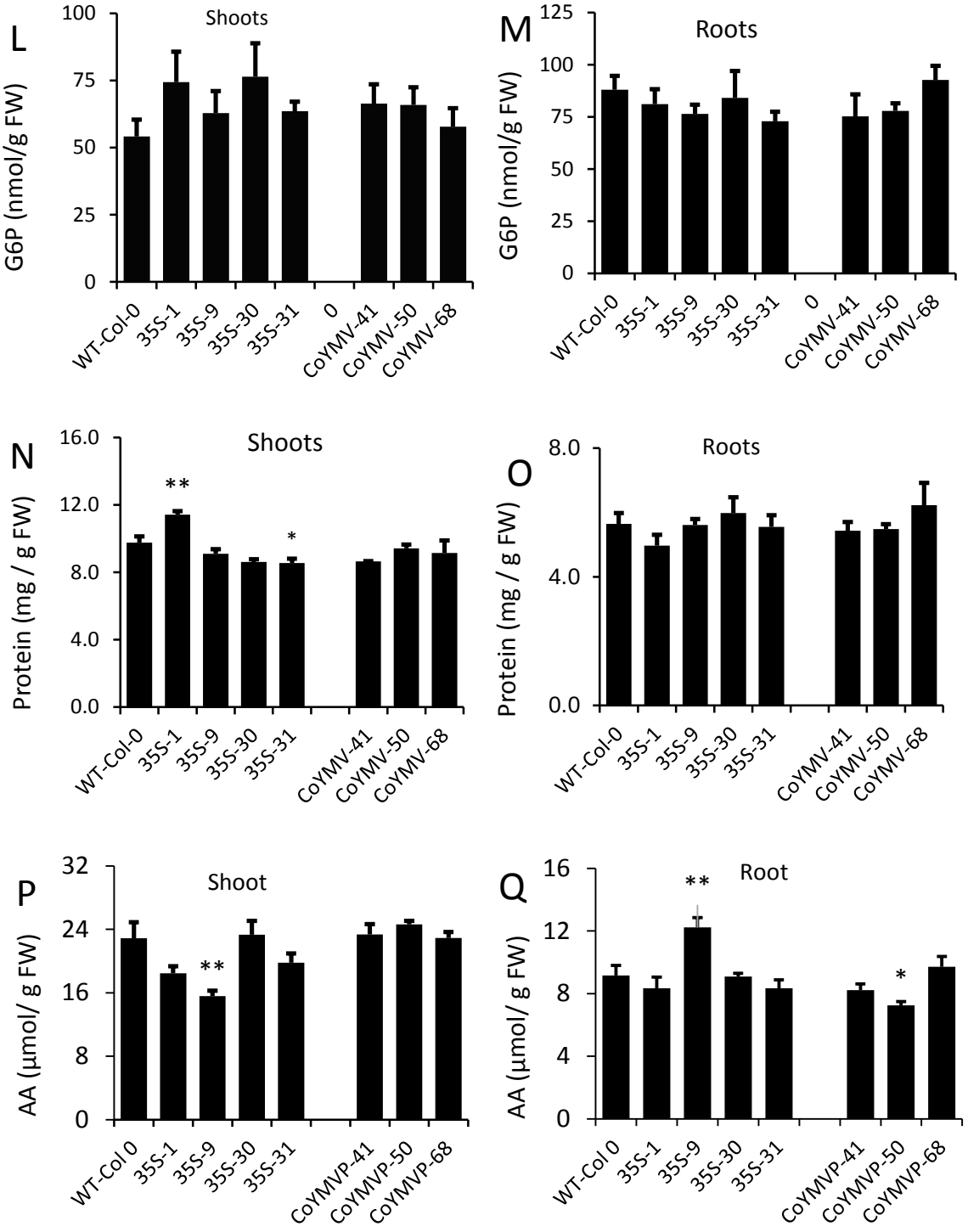

Figure 3-5: Fresh weight, transcript abundance, transient carbohydrates and other primary metabolites from shoots and roots of hydroponically grown tissues. **A**, Fresh weights of shoots and **B**, roots from hydroponically grown 22 d old plants, pools of 3 plants per replicate. RT-qPCR results showing *AVP1* expression from genomic loci (white bars) and cDNA (grey bars) compared to *GAPDH3* of **C**,shoots and **D**,roots of *Pro35S:AVP1* lines; **E**, shoots and **F**, roots of

ProCoYMV:AVP1 lines; Principal soluble sugars, Glc, Fru, Suc from **G**, shoots **H**,roots; **I**, Starch from hydroponically grown shoots; malate and fumarate from **J**,shoots, **K**, roots; glucose-6-phosphate from **L**,shoots, **M**, roots; total protein from, **N**, shoots, **O**, roots. Metabolite measurements expressed as as labeled; variation is SE; n=6 pools, each consisting 4 rosettes or 4 root systems; significant differences from WT are based on Student's T-Test: ^, P ≤0.07; *, P ≤ 0.05; **, P ≤ 0.01; ***, P ≤ 0.001;****, . P ≤ 1×10^{-7}.

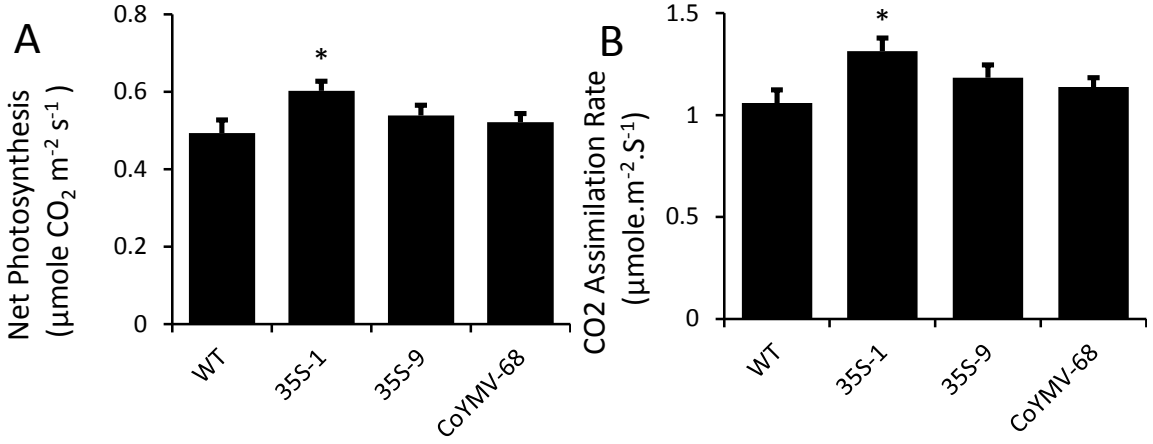

Figure 3-6: Photosynthesis is not significantly increased in Pro35S:AVP1 and ProCoYMV:AVP1 lines. **A**, Net photosynthesis measured as µmoles CO_2 m^{-2} S^{-1}. **B**, CO_2 assimilation rate measured as µmole.m^{-2}.S^{-1}. 35S-1 line has significantly greater photosynthesis rate compared to the other lines, n=12 plants for each line. Significant differences from WT are based on Student's T-Test: *, P ≤ 0.05; **, P ≤ 0.01; ***, P ≤ 0.001.

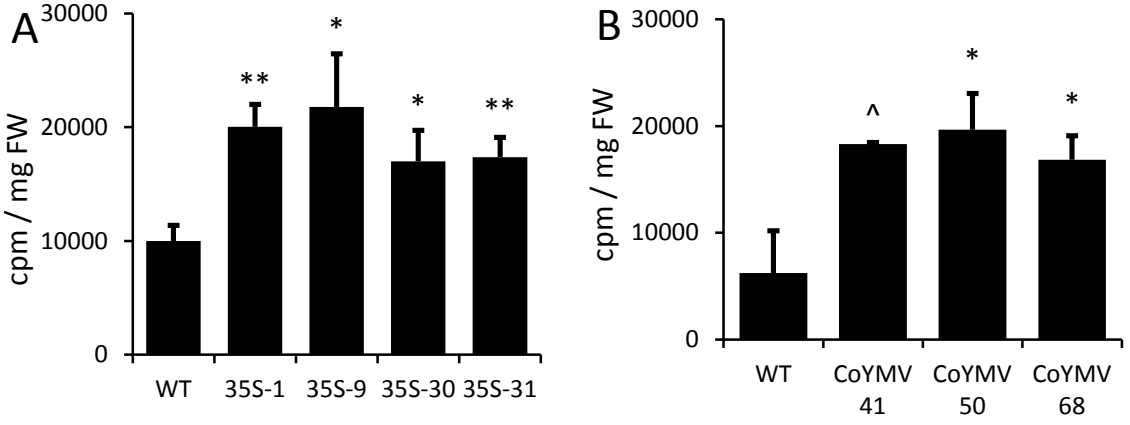

Figure 3-7: Photosynthetic labeling of transgenic and control plants with [^{14}C]-CO_2 for 20 min pulse and 40 min chase. Represented here are counts per min normalized to fresh weights of shoots. **A**, Pro35S:AVP1 and **B**, ProCoYMV:AVP1 shoots have significantly more label in the shoots which supports the hypothesis that *AVP1* overexpression may improve photosynthesis over a period of 20 min of [^{14}C]-CO_2 incorporation. Significant differences from WT are based on Student's T-Test: ^,P ≤0.07; *, P ≤ 0.05; **, P ≤ 0.01; ***, P ≤ 0.001.

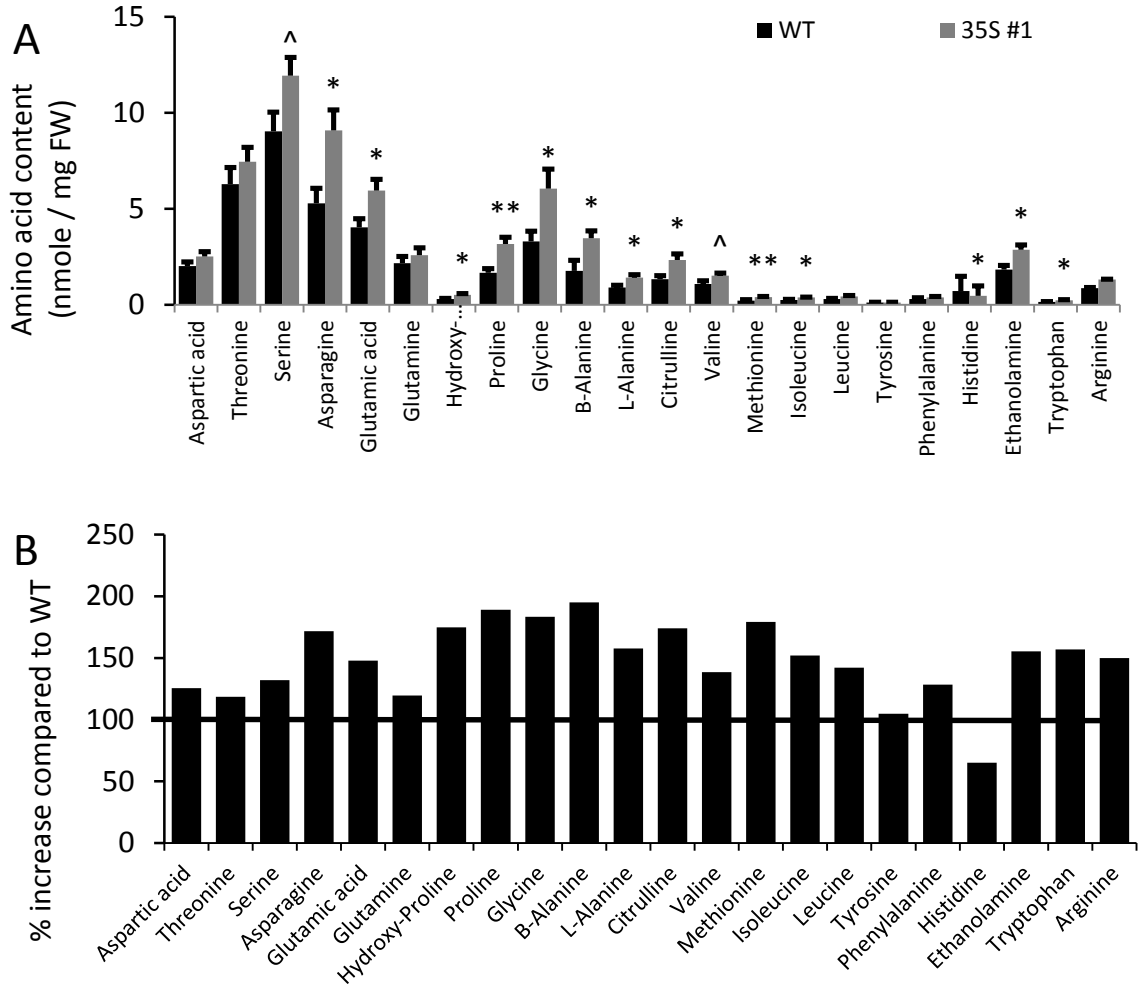

Figure 3-8: Amino acid profiling of Pro35S:AVP1 and WT by AccQ.Tag UPLC-MS.
A, Amino acid abundance is represented as nmol per gram fresh weight (n=6). Significant differences from WT are based on Student's T-Test: ^,P ≤0.07; *, P ≤ 0.05; **, P ≤ 0.01. **B,** Individual amino acids in 35S-1 represented as percentage increase compared to WT.

3.6 Chapter References

Alexandersson E, Saalbach G, Larsson C, Kjellbom P (2004) Arabidopsis plasma membrane proteomics identifies components of transport, signal transduction and membrane trafficking. Plant & Cell Physiology 45: 1543-1556

Arif A, Zafar Y, Arif M, Blumwald E (2012) Improved growth, drought tolerance, and ultrastructural evidence of increased turgidity in tobacco plants overexpressing Arabidopsis vacuolar pyrophosphatase (*AVP1*). Molecular Biotechnology 54: 379-392

Armenta JM, Cortes DF, Pisciotta JM, Shuman JL, Blakeslee K, Rasoloson D, Ogunbiyi O, Sullivan DJ, Shulaev V (2010) Sensitive and rapid method for amino acid quantitation in malaria

biological samples using AccQ.Tag ultra performance liquid chromatography-electrospray ionization-MS/MS with multiple reaction monitoring. Analytical Chemistry 82: 548-558

Atilio B, Causing H (1996) The central role of amino acids on nitrogen utilization and plant growth. Journal of Plant Physiology 149: 358-362

Ayre BG (2011) Membrane-transport systems for sucrose in relation to whole-plant carbon partitioning. Molecular Plant 4: 377-394

Ayre BG, Turgeon R (2004) Graft transmission of a floral stimulant derived from CONSTANS. Plant Physiology 135: 2271-2278

Baltscheffsky H, Von Stedingk LV, Heldt HW, Klingenberg M (1966) Inorganic pyrophosphate: formation in bacterial photophosphorylation. Science 153: 1120-1122

Bantan-Polak T, Kassai M, Grant KB (2001) A comparison of fluorescamine and naphthalene-2,3-dicarboxaldehyde fluorogenic reagents for microplate-based detection of amino acids. Analytical Biochemistry 297: 128-136

Bao A, Suo-Min W, Guo-Qiang W, Jie-Jun X, Jin-Lin Z, Chun-Mei W (2009) Overexpression of the *Arabidopsis* H^+-PPase enhanced resistance to salt and drought stress in transgenic alfalfa (*Medicago sativa* L.). Plant Science 176: 232-240

Boyes DC, Zayed AM, Ascenzi R, McCaskill AJ, Hoffman NE, Davis KR, Görlach J (2001) Growth stage-based phenotypic analysis of Arabidopsis: a model for high throughput functional genomics in plants. The Plant Cell 13: 1499-1510

Bradford MM (1976) A rapid and sensitive method for the quantitation of microgram quantities of protein utilizing the principle of protein-dye binding. Analytical Biochemistry 72: 248-254

Brady SM, Orlando DA, Lee JY, Wang JY, Koch J, Dinneny JR, Mace D, Ohler U, Benfey PN (2007) A high-resolution root spatiotemporal map reveals dominant expression patterns. Science 318: 801-806

Chiou TJ, Aung K, Lin SI, Wu CC, Chiang SF, Su CL (2006) Regulation of phosphate homeostasis by MicroRNA in Arabidopsis. The Plant Cell 18: 412-421

Clough SJ, Bent AF (1998) Floral dip: a simplified method for Agrobacterium-mediated transformation of *Arabidopsis thaliana*. The Plant Journal 16: 735-743

Conn SJ, Hocking B, Dayod M, Xu B, Athman A, Henderson S, Aukett L, Conn V, Shearer MK, Fuentes S, Tyerman SD, Gilliham M (2013) Protocol: optimising hydroponic growth systems for nutritional and physiological analysis of *Arabidopsis thaliana* and other plants. Plant Methods 9: 4

Cross JM, von Korff M, Altmann T, Bartzetko L, Sulpice R, Gibon Y, Palacios N, Stitt M (2006) Variation of enzyme activities and metabolite levels in 24 Arabidopsis accessions growing in carbon-limited conditions. Plant Physiology 142: 1574-1588

Curtis MD, Grossniklaus U (2003) A gateway cloning vector set for high-throughput functional analysis of genes in planta. Plant Physiology 133: 462-469

Dasgupta K, Khadilkar A, Sulpice R, Pant B, Scheible WR, Fisahn J, Stitt M, Ayre BG (2014) Expression of sucrose transporter cDNAs specifically in companion cells enhances phloem loading and long-distance transport of sucrose, but leads to an inhibition of growth and the perception of a phosphate limitation. Plant Physiology 165: 715–731

Davies JM (1997) Vacuolar energization: pumps, shunts and stress. Journal of Experimental Botany 48: 633-641

Etienne C, Rothan C, Moing A, Plomion C, Bodénès C, Svanella-Dumas L, Cosson P, Pronier V, Monet R, Dirlewanger E (2002) Candidate genes and QTLs for sugar and organicacidcontent in peach [*Prunus persica* (L.) Batsch]. Theoretical and Applied Genetics 105: 145-159

Ferjani A, Segami S, Horiguchi G, Muto Y, Maeshima M, Tsukaya H (2011) Keep an eye on PPi: the vacuolar-type H^+-pyrophosphatase regulates postgerminative development in Arabidopsis. The Plant Cell 23: 2895-2908

Fernie AR, Martinoia E (2009) Malate. Jack of all trades or master of a few? Phytochemistry 70: 828-832

Flügge U-I, Häusler RE, Ludewig F, Fischer K (2003) Functional genomics of phosphate antiport systems of plastids. Physiologia Plantarum 118: 475-482

Gaxiola RA, Fink GR, Hirschi KD (2002) Genetic manipulation of vacuolar proton pumps and transporters. Plant Physiology 129: 967-973

Gaxiola RA, Li J, Undurraga S, Dang LM, Allen GJ, Alper SL, Fink GR (2001) Drought- and salt-tolerant plants result from overexpression of the *AVP1* H^+-pump. Proceedings of the National Academy of Sciences of the United States of America 98: 11444-11449

Gaxiola RA, Sanchez CA, Paez-Valencia J, Ayre BG, Elser JJ (2012) Genetic manipulation of a "vacuolar" $H(^+)$-PPase: from salt tolerance to yield enhancement under phosphorus-deficient soils. Plant Physiology 159: 3-11

Gibon Y, Blaesing OE, Hannemann J, Carillo P, Höhne M, Hendriks JH, Palacios N, Cross J, Selbig J, Stitt M (2004) A Robot-based platform to measure multiple enzyme activities in Arabidopsis using a set of cycling assays: comparison of changes of enzyme activities and transcript levels during diurnal cycles and in prolonged darkness. The Plant Cell 16: 3304-3325

Gibon Y, Pyl ET, Sulpice R, Lunn JE, Höhne M, Günther M, Stitt M (2009) Adjustment of growth, starch turnover, protein content and central metabolism to a decrease of the carbon supply when Arabidopsis is grown in very short photoperiods. Plant Cell Environment 32: 859-874

Gibon Y, Vigeolas H, Tiessen A, Geigenberger P, Stitt M (2002) Sensitive and high throughput metabolite assays for inorganic pyrophosphate, ADPGlc, nucleotide phosphates, and glycolytic intermediates based on a novel enzymic cycling system. The Plant Journal 30: 221-235

Gonzalez N, De Bodt S, Sulpice R, Jikumaru Y, Chae E, Dhondt S, Van Daele T, De Milde L, Weigel D, Kamiya Y, Stitt M, Beemster GT, Inze D (2010) Increased leaf size: different means to an end. Plant Physiology 153: 1261-1279

Hammond JP, White PJ (2008) Sucrose transport in the phloem: integrating root responses to phosphorus starvation. Journal of Experimental Botony 59: 93-109

Harrison S, Mott E, Parsley K, Aspinall S, Gray J, Cottage A (2006) A rapid and robust method of identifying transformed *Arabidopsis thaliana* seedlings following floral dip transformation. Plant Methods 2: 19

Hendriks JH, Kolbe A, Gibon Y, Stitt M, Geigenberger P (2003) ADP-glucose pyrophosphorylase is activated by posttranslational redox-modification in response to light and to sugars in leaves of Arabidopsis and other plant species. Plant Physiology 133: 838-849

Hirner B, Fischer WN, Rentsch D, Kwart M, Frommer WB (1998) Developmental control of H^+/amino acid permease gene expression during seed development of Arabidopsis. The Plant Journal 14: 535-544

Hunt E, Gattolin S, Newbury HJ, Bale JS, Tseng HM, Barrett DA, Pritchard J (2010) A mutation in amino acid permease AAP6 reduces the amino acid content of the Arabidopsis sieve elements but leaves aphid herbivores unaffected. Journal of Experimental Botany 61: 55-64

Khoudi H, Maatar Y, Gouiaa S, Masmoudi K (2012) Transgenic tobacco plants expressing ectopically wheat H^+-pyrophosphatase (H^+-PPase) gene *TaVP1* show enhanced accumulation and tolerance to cadmium. Journal of Plant Physiology 169: 98-103

Krebs M, Beyhl D, Gorlich E, Al-Rasheid KA, Marten I, Stierhof YD, Hedrich R, Schumacher K (2010) Arabidopsis V-ATPase activity at the tonoplast is required for efficient nutrient storage but not for sodium accumulation. Proceedings of the National Academy of Sciences of the United States of America 107: 3251-3256

Langhans M, Ratajczak R, Lutzelschwab M, Michalke W, Wachter R, Fischer-Schliebs E, Ullrich CI (2001) Immunolocalization of plasma-membrane H^+-ATPase and tonoplast-type

pyrophosphatase in the plasma membrane of the sieve element-companion cell complex in the stem of Ricinus communis L. Planta 213: 11-19

León P, Sheen J (2003) Sugar and hormone connections. Trends in Plant Science 8: 110-116

Lerchl J, Geigenberger P, Stitt M, Sonnewald U (1995) Impaired photoassimilate partitioning caused by phloem-specific removal of pyrophosphate can be complemented by a phloem-specific cytosolic yeast-derived invertase in transgenic plants. The Plant Cell 7: 259-270

Li B, Wei A, Song C, Li N, Zhang J (2008) Heterologous expression of the *TsVP* gene improves the drought resistance of maize. Plant Biotechnology Journal 6: 146-159

Li J, Yang H, Peer WA, Richter G, Blakeslee J, Bandyopadhyay A, Titapiwantakun B, Undurraga S, Khodakovskaya M, Richards EL, Krizek B, Murphy AS, Gilroy S, Gaxiola R (2005) Arabidopsis H^+-PPase AVP1 regulates auxin-mediated organ development. Science 310: 121-125

Li Z, Baldwin CM, Hu Q, Liu H, Luo H (2010) Heterologous expression of Arabidopsis H^+-pyrophosphatase enhances salt tolerance in transgenic creeping bentgrass (*Agrostis stolonifera L.*). Plant, Cell & Environment 33: 272-289

Lv S, Zhang K, Gao Q, Lian L, Song Y, Zhang J (2008) Overexpression of an *H^+-PPase* gene from *Thellungiella halophila* in cotton enhances salt tolerance and improves growth and photosynthetic performance. Plant & Cell Physiology 49: 1150-1164

Lv SL, Lian LJ, Tao PL, Li ZX, Zhang KW, Zhang JR (2009) Overexpression of *Thellungiella halophila* H($^+$)-PPase (*TsVP*) in cotton enhances drought stress resistance of plants. Planta 229: 899-910

Maeshima M (1991) H($^+$)-translocating inorganic pyrophosphatase of plant vacuoles. Inhibition by Ca^{2+}, stabilization by Mg^{2+} and immunological comparison with other inorganic pyrophosphatases. European Journal of Biochemistry 196: 11-17

Matsuda Y, Liang G, Zhu Y, Ma F, Nelson RS, Ding B (2002) The Commelina yellow mottle virus promoter drives companion-cell-specific gene expression in multiple organs of transgenic tobacco. Protoplasma 220: 51-58

Medberry SL, Lockhart BE, Olszewski NE (1992) The Commelina yellow mottle virus promoter is a strong promoter in vascular and reproductive tissues. The Plant Cell 4: 185-192

Mohammed S, Nishio S, Takahashi H, Shiratake K, Ikeda H, Kanahama K, Kanayama Y (2012) Role of Vacuolar H^+-inorganic pyrophosphatase in tomato fruit development. Journal of Experimental Botony 63: 5613-5621

Paez-Valencia J, Patron-Soberano A, Rodriguez-Leviz A, Sanchez-Lares J, Sanchez-Gomez C, Valencia-Mayoral P, Diaz-Rosas G, Gaxiola R (2011) Plasma membrane localization of the type I H^+-PPase AVP1 in sieve element–companion cell complexes from *Arabidopsis thaliana*. Plant Science 181: 23-30

Paez-Valencia J, Sanchez-Lares J, Marsh E, Dorneles LT, Santos MP, Sanchez D, Winter A, Murphy S, Cox J, Trzaska M, Metler J, Kozic A, Facanha AR, Schachtman D, Sanchez CA, Gaxiola RA (2013) Enhanced proton translocating pyrophosphatase activity improves nitrogen use efficiency in romaine lettuce. Plant Physiology 161: 1557-1569

Pei L, Wang J, Li K, Li Y, Li B, Gao F, Yang A (2012) Overexpression of *Thellungiella halophila* H^+-pyrophosphatase gene improves low phosphate tolerance in maize. PLOS ONE 7: e43501

Pizzio GA, Paez-Valencia J, Khadilkar AS, Regmi KC, Patron-Soberano A, Zhang S, Sanchez-Lares J, Furstenau T, Li J, Sanchez-Gomez C, Valencia-Mayoral P, Yadav UP, Ayre BG, Gaxiola RA (2015) Arabidopsis proton-pumping pyrophosphatase AVP1 expresses strongly in phloem where it is required for PPi metabolism and photosynthate partitioning. Plant Physiology

Rocha Facanha A, de Meis L (1998) Reversibility of H^+-ATPase and H^+-pyrophosphatase in tonoplast vesicles from maize coleoptiles and seeds. Plant Physiology 116: 1487-1495

Salazar C, Armenta JM, Cortes DF, Shulaev V (2012) Combination of an AccQ.Tag-ultra performance liquid chromatographic method with tandem mass spectrometry for the analysis of amino acids. Methods in Molecular Biology 828: 13-28

Schneider CA, Rasband WS, Eliceiri KW (2012) NIH Image to ImageJ: 25 years of image analysis. Nature Methods 9: 671-675

Sonnewald U (1992) Expression of *E. coli* inorganic pyrophosphatase in transgenic plants alters photoassimilate partitioning. The Plant Journal 2: 571-581

Srivastava AC, Ganesan S, Ismail IO, Ayre BG (2009) Effective carbon partitioning driven by exotic phloem-specific regulatory elements fused to the *Arabidopsis thaliana AtSUC2* sucrose-proton symporter gene. BMC Plant Biology 9: 7

Stitt M, Lilley RM, Gerhardt R, Heldt HW (1989) Metabolite levels in specific cells and subcellular compartments of plant-leaves. Methods in Enzymology 174: 518-552

Streb S, Zeeman SC (2012) Starch metabolism in Arabidopsis. Arabidopsis Book 10: e0160

Sturm A (1999) Invertases. Primary structures, functions, and roles in plant development and sucrose partitioning. Plant Physiology 121: 1-8

Tegeder M (2012) Transporters for amino acids in plant cells: some functions and many unknowns. Current Opinion in Plant Biology 15: 315-321

Yang H, Knapp J, Koirala P, Rajagopal D, Peer WA, Silbart LK, Murphy A, Gaxiola RA (2007) Enhanced phosphorus nutrition in monocots and dicots over-expressing a phosphorus-responsive type I H^+-pyrophosphatase. Plant Biotechnology Journal 5: 735-745

Zell MB, Fahnenstich H, Maier A, Saigo M, Voznesenskaya EV, Edwards GE, Andreo C, Schleifenbaum F, Zell C, Drincovich MF, Maurino VG (2010) Analysis of Arabidopsis with highly reduced levels of malate and fumarate sheds light on the role of these organic acids as storage carbon molecules. Plant Physiology 152: 1251-1262

CHAPTER 4

AVP1 ENHANCES PHLOEM LOADING AND PHLOEM TRANSPORT IN CONSTITUTIVE AND PHLOEM SPECIFIC OVEREXPRESSION LINES

4.1 Abstract

We propose a model in which AVP1 in companion cells localizes to the PM and uses the PMF to function as a synthase and increase pyrophosphate levels (Paez-Valencia et al., 2011; Gaxiola et al., 2012). In this model, increased pyrophosphate levels promote Suc oxidation for ATP synthesis, which in turn enhances the PMF across the PM to energize phloem loading. The thereotical maximum for complete oxidation of one molecule of Suc yields 72 ATP (Berg JM, 2002; Amthor, 2003) and thus a small increase in Suc oxidation may dramatically increase the companion cell membrane potential for improved loading. Several experiments were therefore conducted to test for enhanced phloem loading and long distance transport of Suc. To measure the phloem loading capacity of the *Pro35S:AVP1* and *ProCoYMV:AVP1* overexpression lines, [^{14}C]-Suc uptake into veins of leaf discs was conducted. The amount of incorporated label was quantified with scintillation counting. In order to measure the nutrient transport capacity of plants, we conducted [^{14}C]-CO_2 photosynthetic labelling followed by phloem exudation of severed rosettes into EDTA solutions. In order to measure transport to heterotrophic organs, source leaves of two-week-old plants were photosynthetically labeled with [^{14}C]-CO_2 and ^{14}C transport into different root sections was measured by scintillation counting.

4.2 Introduction

The ability to transport nutrients from source to sink tissues in part determines the ability of a plant to accumulate biomass. Alterations in phloem transport have been proposed

as a potential means to enhance plant productivity and yield (Yadav, Ayre and Bush. Frontiers in Plant Sciences, In press)(Ainsworth and Bush, 2011). Reduced phloem transport leads to Suc accumulation in the source tissues, which in turn leads to negative feedback on photosynthesis (Paul et al., 2001; Paul and Foyer, 2001; Srivastava et al., 2008). The corollary of this is that enhanced phloem transport may increase productivity by 1) increasing nutrient transport to growing sinks and storage organs and 2) relieve feedback inhibition on photosynthesis. Suc loading in the phloem is known to be altered based on the needs of the plant and regulation exists to control the amount of Suc loaded into the phloem and transported (Kuhn and Grof, 2010; Ayre, 2011). It was proposed that uncoupling of such regulation by using heterologous promoters that are not controlled by endogenous regulation may be useful tools to maintain elevated levels of phloem loading and consequently phloem transport (Srivastava et al., 2009; Dasgupta et al., 2014). Alternatively or perhaps synergistically, for enhanced phloem loading and transport, energizing the phloem to generate more PMF could help achieve desired goals (Haruta and Sussman, 2012). The PMF is maintained by PM ATPase which require ATP to generate PMF (Sze et al., 1999).

According to our hypothesis AVP1 at the phloem PM uses the PMF to synthesize PPi and provides substrate for ATP synthesis via Suc oxidation. We further propose that this function helps energize the phloem and accounts for the enhanced vitality of *AVP1* overexpressing plants (Gaxiola et al., 2012). Results of phloem-specific overexpression of *AVP1* showed that plants have higher biomass but inconsistent alterations in soluble sugar accumulation (Chapter 3). Here we use combination of ^{14}C labeling, phloem exudation, phloem loading, phloem

transport and unloading in the sink tissues to show that *AVP1* overexpression in the phloem companion cells enhanced Suc loading, transport and unloading.

4.3 Results: ^{14}C-Labeling Indicates Enhanced Phloem Transport and Phloem Loading

To directly test the phloem loading capacity of plants overexpressing *AVP1*, uptake of ^{14}C-Suc into the leaf veins was studied. Leaf discs were vacuum infiltrated with a buffered solution containing [^{14}C]-Suc, incubated for 20 min and then washed throughly to remove ^{14}C-Suc from the apoplasm. The washed disk were blotted dry, frozen on dry ice and lyophilized. Autoradiography confirmed that the majority of ^{14}C label was concentrated in the veins. Scintillation counting showed that all of the Pro35S:AVP1 and ProCoYMV:AVP1 lines absorbed significanlty more [^{14}C]-Suc, indicating that the transgenic lines have enhanced phloem loading compared to WT (Figure 4.1). It is important to note that Pro35S drives *AVP1* expression in the veins as well as more broadly, and thus more incorporation of label in Pro35S:AVP1 lines was expected. But, more label incorporation compared to WT was observed in both Pro35S:AVP1 and ProCoYMV:AVP1 lines, consistent with greater phloem loading due to an energized phloem uptake system.

Enhanced phloem loading mediated by *AVP1* expression in companion cells should lead to greater phloem transport. To study the transport efficiency of Pro35S:AVP1 and ProCoYMV:AVP1 lines, ^{14}C photosynthetic labeling followed by collecting phloem exudations was used to analyze movement of ^{14}C-labeled photoassimilates from the source to the sink. Rosettes were first photosynthetically labled with [^{14}C]-CO_2 and then the stems below the rosettes were cut and maintained in an EDTA solution, such that <2 mm of the cut stem was

submerged. The first 20 min of exudation, which would contain the contents of cut cells, was discarded (Ayre et al., 2003), and ^{14}C exudation over the next two 1-h intervals was measured and expressed as counts per minute exuded per hour per milligram of fresh weight. EDTA chelates the Ca^{2+} ions which are necessary for plugging the damaged sieve tube elements. EDTA is however toxic to the plant cells and thus a dilute concentration of 5mM, pH 6.0, was used. To minimize EDTA entering the rosettes via the xylem and transpiration, exudations were conducted in darkened, sealed chambers to promote stomatal closure and maximize humidity which minimizes uptake (Turgeon and Medville, 2004). Also, enzymes like cell wall invertases released from cut plant material could degrade contents of the phloem sap, thus exudates were immediately chilled on ice after collection, and enzymes were destroyed by addition of chloroform. *AVP1* overexpressing lines had phloem exudation rates 2- to 5-fold higher than those of wild type (Figure 4.2), with the greatest enhancement in the ProCoYMV:AVP1 lines. This indicates more efficient loading and transport of carbon in the phloem. The exudation rates are significatly higher than WT in both one-hour intervals, indicating that the results obtained were consistent and not the result of release from damaged cells. These results indicate that Pro35S:AVP1 and ProCoYMV:AVP1 are more efficient in transporting photoassimilates through phloem from source to sink tissues. This method of assessing phloem transport rates by this EDTA exudation method suffers criticism as these are deemed non-physiological and not sink limited since heterotrophic roots are removed from the plants (Turgeon and Wolf, 2009; Slewinski, 2011) . Hence, the experiment addresses ^{14}C that can enter the phloem transport stream, but does not speak to whether more photoassimilate is reaching and unloading into sink organs.

To assess the efficiency of phloem transport out of leaves and into sink organs, plants were grown on vertical plastic plates and each vertical plate functioned as an independent ^{14}C-CO_2 labeling chamber. The source leaves were photosynthetically labeled for 20 min with [^{14}C]-CO_2 and ^{14}C transport into roots was measured by scintillation counting. Relative to WT, the Pro35S:AVP1 (Figure 4.3 A) and ProCoYMV:AVP1 lines (Figure 4.3 B) incorporated more total ^{14}C per milligram fresh weight. This is consistent with other evidence that *AVP1* expression enhances primary productivity: i.e., the plants are larger (see Chapter 3, Figure 1) and infrared gas analysis suggests increased photosynthesis in 35S-1 (Figure 3.7).

Of the total label incorporated, WT plants transported 5 % to 7 % of the photoassimilated label to roots, Pro35S:AVP1 plants transported more than 15 %, and ProCoYMV:AVP1 transported 25 % to 35 % of the incorporated label to roots (Figure 4.3D-G). This shows that long-distance transport and unloading in the root sink tissues is enhanced by constitutive and especially by companion-cell-specific *AVP1* expression. Furthermore, regions of cell division and elongation constitute the strongest sinks, and thus root was cut into one-cm section, starting at the root tip, to establish where the majority of the photoassimilate was partitioning. The *Pro35S:AVP1* and *ProCoYMV:AVP1* lines transported a greater portion of total ^{14}C out of rosettes (Figure 4.4B and D) to the heterotrophic roots (Figure 4.4 C and E). When dissected into 1 cm sections, it was clear that Pro35S:AVP1 and ProCoYMV:AVP1 lines transported a greater portion of ^{14}C to the growing tip of the primary root (lowest 1 cm in Figure 4.4 C and E) and to the uppermost part of the root which contained emerging lateral roots, than WT.

4.4 Discussion

To test the our hypothesis that the phloem loading and transport capacity is enhanced in transgenic plants, three complementary approaches were used: phloem exudates, phloem loading, and transport capacity. Enhanced phloem loading capacity was demonstrated with [^{14}C]- Suc uptake studies. Phloem exudation studies with ^{14}C labelling showed increased accumulation of Suc in the transport phloem of the transgenic plants. Enhanced transport of photoassimilates to the roots of transgenic plants was shown in the ^{14}C-labeling studied. Increased unloading occurs in the growing apical tip of the roots of transgenic lines. Studies to test the influence of *AVP1* overexpression on Suc synthesis and accumulation of representative primary metabolites was not conclusive based on steady state measurements (Chapter 3). But, ^{14}C labeling studies testing phloem loading, transport and unloading capacities showed that *AVP1* overexpressing plants with CaMV 35 and importantly with CoYMV promoter had enhanced capacity of phloem transport. Thus, more reduced carbon was supplied to the roots which may have been one cause of improved growth by increasing nutrient use efficiency.

4.5.1 How Does Enhanced Suc Transport Contribute to Larger Plants?

During the onset of phosphate starvation several transcriptional, metabolical and physiological alterations occur in plants which either improves ability to aquire more phosphate from the soil or programs plants to more efficiently use in-house phosphate (Hammond and White, 2008, 2011). Shoot derived Suc has been shown to control phosphate starvation responses (Hermans et al., 2006; Karthikeyan et al., 2007). Enhancing phloem transport along with other nutrient translocation and mineral acquisition systems could lead to more efficient mobilization and utilization of resources. In phosphate limiting conditions, increased rates of

phloem transport can not be retained for a long time. In phosphate starved bean leaves, Suc export reverted to basal levels after 9-10 days (Cakmak et al., 1994). In addition, increased phloem transport has been postulated to enhance phosphate transporters (Gaxiola et al., 2012) and in phosphate replenished conditions, plants may be able to retain high transport rates for the whole growth period. In our experiments, in Pro35S:AVP1 and ProCoYMV:AVP1 plants there was more loading and transport, and more unloading in the growing regions of the root. These results are consistent with better phosphate use efficiency. *SUT* over-expressing lines described in Chapter 2 and (Dasgupta et al., 2014) probably do not have better phosphate use efficiency.

In oder to manipulate Suc concentration in phosphate sufficient conditions, tobacco plants were grown in high light conditions and phloem translocation was increased in plants having enhanced photosynthetic capacity (Hammond 2008, Nagel 2006). In our studies, *AVP1* overexpressing plants had higher photosynthetic capacity as demonstrated by ^{14}C labeling experiments (Chapter 3, Figure 3.7). Enhancing phloem transport has been implicated to enhance auxin transport, decreased cytokinin levels, and thus increased lateral rooting. Increased lateral roots may enhance rhizosphere phosphate availability by exuding organic acids and enzymes (Hammond and White, 2008, 2011). In romain Lettuce, Pro35S:AVP1 plants have increased rhizosphere acidification leading to enhanced uptake of nutrients (Paez-Valencia et al., 2013).

The reason *AVP1* overexpressing plants were energy efficient and able to accumulate higher biomass than *AtSUC2* overexpresing plants could be because, in addition to enhanced phloem transport, there are alterations in nitrogen metabolism (Gonzalez et al., 2010). Based on earlier studies (Gonzalez et al., 2010), several Suc and phosphate metabolism genes were

differentially expressed in Pro35S:AVP1 plants. Enhacement in root biomass may be due to the increased supply of nutrients in the growing regions. The phloem loading assay with ^{14}C-Suc showed that the transgenic plants have increased ability of phloem loading. Hence, increased phloem loading, transport, enhanced availability of PMF, better nutrient acquisition and mobilization capacity and altered hormone metabolism might be several different reasons why *AVP1* overexpressing plants have several advantages compared to WT plants.

4.6 Materials and Methods

To test for phloem loading capacity of transgenic and control plants, [^{14}C]-Suc uptake studies were conducted. Leaves of 21 days old plants were harvested by severing the petiole near the base of the lamina. Leaves were submerged in MES buffer (20 mM MES, 2 mM $CaCl_2$, pH 5.5 with KOH) and 5 mm size leaf discs were cut under solution with cork bore. Once all leaf discs were collected, the solution was replaced with 500 µl of fresh buffer containing [^{14}C]-Suc (1 mM Suc, 29 KBq) ml^{-1}, (MP Biomedicals) in MES buffer. Leaves were held down with 4 mm glass beads in a 24-well microtiter plate. Each replicate contained 6 leaf discs from one biological replicate and 6 biological replicates were used for one genotype. The leaf discs were vacuum infiltrated to allow for absorption of labeled solution, and incubated at room temperature for 20 min. Excess solution was removed, followed by three washes in MES buffer. The leaf discs were gently blotted dry, placed in aluminum envelopes, and snap frozen in powdered dry ice. Frozen discs were lyophilized at -30 °C for 48 hour, pressed between steel plates in a vice to bring the labeled phloem close to tissue surface, and exposed to X-ray film (Kodak Biomax MR film) for 24 hour to assess effective labeling. The leaf discs were cleared with 1 ml 95 % ethanol for 30 min, and then bleached with 1 ml commercial bleach for 15 min.

cpm were measured after adding scintillation fluid and [^{14}C]-Suc uptake calculated as cpm per surface area. Blanks contained 95 % ethanol, 1 ml bleach and scintillation fluid (i.e. no leaf tissue). These were used to establish a baseline of autoluminescence.

4.6.1 Measuring the Phloem Contents by Radiolabeling and EDTA Exudation

To measure the transport capacity of transgenic and control plants, an EDTA-exudation method (Srivastava et al., 2008; Dasgupta et al., 2014) was used to collect phloem contents from detached rosettes after photosynthetically labeling with [^{14}C]-CO_2 (Cao et al., 2013; Dasgupta et al., 2014). Transparent catering containers with hinged lids were used for plant growth; drainage holes were created by puncturing and filled half full with potting mix. Plants were grown in these containers for 21 d before labeling. Nine plants were grown in each chamber: 3 replicate plants of 2 independent experimental lines and WT controls, and were arranged in a random fashion. The lids were left open during the growth period. On the day of the labeling, plants were acclimated under 400-W halide lamp for 20 min before the start of the experiment. Chambers were sealed by applying vacuum grease on the lids and were further secured with parafilm. All labeling was conducted in 6 to 8 hour into the 12 hour light period, individual chambers were processed making sure that each chamber was directly under the light source during the period of labeling. Plants were labeled with [^{14}C]-CO_2 which was generated by acidification of 5 µl (5 µCi, 0.185 MBq) of [^{14}C]-HCO_3 (MP Biomedicals) with 15 µl of lactic acid in the barrel of a syringe with a 20-gauge needle inserted into the chamber. The hole was immediately sealed with modeling clay after removal of the needle. Plants were allowed to photosynthesize for 20 min in the presence of [^{14}C]-CO_2 and the excess of [^{14}C]-CO_2 was removed by an air pump connected to a soda lime column to bind residual [^{14}C]-CO_2. Plants

were then allowed to photosynthesize in normal air for an additional 15 min. The rosettes were severed at the hypocotyls and fresh weight determined. Hypocotyls were re-cut under EDTA and placed in coulter counter vials which served as collection chambers, with 5 mM EDTA. For each plant, exudates were collected for 20 min, after which rosettes were transferred to another coulter counter vial and exudate collected for 1 hour, then transferred to a third vial and exudate collected for a second hour. After each time point, exudates were immediately placed on ice and 200 µl of chloroform was added to destroy enzymes released into the exudate that could digest released photoassimilates. 500 µl of exudate was mixed with 5 ml of ScintiSafe Plus 50 % (Phenylxylylethane) scintillation solution (Thermo Fisher Scientific) and cpm determined by scintillation counting (Figure 4.2 A).

4.6.2 Radiolabeling with [^{14}C]-CO_2 to Measure Rates of Phloem Transport

Transgenic and control plants were germinated on 0.5 MS with 1 % Suc for 7 days and transferred to 0.5 MS with 0 % Suc plates to grow vertically for 8 days. Labeling was conducted similar to the method described above, but [^{14}C]-CO_2 was injected into the plates rather than into catering boxes. Each plate served as an individual labeling chamber containing 6 plants, 2 of WT and 2 of 2 different transgenic lines. Plants were labeled with [^{14}C]-CO_2 generated by acidification of 5 µl (5 µCi, 0.185 MBq) of [^{14}C]-HCO_3 (MP Biomedicals) by using 15 µl of lactic acid. Plants were allowed to photosynthesize for 20 min. Excess of [^{14}C]-CO_2 was removed by an air pump connected to a soda lime column. Plants were allowed to photosynthesize for another 40 min in normal air. Shoots and roots were separated and put in scintillation vials containing scintillation fluid and counts measured in scintillation counter. Counts were normalized with

fresh weights for shoots. For experiments with root cuts, roots were cut at 1 cm intervals from the tip of the root and roots from two plants were pooled for analysis (Figure 4.4 A).

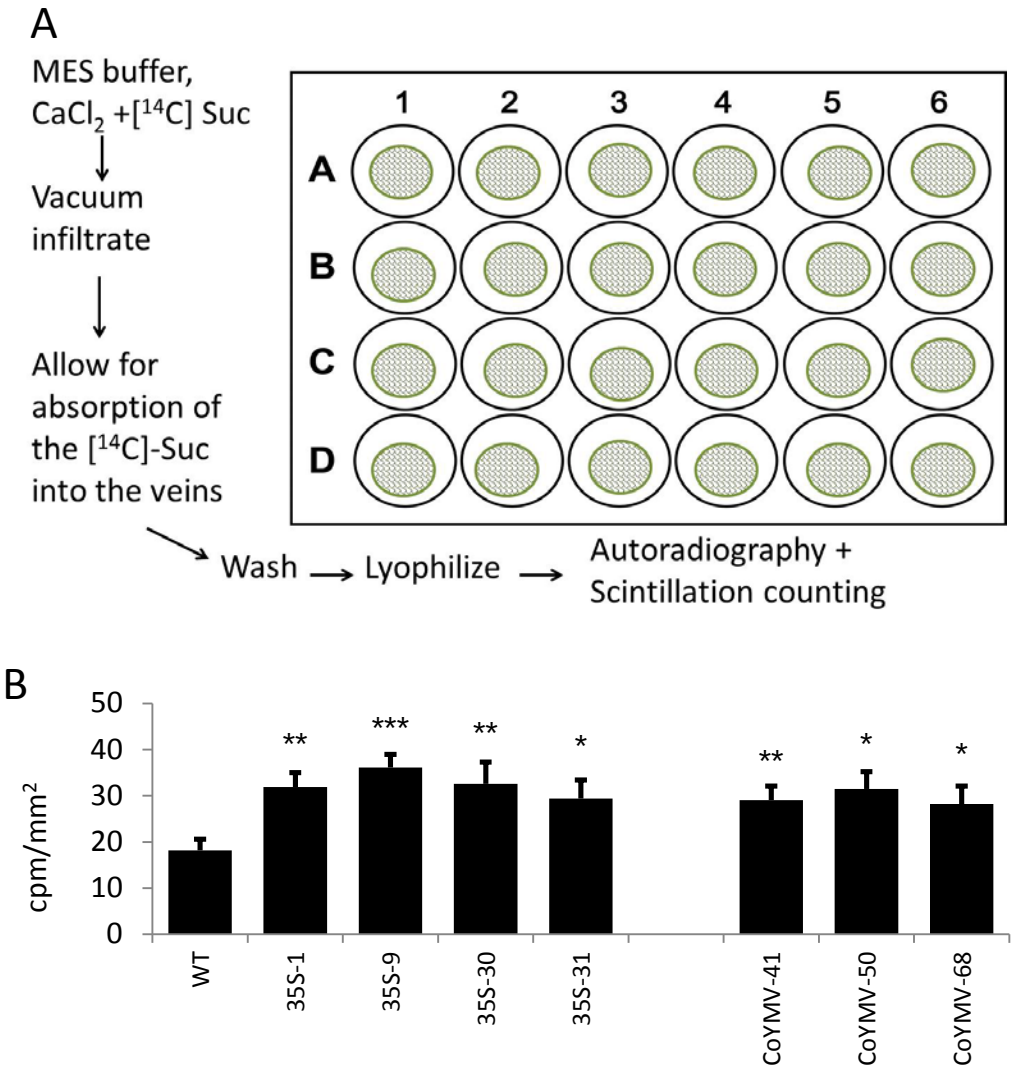

Figure 4-1: Uptake of [^{14}C]-Suc into leaves of WT, Pro35S:AVP1 and ProCoYMV:AVP1 lines to test the phloem loading capacity. **A**, Schematic representation of the experiment: Leaf discs were harvested from leaves of control and Pro35S:AVP1 and ProCoYMV:AVP1 lines, incubated in MES buffer with $CaCl_2$ until all tissues were processed. Previous solutions was replaced with fresh MES buffer with $CaCl_2$ and [^{14}C]-Suc. Leaf discs were vacuum infiltrated to allow for absorption of ^{14}C into the veins. Excess solution was washed with MES buffer, lyophilized and incorporation quantified with scintillation counting. **B**, Uptake of ^{14}C-Suc into the leaf disks of WT and transgenic lines expressed as cpm per mm^2 of leaf area. Variation is SE; n = 8 each containing three randomly pooled leaf discs. Significant differences from WT are based on Student's T-Test: *, $P \leq 0.05$; **, $P \leq 0.01$; ***, $P \leq 0.001$.

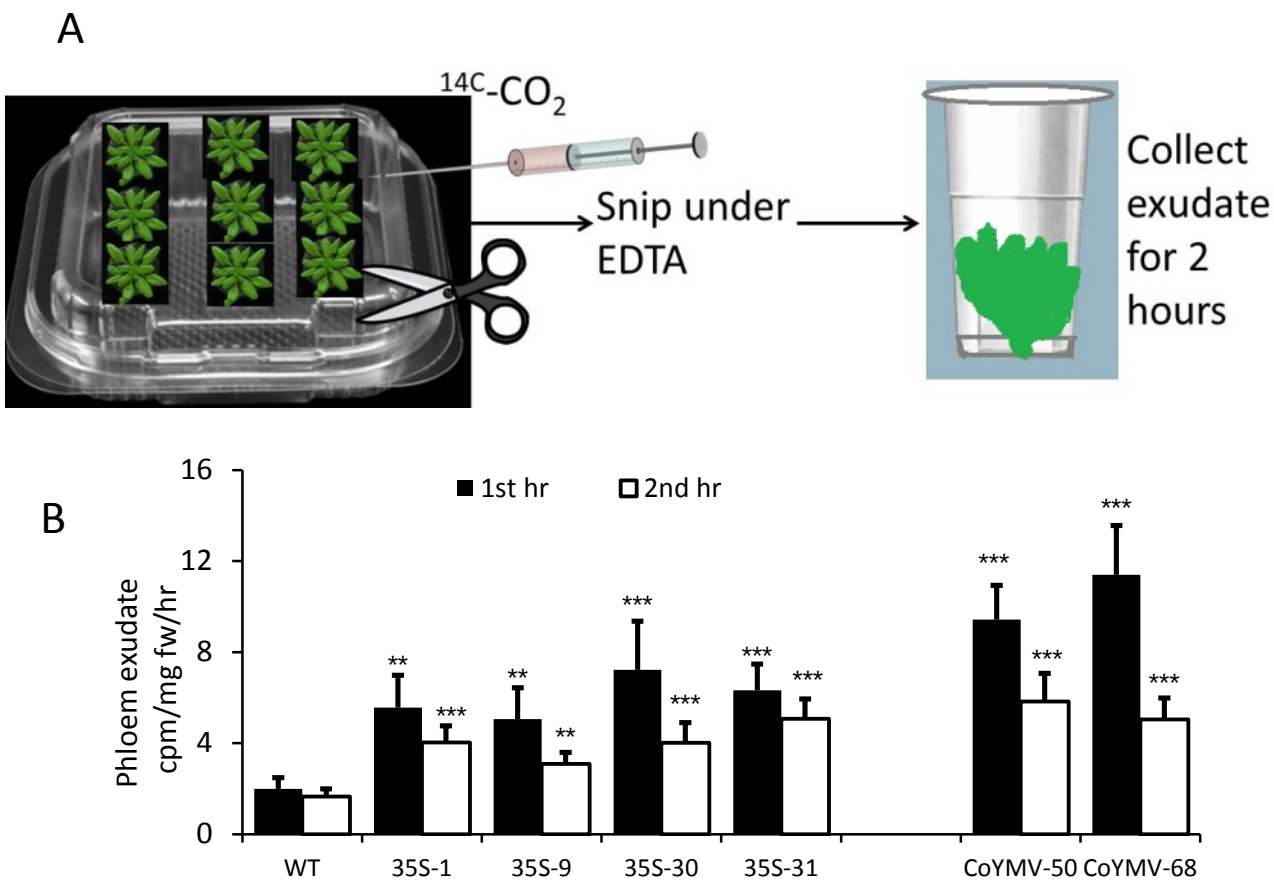

Figure 4-2: Constitutive and phloem-specific overexpression of *AVP1* enhances phloem transport as determined by exudation of cut rosettes. **A**, Schematic representation of experiment. Plants were labeled with [^{14}C]-CO_2 and allowed to photosynthesize for 20 min, afterwhich rosettes were harvested at the hypocotyl, weighed and re-cut under EDTA . Severed rosettes were placed in plastic coulter counter vials with the tip of hypocotyl submerged in EDTA, exudates collected for a total 140 min. **B**, Phloem exudation from detached rosettes of soil-grown plants into EDTA-containing solution after photosynthetic labeling with [^{14}C]-CO_2 shows improved phloem transport of [^{14}C] relative to WT, expressed as a rate of cpm per mg rosette fresh weight per hour. Variation is expressed as SE; n = 9 exudations for each line (3 of each line in 3 labeling chambers). Significant differences from WT are based on Student's T-Test: *, $P \leq 0.05$; **, $P \leq 0.01$; ***, $P \leq 0.001$.

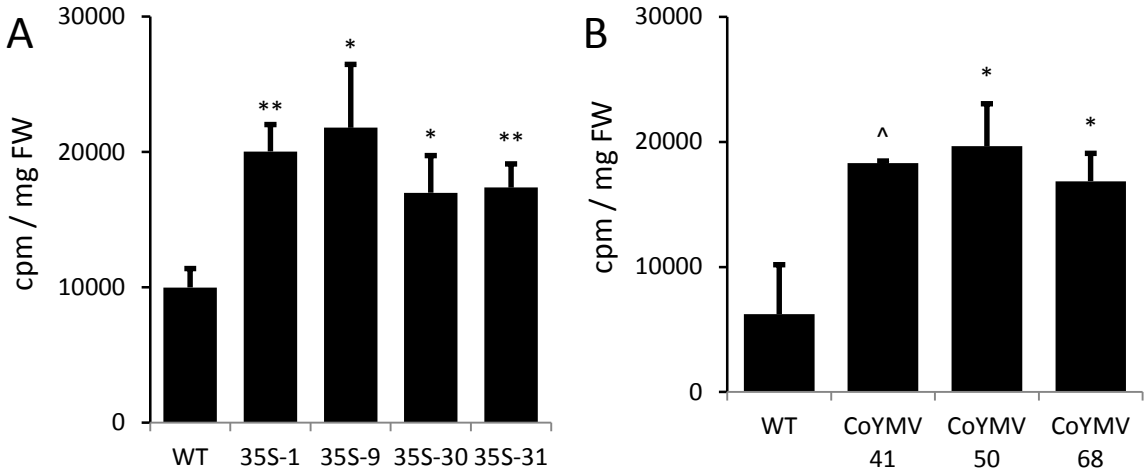
A
30000
20000
10000
0
cpm / mg FW
**
*
*
**
WT
35S-1
35S-9
35S-30
35S-31
B
30000
20000
10000
0
cpm / mg FW
^
*
*
WT
CoYMV 41
CoYMV 50
CoYMV 68

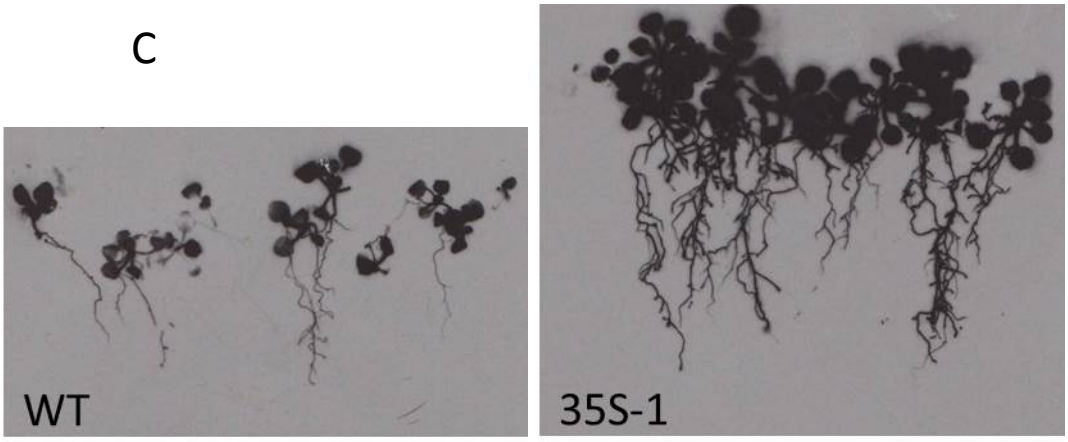
C
WT
35S-1

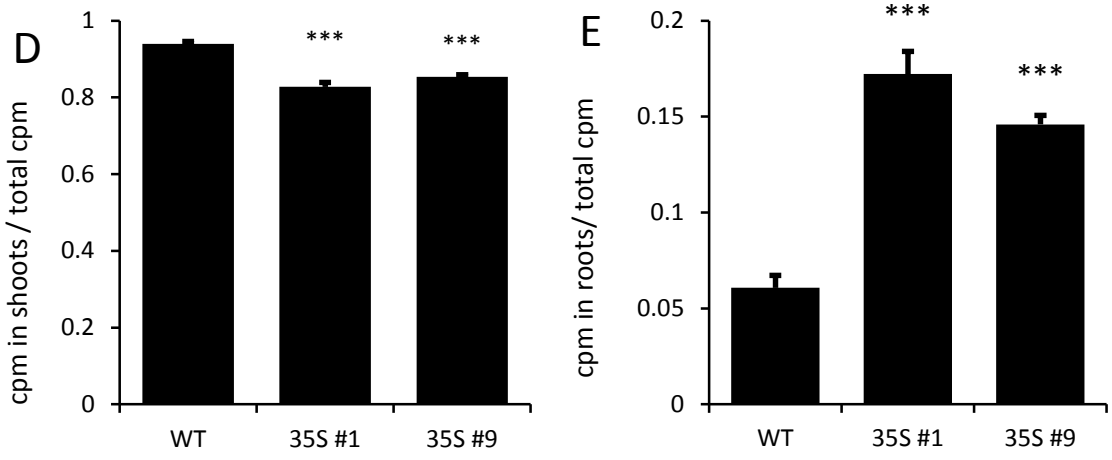
D
1
0.8
0.6
0.4
0.2
0
cpm in shoots / total cpm
***
***
WT
35S #1
35S #9
E
0.2
0.15
0.1
0.05
0
cpm in roots/ total cpm
***
***
WT
35S #1
35S #9

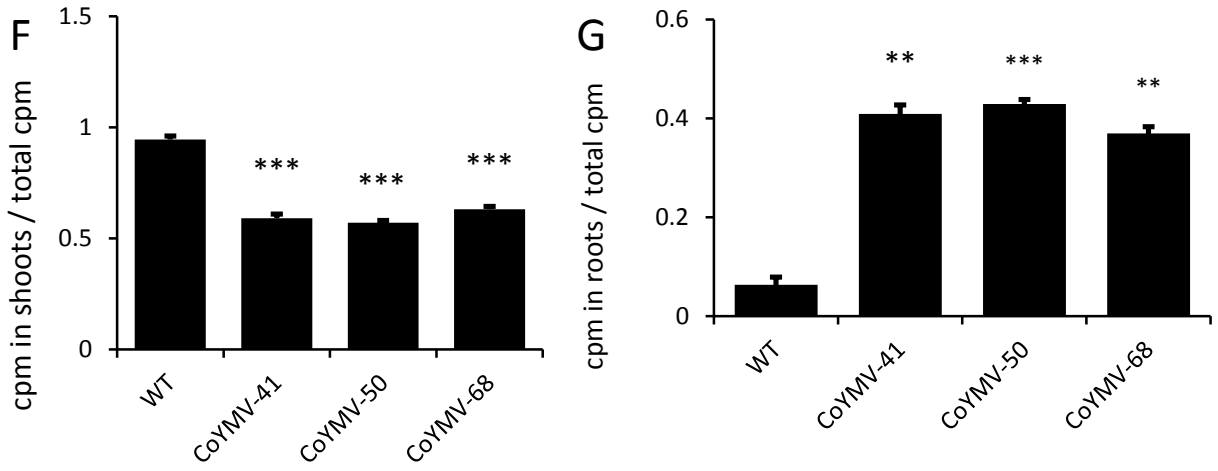

Figure 4-3: Pro35S:AVP1 and ProCoYMV:AVP1 plants have higher phloem transport compared to WT. Ratios of counts per minute (cpm) of ^{14}C after 20 min labeling and 40 min chase in normal air. **A**, cpm per milligram fresh weight in Pro35S:AVP1 plants compared to WT, showing greater assimilation; **B**, cpm per milligram fresh weight in ProCoYMV:AVP1 lines, showing greater assimilation; **C**, Autoradiogram of labeled plants, upper image shows WT and lower image shows 35S-1 having more label compared to WT and plants showing that *AVP1* OE roots accumulated more ^{14}C, and this appears to be concentrated in the growing regions of the main and lateral roots. **D**, Ratios of cpm in shoots to total cpm of *Pro35S:AVP1* plants compared to WT, showing *AVP1* overexpression lines partition greater proportions of ^{14}C to roots (less is retained in the shoot); **E**, Ratios of cpm in roots to total cpm of *Pro35S:AVP1* plants compared to WT, showing greater partitioning of ^{14}C to roots; **F**, Ratios of cpm in shoots to total cpm of *ProCoYMV:AVP1* plants compared to WT. **G**, Ratios of cpm in roots to total cpm of *ProCoYMV:AVP1* plants compared to WT, showing greater partitioning to roots. Variation is expressed as SE. Two plants were pooled for scintillation counting, n=8. Significant differences from WT are based on Student's T-Test: *, $P \leq 0.05$; **, $P \leq 0.01$; ***, $P \leq 0.001$.

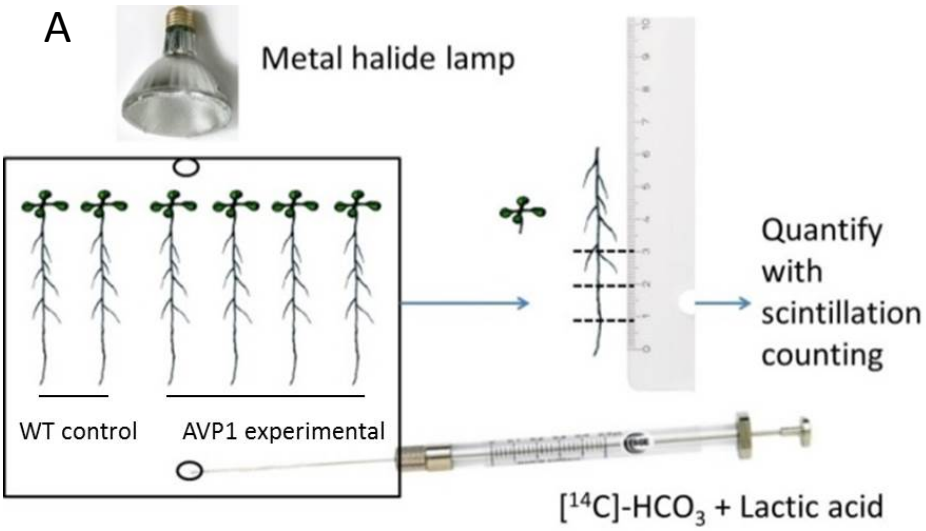

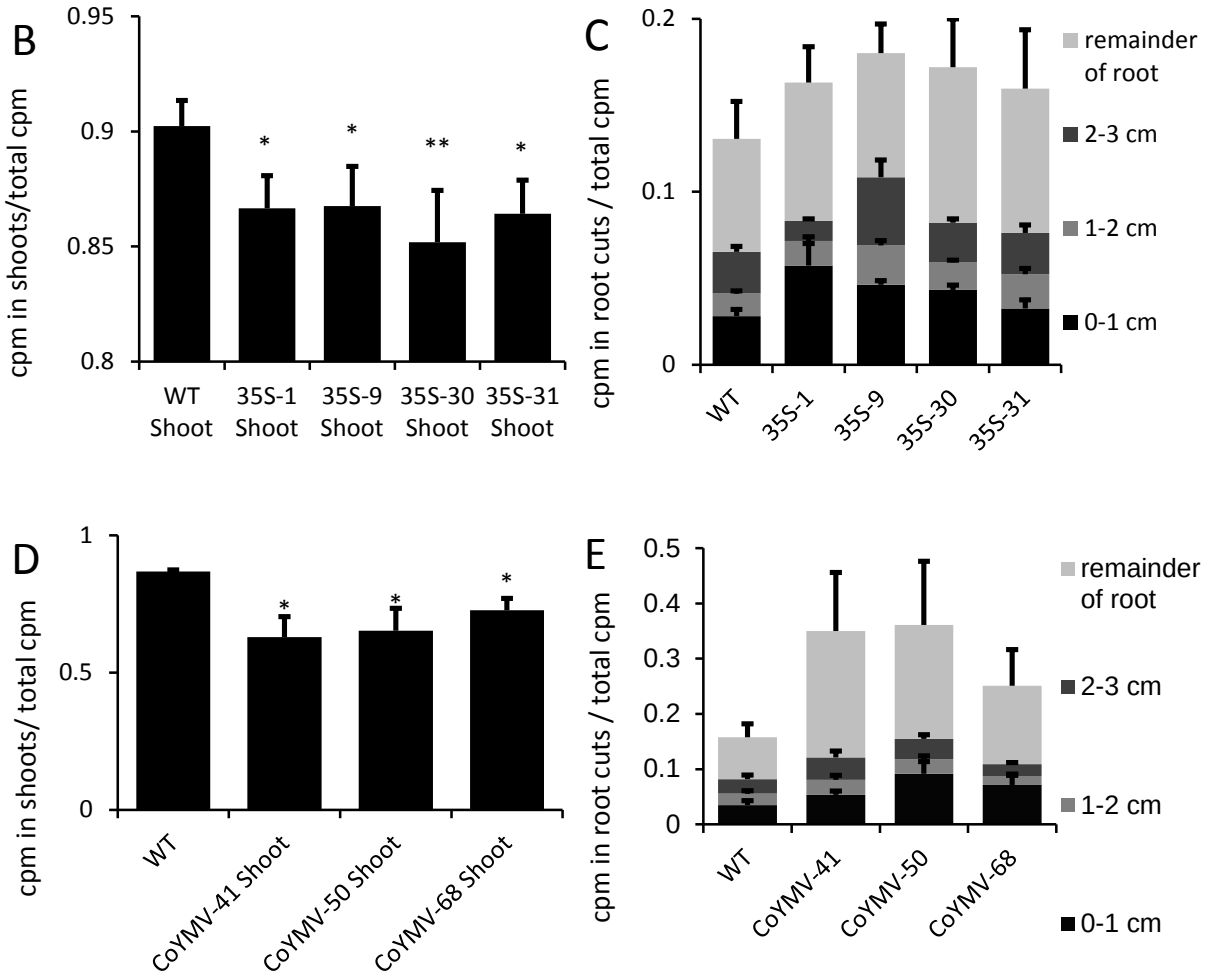

Figure 4-4: Constitutive and phloem-specific overexpression of *AVP1* enhances phloem transport and increased unloading at the terminal growing tip determined by photosynthetic labeling with [^{14}C]-CO_2. **A**, Method of radiolabeling with [^{14}C]-CO_2. Once germinated, plants were transferred to square plates and grown vertically for 8-10 days. Plants were labeled with [^{14}C]-CO_2, which is generated spontaneously by reacting [^{14}C]-HCO_3 and lactic acid. Plants were allowed to photosynthesize for 20 min, excess gas was removed, photosynthesis continued for another 40 min in normal air. Shoots and 1 cm root sections were separated and incorporated label quantified with scintillation counting. **B**, Ratio of cpm in shoots to total cpm of WT and Pro35S:AVP1 lines; **C**, ratio of cpm in roots to total cpm of WT and Pro35S:AVP1 lines; **D**, ratio of cpm in shoots to total cpm of WT and ProCoYMV:AVP1 lines and **E**, ratio of cpm in roots to total cpm of WT and ProCoYMV:AVP1 lines. Averages and SE, n=12, each replicate consisted of a pool of two plants. Shoots of Pro35S:AVP1 and ProCoYMV:AVP1 lines have less ratio of total label incorporated in the shoots compared to WT. Whereas, mainly the terminal 1cm distal tip has significantly higher ratio of label compared to WT indicating increased un-loding in the growing region.

4.7 Chapter References

Ainsworth EA, Bush DR (2011) Carbohydrate export from the leaf: a highly regulated process and target to enhance photosynthesis and productivity. Plant Physiology 155: 64-69

Amthor JS (2003) Efficiency of lignin biosynthesis: a quantitative analysis. Annals of Botany 91: 673-695

Ayre BG (2011) Membrane-transport systems for sucrose in relation to whole-plant carbon partitioning. Molecular Plant 4: 377-394

Ayre BG, Keller F, Turgeon R (2003) Symplastic continuity between companion cells and the translocation stream: long-distance transport is controlled by retention and retrieval mechanisms in the phloem. Plant Physiology 131: 1518-1528

Berg JM TJ, Stryer L (2002) Biochemistry, Ed 5th. W H Freeman, New York

Cakmak I, Hengeler C, Marschner H (1994) Changes in phloem export of sucrose in leaves in response to phosphorus, potassium and magnesium deficiency in bean plants. Journal of Experimental Botany 45: 1251-1257

Cao T, Lahiri I, Singh V, Louis J, Shah J, Ayre BG (2013) Metabolic engineering of raffinose-family oligosaccharides in the phloem reveals alterations in carbon partitioning and enhances resistance to green peach aphid. Frontiers in Plant Science 4: 263

Dasgupta K, Khadilkar A, Sulpice R, Pant B, Scheible WR, Fisahn J, Stitt M, Ayre BG (2014) Expression of sucrose transporter cDNAs specifically in companion cells enhances phloem loading and long-distance transport of sucrose, but leads to an inhibition of growth and the perception of a phosphate limitation. Plant Physiology 165: 715–731

Gaxiola RA, Sanchez CA, Paez-Valencia J, Ayre BG, Elser JJ (2012) Genetic manipulation of a "vacuolar" H($^{+}$)-PPase: from salt tolerance to yield enhancement under phosphorus-deficient soils. Plant Physiology 159: 3-11

Gonzalez N, De Bodt S, Sulpice R, Jikumaru Y, Chae E, Dhondt S, Van Daele T, De Milde L, Weigel D, Kamiya Y, Stitt M, Beemster GT, Inze D (2010) Increased leaf size: different means to an end. Plant Physiology 153: 1261-1279

Hammond JP, White PJ (2008) Sucrose transport in the phloem: integrating root responses to phosphorus starvation. Journal of Experimental Botony 59: 93-109

Hammond JP, White PJ (2011) Sugar signaling in root responses to low phosphorus availability. Plant Physiology 156: 1033-1040

Haruta M, Sussman MR (2012) The effect of a genetically reduced plasma membrane protonmotive force on vegetative growth of Arabidopsis. Plant Physiology 158: 1158-1171

Hermans C, Hammond JP, White PJ, Verbruggen N (2006) How do plants respond to nutrient shortage by biomass allocation? Trends in Plant Science 11: 610-617

Karthikeyan AS, Varadarajan DK, Jain A, Held MA, Carpita NC, Raghothama KG (2007) Phosphate starvation responses are mediated by sugar signaling in Arabidopsis. Planta 225: 907-918

Kuhn C, Grof CP (2010) Sucrose transporters of higher plants. Current Opinion in Plant Biology 13: 288-298

Paez-Valencia J, Patron-Soberano A, Rodriguez-Leviz A, Sanchez-Lares J, Sanchez-Gomez C, Valencia-Mayoral P, Diaz-Rosas G, Gaxiola R (2011) Plasma membrane localization of the type I H^+-PPase AVP1 in sieve element–companion cell complexes from *Arabidopsis thaliana*. Plant Science 181: 23-30

Paez-Valencia J, Sanchez-Lares J, Marsh E, Dorneles LT, Santos MP, Sanchez D, Winter A, Murphy S, Cox J, Trzaska M, Metler J, Kozic A, Facanha AR, Schachtman D, Sanchez CA, Gaxiola RA (2013) Enhanced proton translocating pyrophosphatase activity improves nitrogen use efficiency in romaine lettuce. Plant Physiology 161: 1557-1569

Paul M, Pellny T, Goddijn O (2001) Enhancing photosynthesis with sugar signals. Trends in Plant Science 6: 197-200

Paul MJ, Foyer CH (2001) Sink regulation of photosynthesis. Journal of Experimental Botany 52: 1383-1400

Slewinski TL (2011) Diverse functional roles of monosaccharide transporters and their homologs in vascular plants: a physiological perspective. Molecular Plant 4: 641-662

Srivastava AC, Ganesan S, Ismail IO, Ayre BG (2008) Functional characterization of the Arabidopsis AtSUC2 Sucrose/H^+ symporter by tissue-specific complementation reveals an essential role in phloem loading but not in long-distance transport. Plant Physiology 148: 200-211

Srivastava AC, Ganesan S, Ismail IO, Ayre BG (2009) Effective carbon partitioning driven by exotic phloem-specific regulatory elements fused to the *Arabidopsis thaliana AtSUC2* sucrose-proton symporter gene. BMC Plant Biology 9: 7

Sze H, Li X, Palmgren MG (1999) Energization of plant cell membranes by H^+-pumping ATPases. Regulation and biosynthesis. The Plant Cell 11: 677-690

Turgeon R, Medville R (2004) Phloem loading. A reevaluation of the relationship between plasmodesmatal frequencies and loading strategies. Plant Physiology 136: 3795-3803

Turgeon R, Wolf S (2009) Phloem transport: cellular pathways and molecular trafficking. Annual Review of Plant Biology 60: 207-221

CHAPTER 5

SUMMARY

Phloem transport is one of the most critical processes in establishment of plant growth and development. Understanding how this process is regulated is necessary to manipulate this process to enhance biomass partitioning and subsequently increasing plant productivity and yield. The use of an exotic promoter that is not inhibited in high Suc levels to enhance expression of *AtSUC2* was tested in Chapter 2 of this study. Stunting and carbohydrate accumulation in tobacco plants expressing *ProCoYMV:SUC2* initially seemed to refute our hypothesis that up-regulating *SUT* gene expression would enhance phloem transport and improve the plant growth. More refined analysis of phloem loading and transport did however support our hypothesis: *AtSUC2* overexpressing lines were loading and transporting more Suc than WT, and more ^{14}C was transferred to roots after photosynthetic labeling. This work with *SUT* overexpression in tobacco and prior work in Arabidopsis (Dasgupta et al., 2014) correlate well to argue that enhanced Suc transport has unintended consequences on nutrient use efficiency. Experiments initially conducted in Arabidopsis, and supported here, show that enhanced Suc transport disrupts C/P homeostasis to result in stunting. Through this analysis, we have shown that *AtSUC2* overexpression in tobacco impacts carbohydrate synthesis, transport and allocation to heterotrophic tissues, an interaction with phosphate homeostasis in these processes. The identification of molecular targets of carbohydrate signaling is needed, as are molecular targets of C/P homeostasis, and C homeostasis with other nutrients. In this regard, this work provides an important framework for future experiments involving manipulations of phloem transport as well improving the nutrient requirement and energy

equivalence needed for such enhanced systems. Thus, a strategy where enhanced phloem transport can be supported by enhancing PMF was employed in Chapters 3 and 4. In Chapter 3 the effect of phloem specific *AVP1* overexpression on the growth of plants and on primary metabolites was tested. Analysis of *AVP1* overexpressing plants showed significant increases in growth compared to WT. Measurements of several different primary metabolites did not show consistent alterations in the steady state levels. Flux analysis with ^{13}C or ^{14}C labeling may better address general metabolism. In Chapter 4, flux analysis with ^{14}C was used to study photosynthesis, phloem loading, phloem transport and phloem unloading. Improved Suc transport capacity was demonstrated with array of experiments to test directly phloem loading, transport and ability of delivering nutrients to the heterotrophic tissues. These experiments showed enhancement in each step of the transport pathway.

Thus, in addition to enhanced carbon availability, enhancing other nutrients to support use these additional carbohydrates is needed. Findings presented in Chapter 2 showed that C/P homeostasis was disturbed by enhanced supply of carbon to sink tissues. An approach which increases phloem transport in addition to increasing nutrient use efficiency was warranted. In our second strategy we aimed to simultaneously enhance Suc transport and nutrient uptake by enhancing the PMF in the phloem. As described in Chapter 3 AVP1 was previously shown to enhance nutrient use efficiency, and we hypothesized that it also enhances Suc transport by indirectly energizing the phloem. A portion of Suc that is loaded in phloem for long distance transport is oxidized to generate more ATP. The PM ATPase utilizes this to build up PMF. It was previously shown that inorganic pyrophosphate is necessary for this oxidation: Overexpression of a soluble pyrophosphatase *ppa1* in the phloem prevented Suc oxidation and efficient

transport, and resulted in debilitated plants (Sonnewald, 1992). Also, it was shown that overexpressing the *"vacuolar" proton-pumping pyrophosphatase* (H^+-PPases) *AVP1* enhanced both shoot and root growth, and augmented several energized processes like nutrient acquisition and stress responses (Gaxiola et al., 2001; Li et al., 2005). We tested hypotheses that AVP1 localizes to the PM of phloem cells and uses PMF to synthesize PPi rather than hydrolyze it, and in doing so, maintain PPi levels for efficient Suc oxidation and ATP production and enhanced activity increases phloem energization and phloem transport (Gaxiola et al., 2012). Unlike *SUT* overexpression, enhancing transport by *AVP1* overexpression may also energize the root system to improve nutrient uptake (Gaxiola et al., 2012).In future efforts, the synergistic effects of enhanced phloem transport in *SUT* overexpression lines and the improved PMF energization and enhanced nutrient use efficiency in *AVP1* overexpression lines needs to be assessed by generating crosses between these two lines.

5.1 Chapter Reference

Dasgupta K, Khadilkar A, Sulpice R, Pant B, Scheible WR, Fisahn J, Stitt M, Ayre BG (2014) Expression of sucrose transporter cDNAs specifically in companion cells enhances phloem loading and long-distance transport of sucrose, but leads to an inhibition of growth and the perception of a phosphate limitation. Plant Physiology 165: 715–731

Gaxiola RA, Li J, Undurraga S, Dang LM, Allen GJ, Alper SL, Fink GR (2001) Drought- and salt-tolerant plants result from overexpression of the *AVP1* H^+-pump. Proceedings of the National Academy of Sciences of the United States of America 98: 11444-11449

Gaxiola RA, Sanchez CA, Paez-Valencia J, Ayre BG, Elser JJ (2012) Genetic manipulation of a "vacuolar" H(+)-PPase: from salt tolerance to yield enhancement under phosphorus-deficient soils. Plant Physiology 159: 3-11

Li J, Yang H, Peer WA, Richter G, Blakeslee J, Bandyopadhyay A, Titapiwantakun B, Undurraga S, Khodakovskaya M, Richards EL, Krizek B, Murphy AS, Gilroy S, Gaxiola R (2005) Arabidopsis H^+-PPase AVP1 regulates auxin-mediated organ development. Science 310: 121-125

Sonnewald U (1992) Expression of *E. coli* inorganic pyrophosphatase in transgenic plants alters photoassimilate partitioning. The Plant Journal 2: 571-581

APPENDIX

ESTABLISH THE POTENTIAL OF ECTOPICALLY EXPRESSED *SUTS* TO TARGET CARBOHYDRATE AND BIOMASS TO SPECIFIC TISSUES TO ENHANCE PLANT PRODUCTIVITY

A.1 Abstract

Delivery of carbohydrates through the phloem from photosynthetic source leaves provides the substrate for the growth and maintenance of non-photosynthetic sink tissues like fruits, grains and tubers. Suc is the predominant form in which sugars are transported. The phloem of source leaves has higher concentrations of sugars and other nutrients than sink tissues, and this creates a hydrostatic pressure gradient which drives the flow of phloem sap from source to sink tissues. Once in the recipient sink organs, Suc and other nutrients may move cell to cell through plasmodesmata (i.e., through the symplasm) or across membranes and through the intercellular space. SUTs play important but poorly characterized roles in targeting the distribution of C within sink organs. In this chapter we tested if inducible and ectopic *SUT* expression may be an effective strategy to target carbohydrates to desired tissues and enhance productivity of those tissues. 17-β-estradiol was used as the inducer since it can be applied topically to selected tissues plus spreads minimally since it is lipophilic. *SUT* induction constructs were generated using Gateway recombination cloning technology and transformed in WT Arabidopsis and tobacco. Two-week-old T2 seedlings were incubated in a solution containing Suc and inducer, and semi-qualitative starch staining experiments were conducted to assess the amount of starch accumulated. The understandings from this study may provide future strategies to manipulate photoassimilate distribution.

A.2 Introduction

The in planta ability of Suc transporters to accumulate carbohydrates and contribute to growth in defined or desired tissue is not clearly known. Hence, it is necessary to study the ability of the SUTs to build up carbohydrates into specific target organs. This, in turn may lead

to enhanced development and/or increase in the biomass of the targeted tissue. Here we aim to compare the capacity of one transporter with the capacity of another. Our objective was to use inducible expression to ectopically express selected *SUTs* genes in desired tissues and test their ability of accumulating photoassimilate. Results from this study would test the potential of using SUTs to target biomass partitioning and improve plant productivity. Representatives from the five SUT family subgroups were selected for this study.

A.2.1 Inducible Expression of *SUTs* for Targeted Biomass Partitioning

Delivery of carbohydrates into the sink organs occurs by different pathways. Phloem unloading in strong sinks mostly occurs through symplasm. But Suc is also provided through the apoplasm to several important sinks which are not connected by phloem (Lalonde et al., 2003; Zhang et al., 2006). For example, germinating pollen and developing seeds are isolated from the maternal tissue. Also, ripening fruit or expanding cotton fibers lack plasmodesmatal connections to the vascular tissues at specific developmental stages. The occurrence of symplasmic or apoplasmic unloading domains is dynamic and changes from one to other based on the age of the plants, development stage or organ type (Viola et al., 2001; Stadler et al., 2005; Godt and Roitsch, 2006). In many crop plants, stems and roots are important organs for transient starch storage. These tissues that are adjacent to the transport phloem are symplasmically isolated, thus carbohydrates in these organs depend on apoplasmic movement (Minchin and Thorpe, 1996; Taliercio et al., 2009).

Ectopic *SUT* expression in these lateral tissues may lead to accumulation of carbohydrates leading to enhanced biomass accumulation. Increased biomass accumulation in the lateral tissues of crops like switch-grass would benefit the biofuel industry. As apoplasmic

Suc is available is most tissues in plants, this photoassimiliate can be targeted to desired tissues or organs to improve growth and development. In organs which are symplasmically connected, this approach may lead to changes to carbohydrate allocation leading to changes in metabolism and yield (Sonnewald et al., 1997; Kuhn et al., 2003).

In this study, a well-established inducible system to express selected *SUTs* was selected. In this system, XVE(LexA-VP16-ER) is a chimeric transcription factor which contains the *lex*A DNA binding domain, the VP16 transcriptional activation domain, and an estrogen ligand binding domain, and is expressed from the $P_{G10\text{-}90}$ -strong synthetic promoter. The gene of interest (various *SUT* encoding cDNA) was inserted downstream of the promoter OlexA-46 which is recognized by XVE (Zuo et al., 2000; Curtis and Grossniklaus, 2003). When the hormone 17-β-estradiol binds the ligand binding domain (ER) of XVE, the XVE transcription factor relocalizes from the cytoplasm into the nucleus and binds to the lexA operator region in the $P_{OlexA\text{-}46}$, leading to expression of the gene of interest (Figure A-1). Hence, the gene is expressed only in the organs or tissues treated with the inducer, 17-β-estradiol. 17-β-estradiol can be applied topically and leads to localized induction with minimal dispersion(Curtis and Grossniklaus, 2003). This is beneficial to our study as we may be able to generate our own sink tissues by topical application of 17-β-estradiol after which we can analyze the effect of induced SUT.

Overexpression of *SUTs* is not well emphasized in the literature. In one study, *SoSUT1* from spinach was expressed with the constitutive CaMV 35S promoter in potato and transgenic tubers showed higher sugar accumulation (Leggewie et al., 2003), but this led to little change in the starch content and tuber yield. Constitutive overexpression was believed to hinder the

phloem loading ability and reduced the amount of Suc available for export out of the leaves. Seed-specific overexpression of *StSUT1* using the vicilin promoter in the developing pea cotyledons lead to an increase in [^{14}C]-Suc efflux into the cotyledons. Biomass enhancement was observed in the cotyledons (Rosche et al., 2002). Constitutive overexpression of *SoSUT1* in potato led to enhanced root arbuscular mycorrhizal colonization in phosphorous sufficient soils. Enhanced symbiotic carbon supply was postulated as one of the reasons leading to enhanced mycorrhizal colonization (Gabriel-Neumann et al., 2011).

A.3 Results

A.3.1 Selection of Transgenic Plants Based on Semi-Qualitative Starch Staining Analysis

For each construct (Figure A-2, Table A-2) 25-30 independent lines were screened that showed 3:1 segregation ratio for hygromycin resistance in the succeeding generation, indicating T-DNA at a single locus. T2 and T3 plants containing the XVE:cSUCX cassettes were analyzed with the semi-qualitative starch staining to select ideal lines for further study. The desired lines should show no or very little SUT activity before induction, but high activity after the induction. In order to select which SUT lines were most promising, a high-throughput assay was developed. Two-week old Arabidopsis plants were incubated with a 1 % Suc solution containing 10 µM 17-β-estradiol. Seedlings were allowed to incubate for 8 hours, cleared of pigments and stained with iodine. This screening was fast and effective since inducible SUT activity should be observed in all cells, as leaves take up Suc from the surrounding solution. Suc accumulation leads to starch accumulation. If a particular SUT is capable of Suc uptake when ectopically induced, then we expected starch accumulation in the seedlings incubated with 17-β-estradiol. The independent lines showed differing levels of starch accumulation. Figure A-3 and Table A-2

summarizes the levels of starch accumulation in different lines containing different transporters in the Col-0 WT background. Amongst all tested *SUTs*, *AtSUC1 and AtSUC2* inductions led to the highest starch accumulations in XVE:AtSUC2 line AK2-6-6-11 and XVE:AtSUC1 line AK1-7-2-4, compared to the other XVE:cSUCX lines

For starch staining in tobacco, leaves of eight week old XVE:SUC2-11 and XVE:SUC2-15 plants were treated with 17-β-estradiol in lanolin paste applied on filter paper discs. To test the hypothesis of localized induction, the inductions were carried out over four days with different sections of each leaf induced at 24 hour intervals. We expected to observe a gradient of starch accumulation with the highest starch levels in the 96-hour induced spots compared to the 24-hour induced spots. However, such gradients were not observed. Instead starch was accumulated throughout the leaf, possibly due to movement of accumulated Suc from one cell to the other or more likely, from the spread of the inducer throughout the leaf. Starch accumulation was not observed in the mock induced leaves of different replicates of the same genotype, indicating that the starch accumulation was due to induction of *XVE:SUC2* within the leaf (Figure A-4).

A.4 Discussion

This study allowed us to express *SUT* cDNAs in a controlled manner and monitor the effect of ectopic expression on the carbohydrate accumulation in the induced tissue. The ability to overexpress the *SUTs*, in particular target tissues where it is not naturally expressed, may provide additional information on their physiological role for *in planta* carbon partitioning. The ectopic expression allowed us to create “sinks on demand” which would test the ability of certain tissues to accumulate carbohydrate and that may lead to increase in biomass. Findings

from this study helped formulate experiments where membrane transporters can be used to target photoassimilates to desired organs. Based on the transcript analysis, SUTs with best induction needs to be identified. The semi-qualitative starch accumulation may effectively demonstrate if a particular SUT is capable of Suc uptake when ectopically expressed. Higher uptake capacity may lead to localized starch accumulation when 17-β-estradiol is applied. Based on these experiments, three SUTs from the selected group (Table I) could be used for further analysis. In order to quantify transient carbohydrates, the leaves of T3 homozygous plants would need to be applied with 10 µM 17-β-estradiol. Eight-24 hours post induction; induced leaves could be harvested for quantifying transient soluble sugars and starch.

Once SUT lines leading to shift in photoassimilate accumulation is evaluated, Suc could be targeted to desired organs. The inducer could be applied to the sink organs such as inflorescence stems and the amount of starch and soluble sugars accumulation could be measured. Similarly, inducer could be applied to roots on sterile media containing different Suc concentrations. The starch excess *(sex)* mutants of Arabidopsis roots to accumulated starch when carbohydrate metabolism was disturbed (Vitha et al., 2007). Starch accumulation in roots could be visualized by using iodine staining and may establish the ability of using ectopic *SUT* expression to alter carbon partitioning. Inducer also could be applied to developing siliques, and shifts in carbohydrate partitioning could be quantified.

A.5 Material and Methods

A.5.1 Plasmid Constructions and Plant Transformation

The gateway compatible destination vector pMDC7 was obtained from Dr. Nam-Hai Chua, The Rockefeller University, New York, NY. The full-length open reading frames of selected

SUTs (except AtSUC2 and ZmSUT1) were received from Dr. John M. Ward, University of Minnesota. *AtSUC1*, *AtSUC3*, *AtSUC9* open reading frames were received in the gateway compatible entry vectors, pCR8/GW/TOPO-Spectinomycin^R, namely pCR8:AtSUC1, pCR8:AtSUC3 and pCR8:AtSUC9. Entry clone pCR8:AtSUC1 was recombined with pMDC7 by Gateway LR recombination using LR Clonase II enzyme mix (Life Technologies) to generate pMDC7:AtSUC1. Similarly, pMDC7:AtSUC3 and pMDC7:AtSUC9 were generated. *ZmSUT1* was received in a directional pENTR/TOPO vector as pENTR-ZmSUT1 from Dr. David M. Braun, University of Missouri. pENTR-ZmSUT1 was recombined with the pMDC7 to generated pMDC7:ZmSUT1. *AtSUC2* was PCR amplified from pGEM: ProSUC2:cSUC2 (Srivastava 2008) using oligonucleotides AtSUC2F (5'-CACCATGGTCAGCCATCCAATGGAGAAAGCTGC-3') and AtSUC2R(5'-ATGAAATCCCATAGTAGCTTTGAACGCAGGAGC- 3') using Phusion Hot Start II High-Fidelity DNA polymerase (Finnzymes OY, Thermo-Scientific). PCR product was purified using the Wizard SV gel and PCR clean-up system (Promega, Madison, WI, USA) and cloned into pENTR/D-TOPO using pENTR Directional TOPO cloning kits (Life Technologies) to generate pENTR:AtSUC2. pENTR:AtSUC2 was recombined with pMDC7 to generate pMDC7:AtSUC2 using LR Clonase II enzyme mix (Life Technologies). *LeSUT1, LeSUT2, LeSUT4* and *NtSUT3* were received in Gateway non-compatible vectors as p112A1:LeSUT1, pDR195:LeSUT2, pDR195:LeSUT4 and p195xE-NtSUT3. Each was PCR amplified using LeSUT1F (5'-CACCATGG AGAATGGTACAAAAGGGAAACT-3') and LeSUT1R (5'- AATGGAAACCGCC CATGGCGACTGCTGG- 3'), LeSUT2F (5'-CACCATGGATGCGGTATC GATCAGAGTACCGT- 3') and LeSUT2R (5'-ACCAAAATGGAAGCCAGTTGATTTG- 3'), LeSUT4F (5'- CACCATGCCGGAGATAGA AAGGCATAGAACAAGG-3') and LeSUT4R (5'-TGCAAAGATCTTGGGTCTCTCAACCCGGTGTTCG- 3'),

NtSUT3F (5’-CACCATGGAGAGTGGTA GTATGGGAATG-3’) and NtSUT3R (5’-AAACTTGTTTT GTGATGTCCAGTATTTTGTC- 3’) using Phusion Hot Start II High-Fidelity DNA polymerase (Finnzymes OY) . Oligonucleotides were obtained from Eurofins MWG Operon, Huntsville, AL, USA. PCR products were purified using the Wizard SV gel and PCR clean-up system (Promega) and cloned into pENTR/D-TOPO using pENTR Directional TOPO cloning kits (Life Technologies) to generate pENTR:LeSUT1, pENTR:LeSUT2, pENTR:LeSUT4 and pENTR:NtSUT3 respectively. These entry clones were recombined with pMDC7 to generate pMDC7:LeSUT1, pMDC7:LeSUT2, pMDC7:LeSUT4, pMDC7:NtSUT3 using LR Clonase II enzyme mix. pMDC7:XVE:cSUCX (Figure A-2) cassettes were electroporated into *Agrobacterium tumefaciens* strain GV3101mp90 as described (Ayre 2004). WT Col-0 (ABRC catalog #CS-70000) was transformed with the above constructs by the floral dip method (Clough and Bent, 1998). In addition to Arabidopsis, WT tobacco plants were generated using a protocol described in Chapter 2 of this study. Homozygous plants XVE:SUC2-11 and XVE:SUC2-15 were identified based on resistance to hygromycin and T2 seeds were used for 17-β-estradiol inductions followed by starch staining.

A.5.2 Plant Material

Seeds were selected on the hygromycin and seedlings were transferred to 6 inch pots for tobacco XVE:SUC2 lines. Plantlets were transferred to a growth chamber (Percival AR95L, Percival Scientific, Perry IA) in 12 hour light at 22°C and 12 hour dark at 18°C, 180 µmol photons m^{-2} s^{-1}. Once plants were established, they were transferred to the green house in 14 hour light at 24°C and 12 hour dark at 18°C, 350 µmol photons m^{-2} s^{-1}. For Arabidopsis, T1 generation seeds of plants transformed with pMDC7:cSUCX were selected on sterile medium containing 40 mg/L hygromycin. Seeds were stratified for 72 hours and exposed to light for 7 hours. Seeds

were kept in dark for 5 days to allow hypocotyl elongation to occur. Seedlings resistant to hygromycin were transferred to potting mix. Segregation in T3 generation was used to identify lines homozygous for cDNA (Harrison et al., 2006). For XVE:AtSUC1 lines, AK1-7-2-4, AK1-4-8-8, AK1-5-5-2 were selected. For XVE:SUC2 lines, AK2-14-5-1, AK2-14-3-1 and AK2-6-6-11 were selected. For XVE:ZmSUT1 lines, AK5-5-5-1, AK5-5-8-3 were selected. For semi-qualitative starch staining of the rest of the XVE:cSUCX, T2 lines were used. For XVE:AtSUC3, AK3-2-1, AK3-4-1and AK3-10-1. For XVE:AtSUC9, AK4-13-1, AK4-13-22 and AK4-14-1 were selected. For XVE:LeSUT1, AK6-1-12 and AK6-10-2 were used. For XVE:LeSUT4, AK8-17-1, AK8-24-1 and AK8-14-6 were used. For XVE:NtSUT3, AK9-5-9, AK9-5-4 and AK9-5-11 were used.

A.5.3 Semi-Qualitative Starch Staining

For Arabidopsis, two-week old T3 lines were incubated in 1 % Suc solution containing, 10 µM 17-β-estradiol and 0.01 % Silwett, for 4-8 hour. Seedlings were then depigmented with 70 % ethanol. Seedlings were allowed to rehydrate with two washes each of 60 %, 30 % ethanol and finally two washes of water. The seedlings were stained with 10 % Lugol's iodine (Sigma-Aldrich)

For SUT inductions in tobacco, leaves of eight week old XVE:SUC2-11 and XVE:SUC2-15 and WT were induced with 5 cm diameter filter paper disks with 10 µM 17-β-estradiol in lanolin (Lansinoh HPA, Alexandria VA)for every 24 hour for a period of four days. For negative control, DMSO was dissolved in Lanolin. After four days of inductions, leaves were stained with 10 % Lugol's iodine solution after depigmentation with 70 % ethanol.

Table A-1: The list of selected transporters for the study with summary of their physiological role in plants.

Groups	Functions of Groups	Representative Members	Location And Physiological Function
Group 1	Monocot-specific, high affinity SUTs involved in phloem transport, Suc uptake into sink tissues including grain filling and recovery from the apoplasm.	ZmSUT1	Leaf blades, expanding leaf, Phloem & sinks, loading in source
Group 2	Dicot-specific, high affinity SUTs involved in phloem loading, uptake of Suc into various sink tissues, and recovery from the apoplasm.	AtSUC1	Involved in pollen development and root elongation. Transports Suc to pollen. Suc induced anthocyanin accumulation. Suc signaling in vegetative tissue and male gametophyte function
		AtSUC2	Majorly involved in phloem loading, responsible for hydrostatic pressure gradient across apoplastic space,involved in long distance transport
		AtSUC9	High affinity sucrose transporter. Transports Suc to shoots and flowers. Delays floral transition
		LeSUT1	Involved in phloem loading and accumulation of Suc in few sinks
		NtSUT3	Suc transport into pollen tubes, Suc signaling to pollen tube
Group 3	Found in both Monocots and dicots, low affinity, not well characterized.	LeSUT2	Suc transport to developing sinks, developing pollen
		AtSUT2 (AtSUC3)	Transports Suc to pollen, wounded tissue, developing seed
Group 4	Found in both Monocots and dicots, low affinity, may be involved in transport Suc from the vacuole into the cytoplasm and vice-a-versa.	LeSUT4	Involved in Suc signaling ,Suc transport to sinks, developing ovaries, flowers and fruits
Group 5	Monocot-specific, not well characterized.	None	

Group assignments are based on (Braun and Slewinski, 2009); functions of groups, location and physiological function are based on (Braun and Slewinski, 2009; Ayre, 2011).

Table A-2: Summarizing starch accumulation after semi-qualitative starch staining. Interpretation of observations.

Selected Members	**Level of Starch accumulation**	**Interpretation and Significance from composite assessment of 24-30 lines/XVE:cSUCX**
ZmSUT1	*	Functions in phloem loading in maize (Slewinski et al., 2010), thus we were expecting to have high starch accumulation. Surprisingly, we did not observe significant starch accumulation compared to others. This suggests that other co-factors might be needed for constitutive activity of ZmSUT1.
AtSUC1	****	Transports Suc to pollen. Belongs to Group 2 which is involved in phloem loading and supply of Suc to various sink tissues (Sivitz et al., 2008). Thus as expected it showed high starch accumulation indicating that it has high Suc uptake capacity.
AtSUC2	****	Main player in phloem loading and presumably in Suc retrieval (Srivastava et al., 2009). As expected it showed high starch accumulation indicating that it has high Suc uptake capacity.
AtSUC9	***	As it is a high affinity transporter, supplying Suc to shoots and flowers (Sivitz et al., 2007), we were expecting to have high starch accumulation. We did observe high starch accumulation but 2 other transporters showed higher accumulation.
NtSUT3	***	Involved in Suc transport to pollen tubes and belongs to group 2 which is high affinity group (Lemoine et al., 1999). Showed significant starch accumulation as expected.
LeSUT1	**	We were expecting to have high starch accumulation as this is involved in phloem loading and Suc accumulation in sinks (Hackel et al., 2006). But we did not see significant accumulation compared to others. Needs further analysis.
LeSUT2	**	We were not expecting to have high starch accumulation as this is a low affinity transporter with only known function in developing pollen (Barker et al., 2000). These preliminary results are in congruence with our expectation.
AtSUT2 (AtSUC3)	**	Involved in Suc transport to pollen and T-DNA insertion mutants do not show obvious phenotype (Meyer et al., 2000; Meyer et al., 2004). We were not expecting significant starch accumulation.
LeSUT4	***	Initially this was thought to mediate Suc transport between the cytoplasm and vacuole. Could be involved in Suc transport to developing flowers and fruits. Low affinity transporter (Weise et al., 2000). Hence, we were not expecting high starch accumulation. But we did observe high starch accumulation.

Note: ****: highest, *: lowest

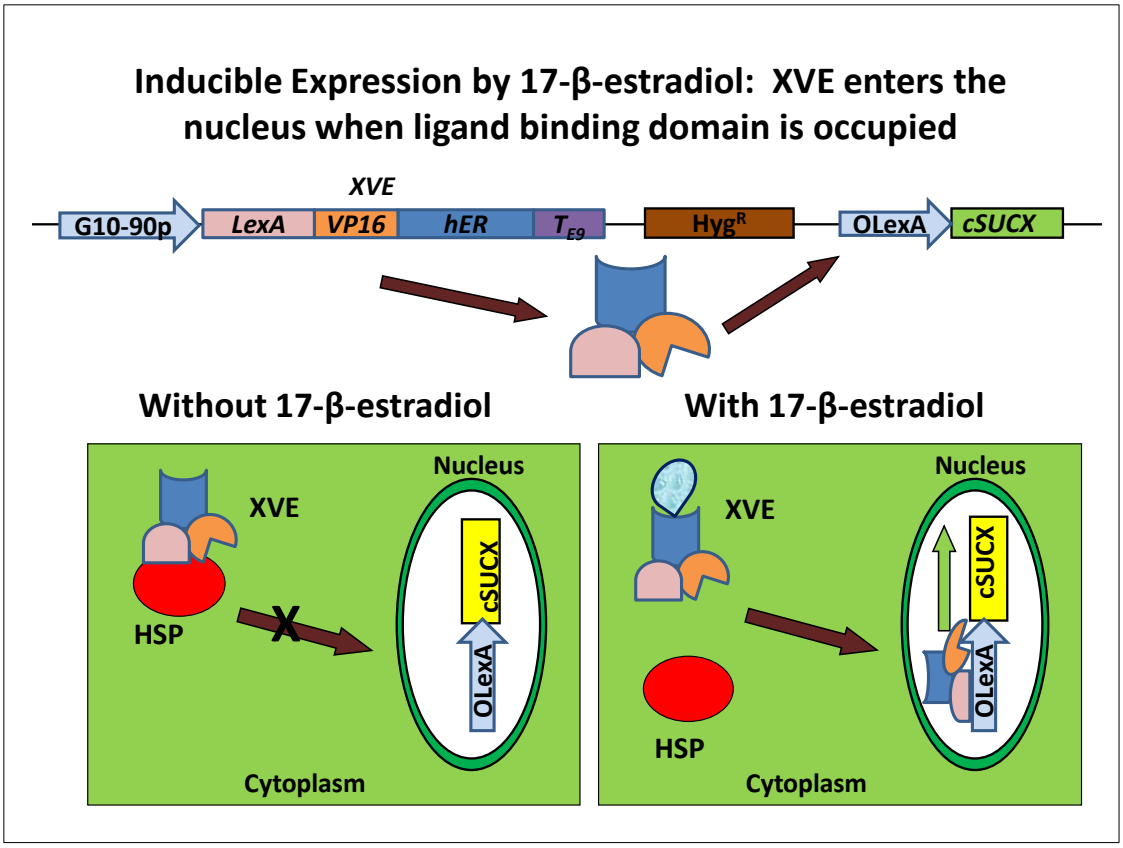

Figure A-1: Mechanism of inducible expression. $P_{G10\text{-}90}$: strong synthetic promoter which expresses *XVE*; *LexA*-encodes for the DNA binding domain, *VP16*-encodes for a transcriptional-activation domain, *hER* encodes for the ER-estrogen ligand binding domain which binds 17-β-estradiol. In presence of estrogen such as 17-β-estradiol-this protein binds to the lexA operator in O_{LexA}-46 which activates transcription (Curtis and Grossniklaus, 2003).

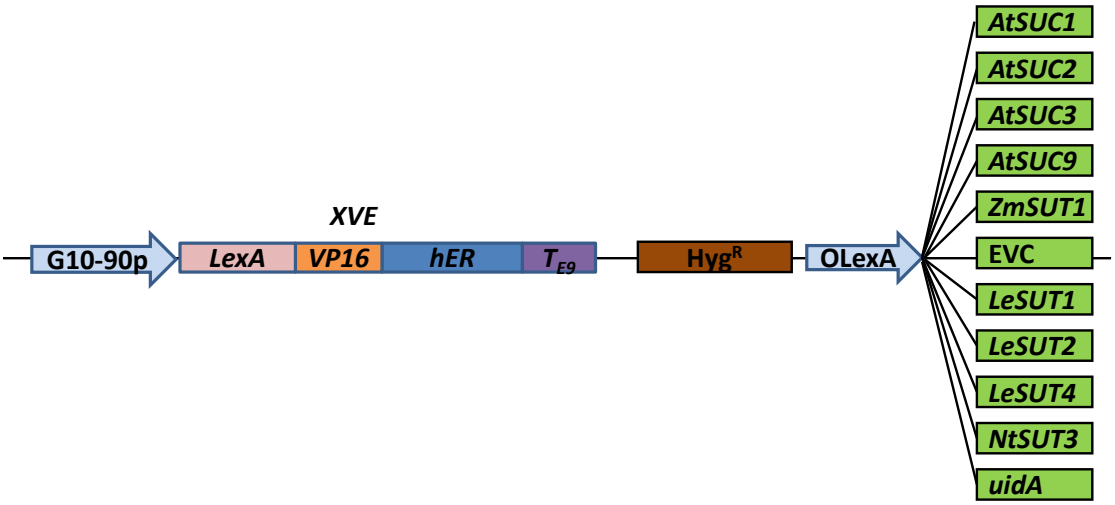

Figure A-2: Summary of SUTs selected for the study. Representation of expression vectors transformed into Arabidopsis.EVC: empty vector control pMDC7 (Curtis and Grossniklaus, 2003) and *uidA* gene from (Srivastava et al., 2008)

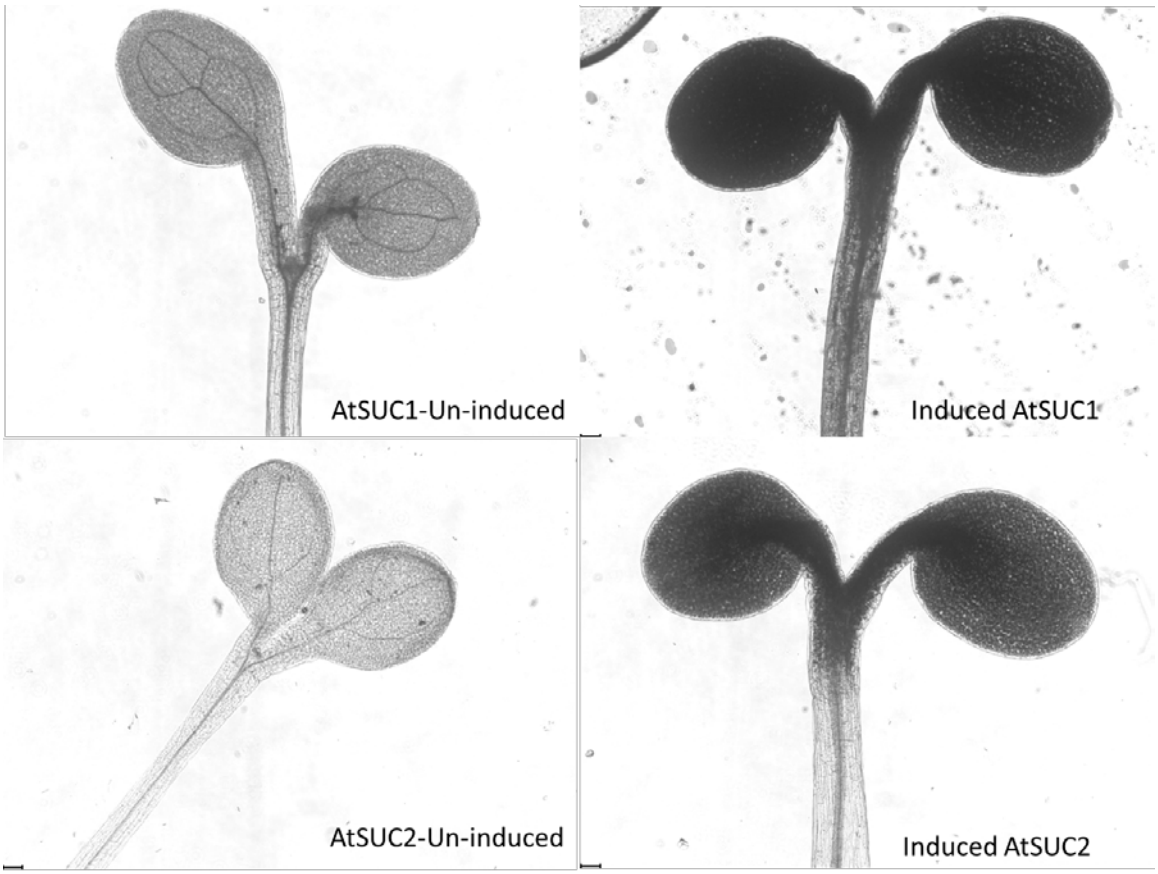

Figure A-3: Starch staining of induced seedlings
Top left: XVE:AtSUC1 line AK1-7-2-4 seedling incubated in 1 % Suc solution without 17-β-estradiol. Top right: XVE:AtSUC1 line AK1-7-2-4 incubated in 1 % Suc plus 17-β-estradiol. Bottom left: XVE:AtSUC2 line AK2-6-6-11 seedling incubated in 1 % Suc solution without 17-β-estradiol. Bottom right: XVE:AtSUC2 line AK2-6-6-11 incubated in 1 % Suc plus 17-β-estradiol. Induced expression of *AtSUC1* and *AtSUC2* led to higher accumulation of starch compared to control conditions.

Figure A-4: Starch staining of induced seedlings. Top left: XVE: AtSUC2-11 leaf induced with 17-β-estradiol. Top right: XVE: AtSUC2-15 leaf induced with 17-β-estradiol. Bottom left: XVE: AtSUC2-11 leaf mock induced without 17-β-estradiol. The leaf is from a sibling plant. Bottom right: XVE: AtSUC2-15 leaf mock induced without 17-β-estradiol. The leaf is from a sibling plant. Induced expression of *AtSUC2* in tobacco led to higher accumulation of starch compared to mock induced conditions.

A.4 Chapter References

Ayre BG (2011) Membrane-transport systems for sucrose in relation to whole-plant carbon partitioning. Molecular Plant 4: 377-394

Barker L, Kuhn C, Weise A, Schulz A, Gebhardt C, Hirner B, Hellmann H, Schulze W, Ward JM, Frommer WB (2000) SUT2, a putative sucrose sensor in sieve elements. The Plant Cell 12: 1153-1164

Braun DM, Slewinski TL (2009) Genetic control of carbon partitioning in grasses: roles of sucrose transporters and tie-dyed loci in phloem loading. Plant Physiology 149: 71-81

Clough SJ, Bent AF (1998) Floral dip: a simplified method for Agrobacterium-mediated transformation of *Arabidopsis thaliana*. The Plant Journal 16: 735-743

Curtis MD, Grossniklaus U (2003) A gateway cloning vector set for high-throughput functional analysis of genes in planta. Plant Physiology 133: 462-469

Gabriel-Neumann E, Neumann G, Leggewie G, George E (2011) Constitutive overexpression of the sucrose transporter *SoSUT1* in potato plants increases arbuscular mycorrhiza fungal root colonization under high, but not under low, soil phosphorus availability. Journal of Plant Physiology 168: 911-919

Godt D, Roitsch T (2006) The developmental and organ specific expression of sucrose cleaving enzymes in sugar beet suggests a transition between apoplasmic and symplasmic phloem unloading in the tap roots. Plant Physiology and Biochemistry 44: 656-665

Hackel A, Schauer N, Carrari F, Fernie AR, Grimm B, Kuhn C (2006) Sucrose transporter LeSUT1 and LeSUT2 inhibition affects tomato fruit development in different ways. The Plant Journal 45: 180-192

Harrison S, Mott E, Parsley K, Aspinall S, Gray J, Cottage A (2006) A rapid and robust method of identifying transformed *Arabidopsis thaliana* seedlings following floral dip transformation. Plant Methods 2: 19

Kuhn C, Hajirezaei MR, Fernie AR, Roessner-Tunali U, Czechowski T, Hirner B, Frommer WB (2003) The sucrose transporter StSUT1 localizes to sieve elements in potato tuber phloem and influences tuber physiology and development. Plant Physiology 131: 102-113

Lalonde S, Tegeder M, Throne-Holst M, Frommer WB, Patrick JW (2003) Phloem loading and unloading of sugars and amino acids. Plant, Cell & Environment 26: 37-56

Leggewie G, Kolbe A, Lemoine R, Roessner U, Lytovchenko A, Zuther E, Kehr J, Frommer WB, Riesmeier JW, Willmitzer L, Fernie AR (2003) Overexpression of the sucrose transporter *SoSUT1* in potato results in alterations in leaf carbon partitioning and in tuber metabolism but has little impact on tuber morphology. Planta 217: 158-167

Lemoine R, Burkle L, Barker L, Sakr S, Kuhn C, Regnacq M, Gaillard C, Delrot S, Frommer WB (1999) Identification of a pollen-specific sucrose transporter-like protein NtSUT3 from tobacco. FEBS Letters 454: 325-330

Meyer S, Lauterbach C, Niedermeier M, Barth I, Sjolund RD, Sauer N (2004) Wounding enhances expression of *AtSUC3*, a sucrose transporter from Arabidopsis sieve elements and sink tissues. Plant Physiology 134: 684-693

Meyer S, Melzer M, Truernit E, Hummer C, Besenbeck R, Stadler R, Sauer N (2000) *AtSUC3*, a gene encoding a new Arabidopsis sucrose transporter, is expressed in cells adjacent to the vascular tissue and in a carpel cell layer. The Plant Journal 24: 869-882

Minchin PE, Thorpe MR (1996) What determines carbon partitioning between competing sinks? Journal of Experimental Botany 47: 1293-1296

Rosche E, Blackmore D, Tegeder M, Richardson T, Schroeder H, Higgins TJ, Frommer WB, Offler CE, Patrick JW (2002) Seed-specific overexpression of a potato sucrose transporter increases sucrose uptake and growth rates of developing pea cotyledons. The Plant Journal 30: 165-175

Sivitz AB, Reinders A, Johnson ME, Krentz AD, Grof CP, Perroux JM, Ward JM (2007) Arabidopsis sucrose transporter AtSUC9. High-affinity transport activity, intragenic control of expression, and early flowering mutant phenotype. Plant Physiology 143: 188-198

Sivitz AB, Reinders A, Ward JM (2008) Arabidopsis sucrose transporter AtSUC1 is important for pollen germination and sucrose-induced anthocyanin accumulation. Plant Physiology 147: 92-100

Slewinski TL, Garg A, Johal GS, Braun DM (2010) Maize SUT1 functions in phloem loading. Plant Signaling & Behavior 5: 687-690

Sonnewald U, Hajirezaei MR, Kossmann J, Heyer A, Trethewey RN, Willmitzer L (1997) Increased potato tuber size resulting from apoplastic expression of a yeast invertase. Nature Biotechnology 15: 794-797

Srivastava AC, Dasgupta K, Ajieren E, Costilla G, McGarry RC, Ayre BG (2009) Arabidopsis plants harbouring a mutation in *AtSUC2*, encoding the predominant sucrose/proton symporter necessary for efficient phloem transport, are able to complete their life cycle and produce viable seed. Annals of Botony 104: 1121-1128

Srivastava AC, Ganesan S, Ismail IO, Ayre BG (2008) Functional characterization of the Arabidopsis AtSUC2 Sucrose/H^+ symporter by tissue-specific complementation reveals an essential role in phloem loading but not in long-distance transport. Plant Physiology 148: 200-211

Stadler R, Lauterbach C, Sauer N (2005) Cell-to-cell movement of green fluorescent protein reveals post-phloem transport in the outer integument and identifies symplastic domains in Arabidopsis seeds and embryos. Plant Physiology 139: 701-712

Taliercio EW, Romano G, Scheffler J, Ayre BG (2009) Expression of genes associated with carbohydrate metabolism in cotton stems and roots. BMC Plant Biology 9: 11-2229-2229-2211

Viola R, Roberts AG, Haupt S, Gazzani S, Hancock RD, Marmiroli N, Machray GC, Oparka KJ (2001) Tuberization in potato involves a switch from apoplastic to symplastic phloem unloading. The Plant Cell 13: 385-398

Vitha S, Yang M, Sack FD, Kiss JZ (2007) Gravitropism in the starch excess mutant of *Arabidopsis thaliana*. American Journal of Botany 94: 590-598

Weise A, Barker L, Kuhn C, Lalonde S, Buschmann H, Frommer WB, Ward JM (2000) A new subfamily of sucrose transporters, SUT4, with low affinity/high capacity localized in enucleate sieve elements of plants. The Plant Cell 12: 1345-1355

Zhang XY, Wang XL, Wang XF, Xia GH, Pan QH, Fan RC, Wu FQ, Yu XC, Zhang DP (2006) A shift of phloem unloading from symplasmic to apoplasmic pathway is involved in developmental onset of ripening in grape berry. Plant Physiology 142: 220-232

Zuo J, Niu QW, Chua NH (2000) Technical advance: An estrogen receptor-based transactivator XVE mediates highly inducible gene expression in transgenic plants. The Plant Journal 24: 265-273